DEVELOPMENT OF NEW FLUOROUS STATIONARY PHASE TECHNOLOGIES FOR IMPROVED ANALYTICAL SEPARATIONS

by

ADAM BRUCE DALEY

A thesis submitted to the Department of Chemistry

in conformity with the requirements for

the degree of Doctor of Philosophy

Queen's University

Kingston, Ontario, Canada

May, 2011

Abstract

Applications taking advantage of fluorine-fluorine interactions for separations are a recent analytical trend, with benefits in terms of cost, ease of use and specificity cited as advantages of these so-called “fluorous” techniques. While most current fluorous separations employ columns packed with microspheres, columns based on entrapped microspheres, porous polymer monoliths (PPMs) and open tubes all represent viable alternatives to conventional packed capillaries. In this thesis, the design, optimization and implementation of fluorous stationary phases based on all three of these new technologies are explored. Development of methods and techniques using these systems are presented, with factors affecting their performance being examined. Doing this, the specificity of the fluorous interaction can also be explored, and potential applications for these new materials can be discussed.

For the work with entrapped microspheres, the columns that were formed did not prove to have an advantage over those that were unentrapped. Although affixing spheres within a matrix is known to have benefits in terms of bed stability over repeated use, the inclusion of a polymer coating proved to represent a greater concern for the availability of the bead-based stationary phases. Layers of polymer forming over the surface were shown to limit the access of analytes to the entrapped microspheres, restricting the usefulness of these materials.

The work with fluorous monoliths proved the most successful, providing clear evidence of improved selectivity when compared to analogs made without fluorination. Fluorous retention specificity was also effectively examined, with secondary effects probed and compared to those that had been discussed for commercially-available

fluorous microspheres. Results showed that the monoliths were very much in-line with what had already been seen for sphere-based systems, with residual substrate character providing only a slight contribution to the observed separations.

Finally, development of open-tubular columns based on microstructured optical fibers was the most speculative of the projects discussed here. The introduction of a fluorous stationary phase through silanization was demonstrated to be an effective method for imparting chromatographic selectivity into these columns, and controllable factors such as treatment protocol and silane character were shown to affect the performance of the resulting materials.

Co-Authorship

All research undertaken for this thesis was completed under the guidance of Dr. Richard Oleschuk. Some of the research presented in Chapter 3 was co-authored by Zhenpo Xu, while some of the research from Chapter 4 was co-authored by Ramin Wright. Portions of this thesis have been published in the following three papers:

Daley, A.B; Oleschuk, R.D. *J. Chromatogr., A* **2009,** *1216*, 772-780.

Daley, A.B.; Xu, Z.; Oleschuk, R.D. *Anal. Chem.* **2011,** *83*, 1688-1695.

Daley, A.B.; Wright, R.D.; Oleschuk, R.D. *Anal. Chim. Acta* **2011,** *690*, 253-262.

Acknowledgements

I would like to take this opportunity to acknowledge those who helped make this thesis possible, as their advice and support were invaluable in allowing me to reach this point. I would particularly like to thank my supervisor, Dr. Richard Oleschuk, for his guidance during the entirety of my time at Queen's, as well as all of the members of the "O" group (past and present) for their friendship, camaraderie and a number of useful discussions. I would also like to thank Dr. David Zechel and Dr. Philip Jessop for their participation as members of my supervisory committee, and Dr. Igor Kozin for his input in a variety of lab-related areas.

To my parents, friends and family who were all so supportive and encouraging during the entirety of this process, I must also extend my thanks. Having that kind of support was invaluable in completing this venture, and I couldn't have made it this far without you. Your contributions will not be forgotten.

Finally, I would like to acknowledge the Natural Sciences and Engineering Research Council of Canada, Walter C. Sumner Foundation, Queen's University, Government of Ontario, R.T. Mohan Graduate Scholarship and R.S. McLaughlin Fellowship for their provision of financial support throughout the duration of my project.

Statement of Originality

The work presented here represents the first known examination and characterization of organic polymer-entrapment conditions as applied to commercially-available fluorous microspheres. Additionally, it also introduces the preparation, characterization and optimization of acrylate-based fluorous monolithic materials for chromatography using fluorous interaction specificity; a topic that had previously been unexplored. Finally, the investigation of fluorous, silane-functionalized open-tubular liquid chromatography columns formed in microstructured optical fibers represents the first known application of these optical materials in a liquid-based, fluorous analytical separation.

Table of Contents

List of Tables

List of Figures

List of Abbreviations

1F-PO – diphenyl-[4-(1H,1H,2H,2H-perfluorodecyl)phenyl]phosphine oxide

2F-PO – bis[4-(1H,1H,2H,2H-perfluorooctyl)phenyl]phenylphosphine oxide

AIBN – azobisisobutyronitrile

BA – butyl acrylate

BDDA – 1,3-butanediol diacrylate

BME – benzoin methyl ether

CEC – capillary electrochromatography

DIOS – desorption/ionization on silicon

EA – ethyl acrylate

ESI – electrospray ionization

FBA – 1H,1H-heptafluorobutyl acrylate

FSPE – fluorous solid-phase extraction

GC – gas chromatography

HILIC – Hydrophilic interaction chromatography

HPLC – high performance liquid chromatography

I.D. – inner diameter

LC – Liquid chromatography

Log *P* – logarithm of octanol-water partition coefficient

MALDI – matrix-assisted laser desorption/ionization

MS – mass spectrometry

MSF – microstructured fiber

N1, N2, N3, N4 – Fluorous-tagged carbamate mixture with an N-substituted 4-nitro-benzyl group ($C_{17+x}H_{17}F_{2x+1}N_2O_4$; x=3, 4, 6 and 8; named N1, N2, N3, N4, respectively, according to increasing fluorous tag length)

NIMS – nanostructure-initiator mass spectrometry

NP – Normal phase

O.D. – outer diameter

OTLC – open-tubular liquid chromatography

P1, P2, P3, P4 – Fluorous-tagged carbamate mixture with an N-substituted 4-phenyl-benzyl group ($C_{23+x}H_{22}F_{2x+1}NO_2$; x=3, 4, 6 and 8; named P1, P2, P3, P4, respectively, according to increasing fluorous tag length)

PAH – polyaromatic hydrocarbon

PFP – pentafluorophenyl

PLOT – porous layer open-tubular

PPM – porous polymer monolith

R-FSPE – reverse fluorous solid-phase extraction

RP – Reverse phase

R_s – resolution

SEM – scanning electron microscopy

SD – standard deviation

SPE – solid-phase extraction

TFBDA – 2,2,3,3-tetrafluoro-1,4-butyl diacrylate

TFEA – 2,2,2-trifluoroethyl acrylate

THF – tetrahydrofuran

TMSPMA – 3-(trimethoxysilyl)propyl methacrylate

TPPO – triphenylphosphine oxide

UPLC – ultra-performance liquid chromatography

XIC – extracted ion current

Chapter 1: Introduction

1.1 – Fluorous Chemistry: One of the newer terms to be added to the chemical lexicon, fluorous chemistry came about predominantly as the result of an introductory paper by Horváth and Rábai in 1994.[1] Originally envisioned to mimic the use of the term aqueous, "fluorous" chemistry was proposed as a definition for any reactions or processes that preferentially occurred in a fluorocarbon phase rather than a conventional aqueous or organic medium. Although the distinct third phase presented by highly-fluorinated reaction components had long been known and employed,[2, 3] this was the first case of it being assigned a specific terminology to set it apart. This simple act of defining the fluorous medium opened the doors for a whole new realm of possibilities, and from there, the field that is now known as fluorous chemistry began to take shape.

With this new area for fluorinated species now delineated, the next logical step was to define the scope and breadth of the fluorous field. Just as every compound containing a carbon atom is not necessarily best defined as being an organic species, so too must distinctions be drawn as to what is and is not a fluorous compound. Curran and Gladysz (two of the more prominent names in the field) proposed the following definition for the term "fluorous":[4]

"Of, relating to, or having the characteristics of highly fluorinated saturated organic materials, molecules or molecular fragments. Or, more simply (but less precisely), 'highly fluorinated' or 'rich in fluorines' and based upon sp^3-hybridized carbon."

This broad definition strays from the original version of the term "fluorous", as it now encompasses a wide range of molecules and fragments that contain fluorine atoms as opposed to simply defining a reaction taking place in fluorinated media. As well, under

this new definition, many species that were once thought of as simply being highly- or perfluorinated-molecules are now more accurately defined as being fluorous compounds. Conversely, this definition also *excludes* many species that might otherwise be thought of as fluorous if it were not for the requirements of saturation and sp^3 hybridization. For example, perfluorinated aromatics are not considered to be fluorous because they will preferentially partition into certain organic phases rather than fluorous ones when both options are present.[4]

Related to the definition provided above, other terminology applied to the fluorous field can also be set out. Species that show a preference for a fluorous medium under a given set of parameters are said to be *fluorophilic*, while those that do not are considered *fluorophobic*. In addition, general reaction terminology such as tagging chemistry or separation processes can also be modified to give their fluorous equivalent (these fields will be discussed in more detail later), generating a broad range of systems, techniques and reactions that can be used in a fluorous capacity.

1.2 – Origin of the Fluorous Interaction: Although it has often been noted that compounds containing fluorine have a strong affinity for each other (the classic "like dissolves like" theory), a conclusive reason for the selectivity of this interaction has been difficult to isolate. Different groups have tried to classify the nature of the interaction, and although a number of mechanisms have been disproved, to this point no definitive explanation has been provided. Fluorous groups are more hydrophobic than hydrocarbons, yet in many cases columns made with fluorous stationary phases showed poorer retention and selectivity than conventional hydrocarbon-based columns for a wide variety of analytes (ruling out interactions based purely on hydrophobic character).[5-10] As an example, specific studies targeting lipophilic structures showed that they were better

retained on hydrocarbon materials than on the fluorous analogue, indicating that fluorous-fluorous selectivity must be distinct from lipophilic interactions.[11, 12]

As another potential avenue for determining the nature of the fluorous-fluorous interaction, it was suggested that when a mobile phase with elevated organic content is employed that a retention mechanism similar to the one seen for Hydrophilic Interaction Chromatography (HILIC) could result.[13] While some would argue that HILIC is just normal-phase (NP) chromatography (where analytes are eluted from a hydrophilic stationary phase using mobile phases with varied, non-polar organic content), HILIC is actually slightly more complex in the nature of the proposed mechanism.[14, 15] As with conventional NP separations HILIC uses an organic mobile phase to effect the elution of analytes, but also differs in that the addition of water to the mobile phase is believed to cause the formation of a thin aqueous layer at the surface of the stationary phase that can affect the analyte partitioning. Because this thin aqueous layer mimics the physical properties of the stationary phase, retention in these systems is believed to be more strongly influenced by their partitioning into the aqueous layer and less by their direct adsorption onto the stationary phase.[14] In the case of fluorous columns with elevated organic content in the mobile phase, the proof of concept used a series of basic analytes with varying compositions of organic solvent and aqueous buffer.[13] Unfortunately, the column that was chosen for the study was a pentafluorophenyl bonded phase, which is not actually fluorous under the classic definition. As such, the argument that relatively high concentrations of buffer cause fluorous columns to behave similarly to reverse-phase materials, while increasing the organic content changes the interaction to one that is reminiscent of an ion exchange material may not be indicative of what happens in a true

fluorous case. This means that although the study employs an interesting method, it cannot help to elucidate the mechanism behind selective fluorous-fluorous interactions.

Although not a purely fluorous interaction, studies on the dipole character of fluorous columns have yielded some of the most concrete data. Given that the electronegativity of fluorine is greater than that of carbon, the C-F bond is strongly polarized.[13] This can lead to increased interactions with aromatics through overlap of their extended π-electron systems with the electron density localized at fluorine, leading to greater selectivity for certain aromatic groups (more conjugated rings leads to better retention).[16] This adds another dimension to the use of fluorous columns, as they can be employed for selective aromatic speciation as well as conventional fluorous processes. Interestingly, polyfluorinated aromatics (which are not truly fluorous species) still show poor retention on fluorous columns even with π-type interactions considered, meaning that fluorous character is a greater determinant on sample selectivity than other possible characteristics.[11]

In a similar vein to these earlier dipole studies, another more recent publication also suggested that polarizability is at least part of the explanation for the fluorous interaction.[17] Affinity between poorly-polarizable fluorinated stationary phases and compounds that are rich in fluorine (which also have low polarizabilities as indicated by low refractive indices) are thought to have the potential to produce the "like-dissolves-like" interaction and desired selectivity, although despite this repetition of a similar theme, it still remains a theory rather than an accepted rule (the retention characteristics of fluorinated stationary phases still remain debateable, primarily as a result of the complexity of the interactions involved).[18, 19] Instead, the best that can currently be done is to provide guidelines that can be used to select molecules that are best equipped to take

advantage of fluorous interactions. Obviously, increasing the amount of fluorine in a molecule should make it more fluorous (so long as it is done in a manner that satisfies the requirements for a structure to be classified as fluorous),[19, 20] but the overall nature of the structure itself can also play a pivotal role. The number of functional groups appended to a structure (fluorous or otherwise) can limit the capacity for intermolecular interactions through steric crowding or inductive effects, potentially reducing fluorous interactions in the process.[19] The way that fluorine atoms are laid out in a structure also plays an important role, since branched structures will not necessarily have the same capability for fluorous interactions as straight-chains do. This makes knowledge of the structures being studied crucial, as different isomers have the potential to exhibit varied fluorous interactions with the same material under otherwise identical separation conditions. Sadly, this level of uncertainty is more often the rule than the exception when it comes to understanding the cause of fluorous interactions, and the mechanism behind the chemistry still requires more study before it can truly hope to be understood.[18]

1.3 – Initial Applications: Fluorous Biphasic Systems: In the original paper by Horváth and Rábai, their purpose was to develop an improved system for the hydroformylation of olefins using the distinct properties of the fluorous phase.[1] Although their specific example employed a modified rhodium catalyst, the same principles could be used for essentially any catalytic species that can be adequately fluorinated by the addition of highly fluorous tags. These tags (used to impart fluorous character on an otherwise metallic or organic species) are generally straight-chain hydrocarbonaceous groups with all of their hydrogen replaced by fluorine. Helping with the attachment chemistry, the fluorous chains are appended to a group with a high degree of selectivity for the target of the tag (e.g. amine, thiol, etc.), making it easier to achieve the needed reactivity. To

prevent the highly electron-withdrawing character of the perfluorinated chains from altering the chemistry of the functional end of the tag, a spacer group (usually comprised of two methylenes) is placed between the fluorous and reactive groups to limit the inductive effects.[1] Depending on the length of the tag, the attached groups are sometimes referred to as "ponytails" in the literature (less than 6 fully-fluorinated sp^3 carbons = tag, more than 6 = ponytail),[4] although this is mostly a naming convention. It is also common to think of ponytails as being permanent attachments to molecules while tags are groups that will ultimately be removed from the substrate, although even then the terms are still used interchangeably by many authors. Regardless of the nomenclature the purpose remains the same, as these groups add fluorous character to the desired targets such that they can be effectively used in biphasic reactions.

Fluorous biphasic chemistry is essentially a variant of heterogeneous catalysis, whereby a fluorous-tagged catalyst is suspended in a fluorocarbon phase while the other components of the reaction start in a second (aqueous or organic) phase.[21] Reaction normally occurs at the interface between these phases, with the catalyst predominantly remaining in the fluorous phase while the desired products prefer the second. This segregation allows for facile recycling of the catalyst from the fluorous phase after the reaction is complete, while the products can also be extracted from their preferred medium. Similarly, another possible reaction can occur if the reagents are sufficiently fluorophilic to enter the fluorous phase. Here, catalysis will take place in the fluorinated medium (rather than at the interface), but at the same time, the reaction will be designed such that the products will be fluorophobic. This means that they should selectively partition back into the second phase, leaving predominantly the reactive components in the fluorous medium. As with the interface-based process this type of reaction facilitates

the isolation of products, because they should largely be focused in the second liquid phase. Similarly, the catalyst can also be reused in these types of reactions, as it should remain almost exclusively in the fluorous phase after the reaction is complete.

A third possible option exists for biphasic systems that can be forced to become a single phase under the application of outside forces. Frequently, heat or pressure can be employed to cause a two-phase system to temporarily mix into a single phase, allowing the desired reaction to take place in the homogeneous state. When the outside force is removed, the two-phase system is quickly regenerated and the products can then be extracted.[22] Although this type of process requires the knowledge of which phase the products will ultimately choose after the reaction (fluorous or secondary) so that they can be recovered, it also provides some of the greatest control over specificity since reactions can essentially be started and stopped by the application of the outside factor. These "switchable" systems are therefore a powerful tool for fluorous chemistry, as they add an even greater degree of control to a process that is already quite selective between the fluorous and secondary phases.[21]

Fluorous biphase chemistry is not limited to catalyst modifications, as reagents can also be rendered fluorous to effect the desired reactions.[23-27] The same ideals as before hold, with the fluorous component allowing selective separation. Depending on where the tag is placed, it will sometimes become a part of the product, while in others it only serves to force the reaction through a particular intermediate and is later removed. Both options are equally effective, with the only difference coming in the phase that the product inhabits upon completion of the reaction (fluorous or secondary).

1.4 – Light versus Heavy Fluorous Tags: Depending on the relative number of fluorine atoms in a tag, as well as the relative mass of the tag in relation to the molecular weight of

the compound, a distinction can be drawn between "light" and "heavy" fluorous groups. In essentially all of the early work done with biphasic systems, fluorous tags contained excessively large numbers of fluorine atoms (60-120) to force selective partitioning into the fluorous phase and ensure the desired specificity. This type of process became known as "Heavy Fluorous Synthesis" (as a result of the inherently bulky fluorous groups), and formed the basis of many of the techniques that have been discussed through the years.[22, 28, 29] Unfortunately, as a result of this highly fluorous character, the tagged molecules have effectively no solubility in aqueous and organic solvents, limiting their broader applicability. As well, with increasing concerns over the persistence of fluorinated substances in the environment and the potential effects therin,[30] techniques requiring large volumes of highly fluorinated liquids have become less and less popular if they can be replaced by more environmentally-friendly processes.

As a novel alternative to the heavy fluorous process, Curran and Luo introduced the concept of "Light Fluorous Synthesis" in a paper published in 1999.[31] Here, the size of the tag is drastically decreased, giving the labelled compound a much greater miscibility with organic media. While this increases the number of reactions that the tagged compound can undergo (it is no longer limited to just the fluorous domain), the trade-off is a marked decrease of the solubility in fluorous media. This eliminates the liquid-liquid separation specificity that had originally defined fluorous biphasic systems, meaning that new methods to force partitioning of the fluorous groups would be needed.

One such method is solid-phase extraction (SPE), which mimics conventional column chromatography in its separation mechanism, and can be used to differentiate between species with widely different retention values on the same solid support.[32] After loading a mixture of samples onto a SPE column, two distinct washing solvents can be

used in sequence to elute the different types of compounds (one class of samples in each fraction), which in turn gives the desired separation when the fractions are analyzed. Obviously, the unique characteristics of fluorous molecules should place them in a distinct class that is separate from other organic species, making SPE a logical method to achieve their fractionation from complex mixtures. One caveat to this idea is that the unique fluorous properties should be imparted onto the target structure with a minimal number of fluorine groups in the tag (the "light" fluorous component),[31] as otherwise, the tagged species would still be in the "heavy" classification and be quite difficult to mix with organic components for reaction chemistry and any subsequent workup.

As briefly mentioned earlier, the general distinction that has been proposed to determine whether a compound is classified as light or heavy is based on the number and relative percentage of fluorine atoms in the structure. Typically, a structure that contains more than 60% fluorine atoms (by molecular weight) is considered to be in the heavy classification, while those that are less than 40% fluorine by molecular weight, or contain less than 21 total fluorine atoms (regardless of size) fall into the light grouping.[29] Structures in the intermediate range of percentages (41-59% fluorine) are difficult to classify one way or the other, depending instead on the presence or absence of other functional groups to dictate the physical characteristics (e.g. polar functional groups would increase organic character at the expense of fluorous).[31]

This system for deciding between light and heavy classification has been widely adopted in the literature, with many occurrences where it is cited as the determining factor in a specific classification scheme.[11, 19, 24, 25, 27, 32-34]

1.5 – Fluorous Solid-Phase Extraction (FSPE): Silica gel with a fluorocarbon bonded-phase (i.e. "fluorous" silica gel) was actually known in the literature well before the

advent of fluorous chemistry and light fluorous reactions. Berendsen et al. reported on the unique liquid chromatography (LC) properties of a highly fluorinated bonded phase for reverse-phase separations almost 30 years ago,[35] sparking an initial surge of papers investigating the chromatographic behaviour of these materials.[5-10, 36-38] Some of these investigations were actually the first to note that fluorinated phases exhibit preferential interactions with analytes containing fluorine,[35-38] using the columns to separate fluorinated molecules from other organics, and to separate groups of fluorinated species by their relative fluorine content (more fluorine equalled longer retention on-column). While it would later be proven that these fluorous-fluorous separations were the true niche for fluorinated silica gel, a majority of the initial studies instead chose to use it for its strongly hydrophobic character as a variant on typical reverse-phase (RP) chromatographic beds.[5-10] The results from these experiments proved to be less than stellar in many cases (no improvement over conventional RP phases), and may have led to the lack of research on fluorous bonded-phases for a good number of years.

The renaissance for fluorous silica gel came in the form of light fluorous chemistry, which as mentioned earlier, requires the use of a SPE column to recover the tagged components from a reaction mixture. The strong nature of fluorous-fluorous interactions makes fluorinated silica gel preferable to essentially all other bonded-phases for these types of recoveries, giving a new life to the material. Initially, groups were forced to functionalize their own silica gel with fluorous groups,[8, 34-37, 39] arising from the lack of viable commercial sources of the needed materials (while many distributors had pentafluorophenyl (PFP) bonded phase columns for either SPE or LC applications, these are not truly fluorous based on their aromatic nature). At this time, the silica gel and related SPE were both commonly referred to as "fluorous reverse-phase" processes,

owing to their perceived similarities to the non-polar interactions that define RP chemistry. Although this was later decided to be a misnomer (since fluorine-fluorine interactions are distinct from those that take place in conventional RP materials), some groups still maintain the use of the reverse-phase designation in addition to the fluorous label in their publications.[12, 40]

Fluorous bonded-phases of the correct design (straight-chain or branched polyfluorinated hydrocarbons) are now commercially available from retailers like Fluorous Technologies and Silicycle, giving the field of FSPE a much more consistent source of materials. As well, standard protocols for the use of FSPE have been developed, helping to make the process much more universal.[22, 25, 27, 29, 32, 41-44] Typically, a sample is initially loaded onto the FSPE column, and any contaminants and undesired components are removed with a fluorophobic wash. This usually consists of an organic solvent with a relatively high aqueous content (greater than 20% aqueous is "high" for fluorous materials), allowing for the broad removal of organic compounds and contaminants like salts, while leaving fluorous components retained on the column. Afterwards, the desired fraction is recovered from the column with a second (fluorophilic) wash. Because essentially all of the interfering species have previously been removed, the solvent used for the fluorophilic wash can actually be a simple organic liquid with a high affinity for fluorous compounds (e.g. acetonitrile, methanol, etc.) rather than a fluorous solvent as might be expected. This makes the entire FSPE process quite attractive, as it is selective, efficient and simple, and also uses readily available solvents as opposed to the fluorous liquids that were needed in biphasic separations.

1.6 – Competition for FSPE: As with most techniques, researchers are always looking for alternate options that improve upon the process. Separation by FSPE is no different,

and although it currently sets the benchmark for fluorous isolation and purification, if a technique that is faster, more selective, or more efficient could be found it would quickly supplant it as the new method of choice. Although reverse-phase chromatography can be used to separate fluorous species on the basis of their polarity, it is hardly selective enough to compete with FSPE (especially in cases where the compounds contain a similar number of fluorine atoms such that their polarities cannot easily be differentiated). As a result, any new methods that are proposed must make use of an interaction that is equally selective when compared to the fluorous interaction if they hope to be competitive.

Although not a truly "new" technique, the method of reverse fluorous solid-phase extraction (R-FSPE) provides an interesting variant on the conventional FSPE process.[45] Not to be confused with fluorous reverse-phase processes (which are just another way of describing fluorous techniques based on their perceived similarities to RP separations), R-FSPE is an inversion of conventional FSPE in that it uses regular silica gel with a fluorous elution solvent to separate the fluorinated components from a reaction medium while leaving the undesired components retained on the column. This technique is actually reminiscent of fluorous biphasic systems in that regard (with the same associated environmental concerns regarding the use of fluorous solvents), possibly explaining why it has not been widely adopted as an extraction technique (only a few citations for this method were noted in a recent review of fluorous separations).[43, 46] Still, despite these concerns, R-FSPE does represent a legitimate competitor to FSPE in terms of fluorous separation selectivity. Should better solvent options present themselves, R-FSPE could easily expand into a much more important application for fluorous chemical analysis.

Another possible method to retain fluorous species is through the use of β-cyclodextrin columns. Stemming from a study of relative inclusion of hydrocarbon and

fluorocarbon analogues within cyclodextrins,[47] the idea was later revised and applied to the creation of SPE columns for selective fluorous separation.[48] Although it was initially reported that these new columns were superior to fluorous columns on account of their improved separation of compounds with differing fluorous tag lengths, proponents of the fluorous method were quick to issue a rebuttal. Their primary criticism of the study on the cyclodextrin columns was that all of the separated compounds were identical, differing only in the length of the fluorous tags in the series. It was therefore argued that since fluorine is also hydrophobic, simply increasing the amount of it in a series of tags should allow a number of different types of columns to separate that series on account of the differences in polarity (totally independent of fluorous effects).[49] It was also noted that no tests were done in the absence of fluorous tags to verify whether there was actually a selective interaction between the cyclodextrin and fluorine, thereby hurting the argument for a specific separation. Although these arguments would appear to be quite damaging, β-cyclodextrin columns have still managed to find a niche in the fluorous field. Mixtures that contain only very short fluorous tags (C_3F_7 or less) and require rapid separation,[50] as well as chiral fluorous molecules[51, 52] have been successfully separated by β-cyclodextrin columns. As well, because these columns are actually quite selective for hydrocarbonaceous compounds as well as for fluorous,[49] they can sometimes be used as general-purpose substrates for separations that need to be run under a variety of different conditions (fluorous, reverse-phase, and normal-phase).[53]

1.7 – Proteomic Applications of FSPE: No good technique is without applications, and FSPE is rapidly starting to find a role in a number of different analyses. Although many such applications are conventional organic reactions modified to make use of fluorous-tagged substrates as mentioned earlier,[23-27, 29] one of the newer uses involves fluorous tags

in biochemical processes to improve proteomic applications (studies devoted to the structure, function, and interaction of proteins).[27, 54-58] Because these techniques deal with very small sample volumes that are frequently derived from complex biological matrices, separation efficiency and capacity for selective purification are at a premium. A typical proteomic analysis involves the initial step of tagging a selected peptide or protein with a marker that can be easily recognized, allowing the desired component to later be identified. After a series of analysis-specific steps (e.g. digestion, coupling, etc.) the desired component can be identified by looking for the tag (usually via mass spectrometry or fluorescence), allowing any changes to the structure that occurred during the analysis to be determined. Conventional labels for proteomic studies make use of either metal affinity or biochemical interactions (biotin-streptavidin is a common pair) to isolate the desired component,[54] although these species are also known to suffer from additional non-specific interactions such that they are not considered "optimal". The cost of these reagents is also somewhat inhibitory, so a more economical option that still allows a high degree of selectivity is widely desired.

In a paper published in 2005, Brittain et al. introduced the novel concept of fluorous affinity tags for proteomic analysis.[54] Here, fluorous reagents designed to selectively label specific amino acid residues in a biological sample were employed to effect their separation. This process greatly improved upon conventional labelling techniques in proteomic studies, as the unique and highly selective fluorous interactions allowed for very specific recovery of the tagged analytes without additional interferences. As well, the growing range of commercially-available fluorous reagents will allow for compound-specific reaction chemistries to be employed in many cases, further improving the specificity of the process.

Although it would not be fair to say that this technique has reached widespread popularity in the years since its introduction, it *has* already been applied successfully to the specific fractionation of individual amino acids,[56] oligonucleotides,[55] and peptides.[57, 58] The primary factor limiting the further growth of fluorous affinity methods is the lack of a true online coupling medium for FSPE with an analysis method like mass spectrometry (MS), limiting the ability for high-throughput proteomics. Currently, most reported applications perform FSPE as an initial step, later using electrospray ionization (ESI),[59] matrix-assisted laser desorption/ionization (MALDI),[60-63] desorption/ionization on silica (DIOS),[64-66] or nanostructure-initiator mass spectrometry (NIMS)[67] to perform analysis in an offline manner. Should an online coupling method for FSPE with MS become commercially available, it would greatly enhance the popularity of the technique as it would provide the high-throughput method for rapid proteomic analysis that many groups in the field desire.

1.8 – Fluorous Chromatography: Sharing many similarities with FSPE (they are mechanistically identical, taking advantage of fluorous silica gel to achieve separations; *vide supra*), fluorous chromatography also has the distinct benefit of online coupling with detectors that can take advantage of its specificity to allow even more complicated analyses to be introduced (it is no longer limited by having to collect fractions in an offline fashion).[68, 69] In the case of liquid chromatography (LC), it also allows for more involved pumping systems to be introduced (both in isocratic and gradient-elution modes), which in-turn greatly facilitates switching between fluorophobic and fluorophilic solvent compositions to allow a greater degree of control over the elution of any species (fluorous or otherwise) that are retained on the column. While many of the earliest publications in the area of fluorous stationary phases alluded to the potential usefulness of

columns of this type for separations involving fluorinated analytes,[35-38] it strangely remains an under-represented area of research in the literature even to this day. While this can partially be attributed to the lack of commercially-available materials for a great number of years, the recent growth in the realm of LC column development now means that most major manufacturers offer materials with perfluorinated bonded phases that can be used for proper fluorous separations. That aside then, it would seem that other reasons must now be behind the lack of discussion with respect to fluorous LC separations. When you also consider the potential that integrated fluorous LC systems would seem to offer in proteomic applications (eliminating many of the aforementioned issues), it becomes even more puzzling that there has not been more work dedicated to expanding this area.

1.9 – Chromatographic Columns: When designing columns for chromatography, there are three primary means of fabrication currently in use: traditional columns packed with spherical stationary phase materials (as discussed for the fluorous case), continuous rods of chromatographic materials (monolithic columns; see Chapter 3), and hybrid columns combining particulate materials and a continuous phase (entrapped microsphere columns; Chapter 2).[70-72] Since it is not reasonable to try and compare these different methods in a purely qualitative sense, two parameters have been defined as quantitative measures of column effectiveness: plate height (H), and number of theoretical plates (N). These terms arise from historical use; developed in the 1920's as a method of describing separations on a fractional distillation column (which contains a series of plates at different heights), and effectively explain the Gaussian nature of chromatographic peaks.[73] Although they have no significance for current chromatographic techniques in terms of the way the methods are now performed (the old system assumed equilibrium conditions throughout a column, which makes no sense for a dynamic process like liquid chromatography), the

terminology has been retained for nostalgic reasons. Fortunately, the N and H parameters have also been described by a series of equations that allow efficiency to be quantified (including the *van Deemter* equation), permitting different columns to be compared in a more specific manner.[74]

The width of a peak in a chromatogram (w) can be expressed as a time value if the difference between the first and last signs of elution (the shoulders of the peak) is taken. The retention time of the peak (t_R) can then be calculated as the midpoint of these two times, giving the second required parameter. Using these two values, N can be calculated as follows:

$$N = 16\left(\frac{t_R}{w}\right)^2 \tag{1}$$

From here, the value for the plate height can also be calculated using Equation 2 if the length of the chromatographic column (L; usually in centimeters) is known.

$$N = L/H \tag{2}$$

Large numbers of theoretical plates and small theoretical plate heights are the desired results for efficient columns. Band broadening is a primary concern, with broad signals causing an increase in the value of w, lowering N, increasing H, and drastically reducing column efficiency. The primary factors contributing to this band broadening are summarized below in the classic *van Deemter* equation:

$$H = A + B/u + (C_s + C_M)u \tag{3}$$

A (The Multipath Term) refers to the number of paths analytes moving through a porous column can choose to follow and is sometimes called the "eddy diffusion" parameter.

B (Longitudinal Diffusion Term) defines the spreading of a narrow plug of analyte towards and away from the direction of flow within the mobile phase.

u (Linear Velocity of the Mobile Phase) affects the length of time that analytes in the mobile phase remain in contact with the stationary phase.

C_s (Stationary Phase Mass-Transfer) defines the equilibration time required between analytes in the mobile phase and the stationary phase material.

C_M (Mobile Phase Mass-Transfer) is mostly related to the diffusion coefficient of the analytes in the mobile phase, with smaller stationary phase particles helping to improve this term.

To summarize then, easily controllable factors for dealing with band broadening include the diameter of the stationary phase particles, as well as the diameter of the column itself. Decreasing both can greatly improve column efficiency and generate better separations, although this can also lead to increased pressure and resistance to flow that can become problematic. Similarly, increasing the length of the column can improve the number of theoretical plates, as can reducing the flow rate of the mobile phase. As such then, careful control over all of these parameters is ideally required to produce the most effective separations in any column of choice.

1.10 – Further Expansion of Fluorous Separation Techniques: Proteomics aside, there are also a number of other applications starting to appear in the literature that take advantage of fluorous techniques to achieve a variety of unique goals.[75] For example, modification of poly(dimethylsiloxane) with fluorinated groups has recently been undertaken,[76, 77] with the effects on the surface of the material and potential applications derived thereof being explored. Alternatively, another group has looked at the ability to introduce fluorous tags in natively-fluorescent species,[78] introducing a separation handle to use in tandem with the detection capabilities conferred by the native structure. They feel that this holds great potential in the realm of LC quantification, although in principle,

it (and the surface modification studies as well) still remain conceptually similar to FSPE in their design and use for isolating species with fluorous labels (either native or otherwise introduced).

Interestingly, even with these applications in mind, it is still surprising to note the comparative lack of chromatographic studies that seek to take advantage of fluorous affinity relative to other separation modes. With microsphere-based columns already presenting a well-developed avenue for fluorous separations (*vide supra*), it does not seem likely that technology is the issue. Perhaps then, it is more a question of versatility that is hindering the use of fluorous chromatography. Not all applications are suited to the use of packed columns for separation/isolation, and with the growing trend toward system miniaturization and lab-on-a-chip technologies replacing the larger volumes of conventional LC columns,[79-81] it is conceivable that fluorous separations have simply not adapted to meet the needs of this new regime. Small channels and unique geometries (such as those in most integrated microfluidic chips) do not always lend themselves to the facile packing of microspheres,[82-85] so if fluorous phases remain largely confined to silica particles (or liquids) as they have been in the past, then they simply will not be useful in a large portion of these new analytical devices and will lead to researchers using other methods. Adding in the concerns with the understanding of the mechanism behind fluorous affinity might also lead to a certain degree of hesitation, which in turn could cause a trend toward the use of better-understood columns and methods rather than exploring the potential that fluorous columns might provide. The sum of these factors could at least partially explain the lack of attention fluorous chromatography columns receive, and fortunately, they are also easily corrected given the proper motivation

1.11 – Objectives: With these factors in mind then, the goal of my research has been to expand the scope of fluorous chromatography through the exploration of new stationary phase materials. In cases where microspheres are still employed, void formation that can arise during the lifetime of their usage remains a concern. One way that this can potentially be alleviated is through the use of entrapment; bonding the spheres in a particular alignment to prevent any unwanted motion. Alternatively, while microspheres still comprise the majority of columns that are used today, porous polymer monoliths and open tubes with thin layers of stationary phase both represent viable alternatives to be explored. These two methods completely eliminate particles (and their associated issues) rather than trying to circumvent them, meaning that they also have advantages in newer applications where microsphere use is not desirable or practical.

In terms of my research, it has been focused on taking these three main areas (microsphere entrapment, monoliths and open tubes) and applying them to the fluorous domain. By exploring these new varieties of fluorous stationary phase, the goal was to expand the usefulness of fluorous chromatography. Ideally this will ultimately lead to a wider implementation of the technique in analytical applications, as it has been well-documented that fluorous techniques are desirable if their limitations can be overcome (*vide supra*). Additionally, through the exploration of these new fluorous stationary phases, it presents the opportunity to examine the specificity of the fluorous interaction in these materials. This in turn allows for a discussion on their similarity to existing fluorous phases, as well as a wider examination of the interaction as a whole and its usefulness in an array of analytical situations.

1.12 – References

(1) Horvath, I. T.; Rabai, J. *Science* **1994**, *266*, 72-75.

(2) Simons, J. H.; Block, L. P. *J. Am. Chem. Soc.* **1937**, *59*, 1407.

(3) Grosse, A. V.; Cady, G. H. *Ind. Eng. Chem.* **1947**, *39*, 367-374.

(4) Gladysz, J. A.; Curran, D. P. *Tetrahedron* **2002**, *58*, 3823-3825.

(5) Haas, A.; Koehler, J.; Hemetsberger, H. *Chromatographia* **1981**, *14*, 341-344.

(6) Xindu, G.; Carr, P. W. *J. Chromatogr.* **1983**, *269*, 96-102.

(7) Sadek, P. C.; Carr, P. W. *J. Chromatogr.* **1984**, *288*, 25-41.

(8) Bicking, M. K. L.; Bicking, M. L.; Longman, W. E. *Anal. Chem.* **1986**, *58*, 499-501.

(9) Sadek, P. C.; Carr, P. W.; Ruggio, M. J. *Anal. Chem.* **1987**, *59*, 1032-1039.

(10) Danielson, N. D.; Beaver, L. G.; Wangsa, J. *J. Chromatogr.* **1991**, *544*, 187-199.

(11) Andrushko, V.; Schwinn, D.; Tzschucke, C. C.; Michalek, F.; Horn, J.; Moessner, C.; Bannwarth, W. *Helv. Chim. Acta* **2005**, *88*, 936-949.

(12) Beller, C.; Bannwarth, W. *Helv. Chim. Acta* **2005**, *88*, 171-179.

(13) Euerby, M. R.; McKeown, A. P.; Petersson, P. *J. Sep. Sci.* **2003**, *26*, 295-306.

(14) Alpert, A. J. *J. Chromatogr.* **1990**, *499*, 177-196.

(15) Strege, M. A. *Anal. Chem.* **1998**, *70*, 2439-2445.

(16) Yamamoto, F. M.; Rokushika, S. *J. Chromatogr., A* **2000**, *898*, 141-151.

(17) Marchand, D. H.; Croes, K.; Dolan, J. W.; Snyder, L. R.; Henry, R. A.; Kallury, K. M. R.; Waite, S.; Carr, P. W. *J. Chromatogr., A* **2005**, *1062*, 65-78.

(18) Wang, Y.; Harrison, M.; Clark, B. J. *J. Chromatogr., A* **2006**, *1105*, 77-86.

(19) Kiss, L. E.; Kovesdi, I.; Rabai, J. *J. Fluorine Chem.* **2001**, *108*, 95-109.

(20) Narang, P.; Colon, L. A. *J. Chromatogr., A* **1997**, *773*, 65-72.

(21) Horvath, I. T. *Acc. Chem. Res.* **1998**, *31*, 641-650.

(22) Gladysz, J. A.; Curran, D. P.; Horvath, I. T., Eds. *Handbook of Fluorous Chemistry*; Wiley-VCH: Weinheim, Germany, 2004.

(23) Studer, A.; Jeger, P.; Wipf, P.; Curran, D. P. *J. Org. Chem.* **1997**, *62*, 2917-2924.

(24) Curran, D. P. *Pure Appl. Chem.* **2000**, *72*, 1649-1653.

(25) Curran, D.; Lee, Z. *Green Chem.* **2001**, *3*, G3-G7.

(26) de Visser, P. C.; van Helden, M.; Filippov, D. V.; van der Marel, G. A.; Drijfhout, J. W.; van Boom, J. H.; Noort, D.; Overkleeft, H. S. *Tetrahedron Lett.* **2003**, *44*, 9013-9016.

(27) Dandapani, S. *QSAR Comb. Sci.* **2006**, *25*, 681-688.

(28) Bergbreiter, D. E.; Franchina, J. G.; Case, B. L. *Org. Lett.* **2000**, *2*, 393-395.

(29) Ubeda, M. A.; Dembinski, R. *J. Chem. Educ.* **2006**, *83*, 84-92.

(30) Schultz, M. M.; Barofsky, D. F.; Field, J. A. *Environ. Sci. Technol.* **2006**, *40*, 289-295.

(31) Curran, D. P.; Luo, Z. *J. Am. Chem. Soc.* **1999**, *121*, 9069-9072.

(32) Curran, D. P. *Synlett* **2001**, 1488-1496.

(33) Zhang, Q.; Luo, Z.; Curran, D. P. *J. Org. Chem.* **2000**, *65*, 8866-8873.

(34) Jenkins, P. M.; Steele, A. M.; Tsang, S. C. *Catal. Commun.* **2003**, *4*, 45-50.

(35) Berendsen, G. E.; Pikaart, K. A.; De Galan, L.; Olieman, C. *Anal. Chem.* **1980**, *52*, 1990-1993.

(36) Billiet, H. A. H.; Schoenmakers, P. J.; De Galan, L. *J. Chromatogr.* **1981**, *218*, 443-454.

(37) Krafft, M. P.; Jeannaux, F.; Le Blanc, M.; Riess, J. G.; Berthod, A. *Anal. Chem.* **1988**, *60*, 1969-1972.

(38) Hirayama, C.; Ihara, H.; Nagaoka, S.; Hamada, K. *J. Chromatogr.* **1989**, *465*, 241-248.

(39) Curran, D. P.; Hadida, S.; He, M. *J. Org. Chem.* **1997**, *62*, 6714-6715.

(40) Glatz, H.; Blay, C.; Engelhardt, H.; Bannwarth, W. *Chromatographia* **2004**, *59*, 567-570.

(41) Zhang, W.; Curran, D. P.; Chen, C. H.-T. *Tetrahedron* **2002**, *58*, 3871-3875.

(42) Zhang, W.; Lu, Y.; Nagashima, T. *J. Comb. Chem.* **2005**, *7*, 893-897.

(43) Zhang, W.; Curran, D. P. *Tetrahedron* **2006**, *62*, 11837-11865.

(44) Zhang, W.; Lu, Y. *J. Comb. Chem.* **2006**, *8*, 890-896.

(45) Matsugi, M.; Curran, D. P. *Org. Lett.* **2004**, *6*, 2717-2720.

(46) Del Pozo, C.; Keller, A. I.; Nagashima, T.; Curran, D. P. *Org. Lett.* **2007**, *9*, 4167-4170.

(47) Wilson, L. D.; Verrall, R. E. *J. Phys. Chem. B.* **1997**, *101*, 9270-9279.

(48) Matsuzawa, H.; Mikami, K. *Synlett* **2002**, 1607-1612.

(49) Curran, D. P.; Dandapani, S.; Werner, S.; Matsugi, M. *Synlett* **2004**, 1545-1548.

(50) Mikami, K.; Matsuzawa, H.; Tekeuchi, S.; Nakamura, Y.; Curran, D. P. *Synlett* **2004**, 2713-2716.

(51) Matsuzawa, H.; Mikami, K. *Tetrahedron Lett.* **2003**, *44*, 6227-6230.

(52) Nakamura, Y.; Takeuchi, S.; Okumura, K.; Ohgo, Y.; Matsuzawa, H.; Mikami, K. *Tetrahedron Lett.* **2003**, *44*, 6221-6225.

(53) Mikami, K.; Tonoi, T.; Matsuzawa, H. *QSAR Comb. Sci.* **2006**, *25*, 766-768.

(54) Brittain, S. M.; Ficarro, S. B.; Brock, A.; Peters, E. C. *Nat. Biotechnol.* **2005**, *23*, 463-468.

(55) Pearson, W. H.; Berry, D. A.; Stoy, P.; Jung, K.-Y.; Sercel, A. D. *J. Org. Chem.* **2005**, *70*, 7114-7122.

(56) Hu, G.; Lee, J. S. H.; Li, D. *J. Colloid Interface Sci.* **2006**, *301*, 697-702.

(57) Yoder, N. C.; Yueksel, D.; Dafik, L.; Kumar, K. *Curr. Opin. Chem. Biol.* **2006**, *10*, 576-583.

(58) Go, E. P.; Uritboonthai, W.; Apon, J. V.; Trauger, S. A.; Nordstrom, A.; O'Maille, G.; Brittain, S. M.; Peters, E. C.; Siuzdak, G. *J. Proteome Res.* **2007**, *6*, 1492-1499.

(59) Manisali, I.; Chen, D. D. Y.; Schneider, B. B. *Trends Anal. Chem.* **2006**, *25*, 243-256.

(60) Zenobi, R.; Knochenmuss, R. *Mass Spectrom. Rev.* **1999**, *17*, 337-366.

(61) Jagtap, R. N.; Ambre, A. H. *Bull. Mater. Sci.* **2005**, *28*, 515-528.

(62) Knochenmuss, R. *Analyst* **2006**, *131*, 966-986.

(63) Ying, W.; Perlman, D. H.; Li, L.; Theberge, R.; Costello, C. E.; McComb, M. E. *Rapid Commun. Mass Spectrom.* **2009**, *23*, 4019-4030.

(64) Wei, J.; Buriak, J. M.; Siuzdak, G. *Nature* **1999**, *399*, 243-246.

(65) Lewis, W. G.; Shen, Z.; Finn, M. G.; Siuzdak, G. *Int. J. Mass Spectrom.* **2003**, *226*, 107-116.

(66) Trauger, S. A.; Go, E. P.; Shen, Z.; Apon, J. V.; Compton, B. J.; Bouvier, E. S. P.; Finn, M. G.; Siuzdak, G. *Anal. Chem.* **2004**, *76*, 4484-4489.

(67) Northen, T. R.; Lee, J.-C.; Hoang, L.; Raymond, J.; Hwang, D.-R.; Yannone, S. M.; Wong, C.-H.; Siuzdak, G. *Proc. Natl. Acad. Sci. U. S. A.* **2008**, *105*, 3678-3683.

(68) Zhang, W. *J. Fluorine Chem.* **2008**, *129*, 910-919.

(69) Xiao, N.; Yu, Y. B. *J. Fluorine Chem.* **2010**, *131*, 439-445.

(70) Xie, R.; Oleschuk, R. *Electrophoresis* **2005**, *26*, 4225-4234.

(71) Xie, R.; Oleschuk, R. *Anal. Chem.* **2007**, *79*, 1529-1535.

(72) Gibson, G. T. T.; Koerner, T. B.; Xie, R.; Shah, K.; de Korompay, N.; Oleschuk, R. D. *J. Colloid Interface Sci.* **2008**, *320*, 82-90.

(73) Skoog, D. A.; West, D. M.; Holler, F. J., Eds. *Fundamentals of Analytical Chemistry*, 7th ed.; Saunders College Publishing: Fort Worth, 1996.

(74) Skoog, D. A.; Holler, F. J.; Nieman, T. A., Eds. *Principles of Instrumental Analysis*, 5th ed.; Harcourt Brace College Publishers: Orlando, Florida, 1998.

(75) Zhang, W.; Cai, C. *Chem. Commun.* **2008**, 5686-5694.

(76) Wang, D.; Oleschuk, R. D.; Horton, J. H. *Langmuir* **2008**, *24*, 1080-1086.

(77) Wang, D.; Douma, M.; Swift, B.; Oleschuk, R. D.; Horton, J. H. *J. Colloid Interface Sci.* **2009**, *331*, 90-97.

(78) Sakaguchi, Y.; Yoshida, H.; Todoroki, K.; Nohta, H.; Yamaguchi, M. *Anal. Chem.* **2009**, *81*, 5039-5045.

(79) Ohno, K.-i.; Tachikawa, K.; Manz, A. *Electrophoresis* **2008**, *29*, 4443-4453.

(80) Faure, K. *Electrophoresis* **2010**, *31*, 2499-2511.

(81) Mark, D.; Haeberle, S.; Roth, G.; von Stetten, F.; Zengerle, R. *Chem. Soc. Rev.* **2010**, *39*, 1153-1182.

(82) Oleschuk, R. D.; Shultz-Lockyear, L. L.; Ning, Y.; Harrison, D. J. *Anal. Chem.* **2000**, *72*, 585-590.

(83) Ehlert, S.; Kraiczek, K.; Mora, J.-A.; Dittmann, M.; Rozing, G. P.; Tallarek, U. *Anal. Chem.* **2008**, *80*, 5945-5950.

(84) Jemere, A. B.; Martinez, D.; Finot, M.; Harrison, D. J. *Electrophoresis* **2009**, *30*, 4237-4244.

(85) Trusch, M.; Ehlert, S.; Bertsch, A.; Kohlbacher, O.; Hildebrand, D.; Schlueter, H.; Tallarek, U. *J. Sep. Sci.* **2010**, *33*, 3283-3291.

Chapter 2: Entrapped Microsphere Column Development

2.1 - Introduction

2.1.1 – Packed Chromatographic Columns: The most common choice that is currently available for chromatography is a column that is packed with a particulate stationary phase. A wide variety of methods exist for introducing this stationary phase into the column,[1] although for general ease of use, the classic slurry-packing method requires the least complicated setup to give adequate packing in a reasonable amount of time. No matter which packing method is chosen, the key factor affecting the success of packed beds is the formation of retaining frits to keep the stationary phase in place. Frits must be strong enough to withstand pressure during packing and column use, while also remaining adequately permeable to not inhibit flow.[1, 2] Ideally, fabrication of frits is also facile and reproducible, ensuring that all columns made using the same technique are consistent.

Common methods for frit fabrication include sintering of packing materials, formation of sol-gel materials, or polymerization of a porous plug.[2] Sintering is the simplest of these methods, requiring the application of heat to bond a small plug of the stationary phase material to both itself and the column to produce a retaining frit. This can unfortunately lead to irreproducible flow through the columns though (little control over frit formation), and a decrease in structural integrity at the point of frit formation makes sintering less desirable than other options.[2] The sol-gel process has been effectively reviewed a number of times,[3-5] and describes the formation of an interconnected solid network from the hydrolysis and polycondensation of organometallic precursors.[3] The ease of formation allows sol-gel frits to be selectively patterned in

capillaries much more effectively than sintering,[6, 7] and they are characterized by a high degree of stability (good day-to-day reproducibility) and relative ease of flow (little resistance).[2] Formation of a porous polymer monolith (PPM) is similar to the sol-gel process, although it involves the use of organic monomers, cross-linking agents, porogenic solvent and polymerization initiator (UV or thermal activated) to form a solid support that will retain the packing material.[8, 9] These materials are quite stable, and show a very high level of column-to-column reproducibility (indicating the reliability of the method).[2] Frits based on PPM technology also have the advantage of selective patterning within a column if photopolymerization and UV-transparent capillaries are employed, and are typically formed much more quickly than sol-gel columns based on the rapid nature of the UV initiation.

No matter which frit formation method is used, one problem that cannot be avoided with packed columns is the potential for movement of the stationary phase particles. With repeated use, voids can eventually be formed by the shifting and compression of the particles, leading to degraded column performance and irreproducible results. This has been one of the primary concerns with conventional packed columns for many years (along with the effort required to prepare and fill the column with stationary phase particles), and has led to much of the impetus for developing newer stationary phase options.

2.1.2 –Entrapped Microsphere Columns: As attractive as PPM technology currently is as a chromatographic substrate,[10] one slight disadvantage that can be found is that the formation of columns with specific functionalities (e.g. protein affinity, ion exchange, etc.) often requires an additional step after the monolith has been formed to impart the desired effect.[11-14] If this additional functionalization could be avoided it would make

column preparations much easier, which is where microsphere entrapping comes into play. Many different varieties of pre-functionalized microspheres ("beads") can be purchased commercially, making them an interesting option. With the problems of conventional packed columns already established it is clear that simply packing these beads is not the ideal option, but if they could somehow be fixed in a column without destroying their desired functionality it could greatly improve the way that packed-column chromatography is performed.

Early attempts to affix microspheres within columns made use of the sintering process mentioned previously, although here it was not simply used to form a frit, but rather to form a monolithic material of microspheres that were bonded together by the heating process.[15] While this succeeded in providing a bed of entrapped beads, the products of the sintering process were still subject to all of the concerns detailed previously (poor flow characteristics and structural instability). Additionally, the heat that needs to be applied for sintering can also be sufficient to degrade certain chemical or biological functionalities that are often present on the surface of the spheres for desired interactions after entrapment, further limiting its usefulness.

Sol-gel technologies have been applied to the process of microsphere entrapping, serving as a "nanoglue" to hold the chromatographic bed together.[16] Formation of a monolithic support structure as a backbone to retain the beads eliminates the need for retaining frits, as well as producing a relatively uniform structure for highly efficient chromatography in a variety of applications.[17-21] Despite this relative strength, one problem that exists with the sol-gel process is that the formation of the monolithic support structure is non-specific, frequently leading to encapsulation of the stationary phase particles.[22-24] This in turn can lead to a subsequent decrease in the selectivity of the

stationary phase material, as the porous nature of the entrapped beads can be partially occluded by the formation of the sol-gel (decreasing the available surface area).[22, 24] This partial loss of selectivity is particularly concerning for applications that require functionalized microspheres, as it is the specific interactions of analytes with the surface of the functionalized spheres that brings about the advantages of the method, and this benefit is lost if the surface is no longer available.

Another option for entrapment uses a technique similar to that which is employed in the formation of a porous polymer monolith, using a matrix generated from organic monomers to affix beads within a column.[25-28] This process is believed to arise from preferential partitioning, whereby a polymerization system with polarity that is similar to that of the beads being entrapped and dissimilar to the porogenic solvent should force selective polymerization at bead-bead and bead-capillary contact points. So far, evidence of this process has been suggested by the formation of polymer "webs" between beads, holding them in place after packing and eliminating potential motion.[26-29] This in turn should provide the subsequent columns with a high degree of mechanical stability, excellent flow properties, and sufficient free surface area to achieve efficient separations; all very desirable parameters for column design. The lack of a visible polymer coating on the surface of the particles might also suggest that the functionalized beads will retain their capacity for specific interactions, making microsphere entrapped columns one of the more interesting options for complex separations as they can seemingly be tailored with a wide variety of unique surface chemistries to effect column chromatography.[29]

With this in mind, one of the thrusts of research in our group has focused on the entrapment of microspheres within PPM materials for a variety of applications including SPE,[26] LC and capillary electrochromatography (CEC),[27, 29] and use as novel electrospray

emitter tips.[30] When the applications of fluorous silica gel and fluorous chemistry are also taken into consideration however, a logical extension presents itself in the adaptation of the microsphere entrapping process to the fluorous case. Fluorous silica gel is already a type of microsphere (5 μm diameter; 90 Å pore size), making it an interesting choice for entrapment. The possibility of developing a new variation on FSPE or fluorous column chromatography through microsphere entrapment has therefore been one of the avenues of my research, focusing on the design and optimization of appropriate entrapment conditions for the system in question.

2.2 Experimental

2.2.1 – Materials: Water for all solutions was purified by a Milli-Q system (Millipore; Bedford, MA, USA) to a value of 18.2 MΩ. Butyl acrylate (BA; Figure 2.1), 1,3-butanediol diacrylate (BDDA), benzoin methyl ether (BME), 3-(trimethoxysilyl)propyl methacrylate (TMSPMA), 2,2,2-trifluoroethyl acrylate (99%; TFEA), ethyl acrylate (99%; EA) and pentane were obtained from Aldrich (Oakville, ON). Fluoro Flash silica gel (silica gel with a perfluorooctylethylsilyl bonded phase; 5 μm particle; 90 Å pore size) came from Fluorous Technologies (Pittsburgh, PA, USA), while glacial acetic acid, acetonitrile (HPLC grade), toluene (certified), acetone (certified) and tetrahydrofuran (certified) were purchased from Fisher Scientific (Nepean, ON). Formic acid (98%) was purchased from BDH Chemicals (Toronto, ON), and ethanol (95%) was acquired from Commercial Alcohols (Brampton, ON). All reagents were used as received without any additional purification.

The capillary for all tests was supplied by Polymicro Technologies (product TSU075375; Phoenix, AZ, USA). Column dimensions were a 75 μm I.D. and 363 μm O.D., and all capillaries had a UV-transparent coating to facilitate polymerization.

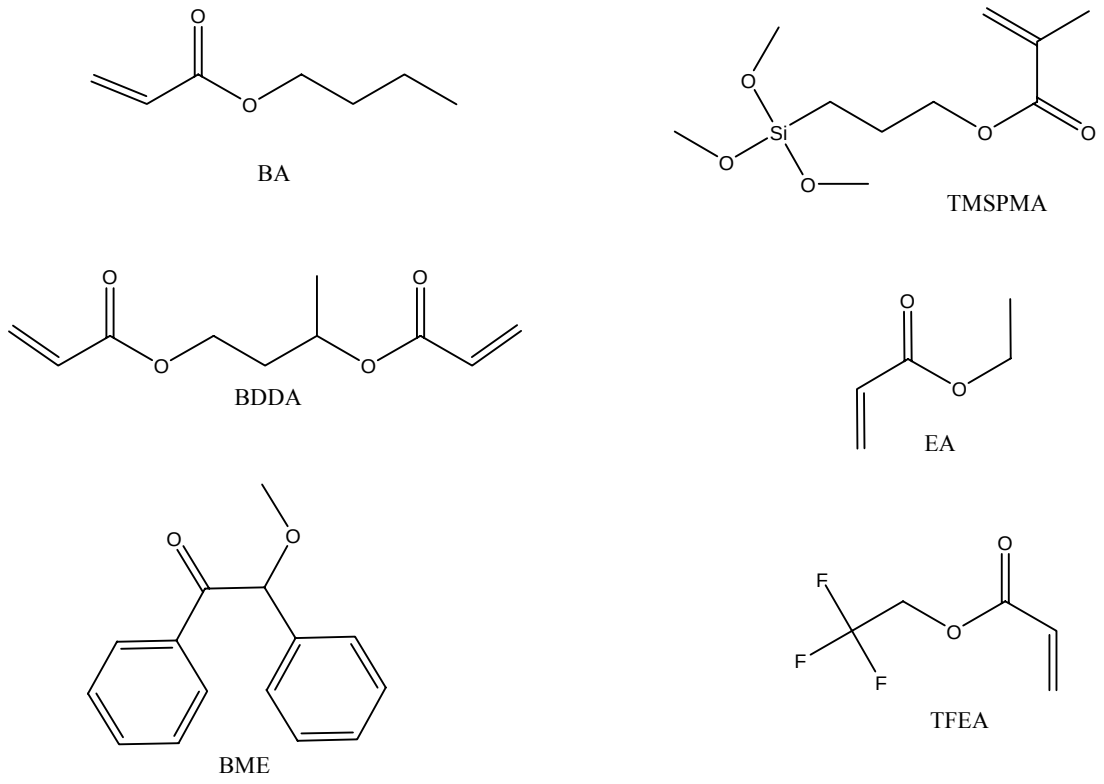

Figure 2.1: Structures of relevant compounds.

2.2.2 – Column Fabrication: The general method used for entrapping beads remains the same for both fluorous and non-fluorous spheres alike, and is detailed visually in Figure 2.2. Capillaries are initially pre-treated by filling with a mixture of 50% water, 20% TMSPMA and 30% glacial acetic acid, and allowed to remain static overnight to graft the silica walls with vinyl groups (improving subsequent polymer binding).[31] Subsequently, the capillary is flushed with a mixture of acetonitrile (60%), ethanol (20%) and purified water (20%), and can then be used immediately or stored indefinitely (filled with the flushing solution).

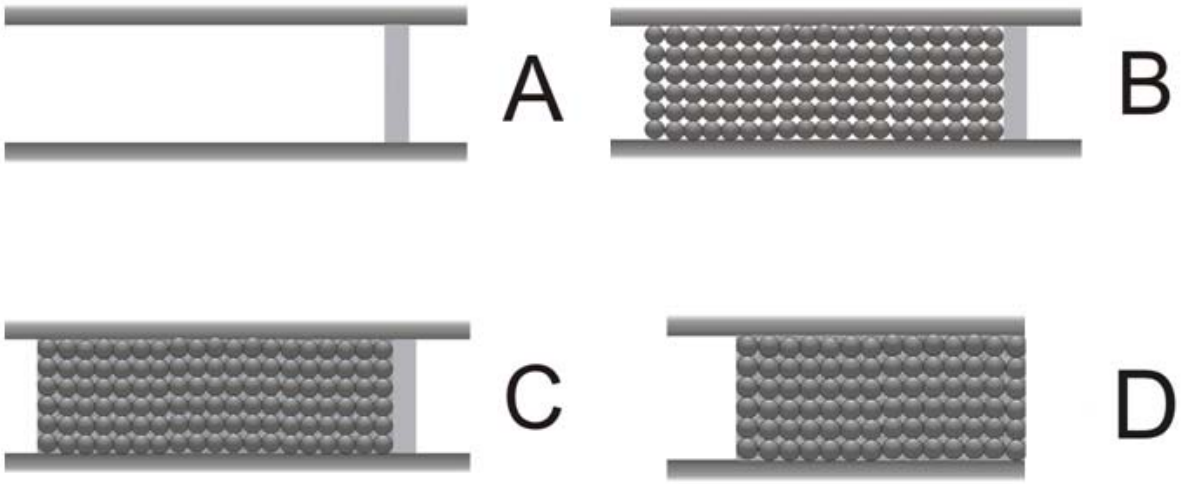

Figure 2.2: The standard protocol for microsphere entrapment, with steps as follows: A) Formation of a polymeric frit. B) Capillary filling with microsphere slurry to a desired length. C) Filling column with polymerization mixture. D) Trimming of any unentrapped areas and retaining frit after UV irradiation causes polymerization and microsphere entrapment.

Polymerization of temporary retaining frits follows a PPM method first proposed by Shepodd et al.,[32] with the modification of using benzoin methyl ether as the radical initiator in place of azobisisobutyronitrile (AIBN). The composition of this mixture included 23% BA (all percentages by volume unless otherwise noted), 10% BDDA, 40% acetonitrile, 13.25% ethanol and 13.25% water. Additionally, 0.1% TMSPMA relative to the total volume of polymerization mixture was included to further encourage polymer attachment to the capillary walls during frit formation, and 2 mg of BME per milliliter of polymerization solution was used as the initiator.

Prior to polymerization, the entire capillary (other than an area of approximately 2 mm) was placed under a photomask to prevent UV initiation in those places. This helps to create a small, well-focused frit, as well as preventing undesirable polymerization in areas that need to be subsequently packed with microspheres. After manually filling the capillary with polymerization mixture by syringe (3 mL Luer-Lok Tip; BD; Franklin Lakes, NJ, USA), initiation was catalyzed by a UV lamp (Spectroline 8 W UV lamp; model ENF-280C; Fisher Scientific) emitting a wavelength of 254 nm at a distance of ~2 cm from the capillary being irradiated. Polymerization was allowed to proceed for 5 min, after which the column was flushed with a solution of acetonitrile and water (95:5 v/v) using a Waters model 590 HPLC pump (Milford, MA, USA) at a flow rate of ~10 μL/min to remove any unreacted monomer or cross-linker prior to microsphere packing. Additionally, the flushing step also allows the durability of the frit to be verified, as it should easily withstand the pressure generated by the solvent flow if fabrication was successful.

Introduction of the fluorous spheres employed a slurry-packing method, with about 10-20 mg of the Fluoro Flash particles suspended in 1 mL of methanol. A syringe was used to manually fill the capillary to a desired length with a loose bed of spheres, which were subsequently compacted using the Waters 590 LC pump to provide a pressure of ~14 MPa that helped to minimize voids and ensure optimal packing. After this, a polymerization mixture could then be manually introduced by syringe into the packed columns for entrapment. These mixtures comprised a variety of combinations of monomer, cross-linker and porogen, and will be discussed in more detail in the Results section. Once the column was filled with a polymerization mixture, areas where sphere entrapment was not desirable were masked (identically to the method used during frit

formation), and irradiation with 254 nm UV light (for varying amounts of time) was used to produce an entrapped bed.

Next, the column was again flushed using the Waters 590 pump, although this time it was essential to ensure that the column was flushed from both ends rather than in only a single direction. It was necessary to remove any unentrapped particles as well as residual polymerization solution prior to column use, but with the bed of entrapped spheres now affixed, there was only one direction that would allow loose particles to be removed (either flow direction could be used to remove residual solution). Finally, after all appropriate flushing had been completed, the frit was removed (by cleaving with a ceramic cutter), leaving an entrapped fluorous column that was ready for use.

2.2.3 – Scanning Electron Microscopy: Images were obtained using a Jeol JSM-840 scanning microscope (Tokyo, Japan). After columns had been fabricated and otherwise tested, pieces were then cut from the tip to provide a view of the microsphere entrapment and polymer morphology. The cuts were subsequently mounted on aluminum stubs using tape such that an unobstructed view of their cross-section was possible. Prior to imaging, the stubs were coated with a thin layer of gold using a Hummer 6.2 Sputtering System (Anatech; Hayward, CA, USA).

2.2.4 – Backpressure Testing: Flow-induced backpressure was assessed using an Eksigent NanoLC pump (Livermore, CA, USA) with a 1:1 acetonitrile/purified water solvent composition. For analysis, columns were cut to a total length of 4 cm (1 cm of entrapped particles and 3 cm of empty capillary left prior to the spheres to facilitate fluidic connections). Each column was flushed for 30 min prior to the start of data collection, with measurements then taken at five different flow rates between 200 and 1000 nL/min. At each rate, the column was allowed to flush with the 50:50 mobile phase

for 5 min, after which time 15 readings of back pressure were recorded at 3 s intervals. This process was repeated twice, and the data averaged to get the value for back pressure at a particular flow rate.

2.3 Results and Discussion

2.3.1 – "Shepodd-Type" Polymer for Entrapping Fluorous Microspheres: Initially, trapping of the fluorous spheres was tested with the same polymerization mixture used for frit fabrication (the so-called "Shepodd-Type" PPM mixture; Experimental section 2.2.2)[32] based on the relative polarities. Since both the polymerization mixture and fluorous spheres were largely non-polar, it was posited that partitioning should occur in a similar manner to that which has previously been suggested to give the desired webbing between spheres.[26-28] Unfortunately, this did not turn out to be the case, as all of the columns produced by this method showed a heterogeneous polymer distribution that completely coated the beads (Figure 2.3). Changes in the UV irradiation time from 90 s down to 15 s all produced similar results, with excessive polymer coating resulting in each case.

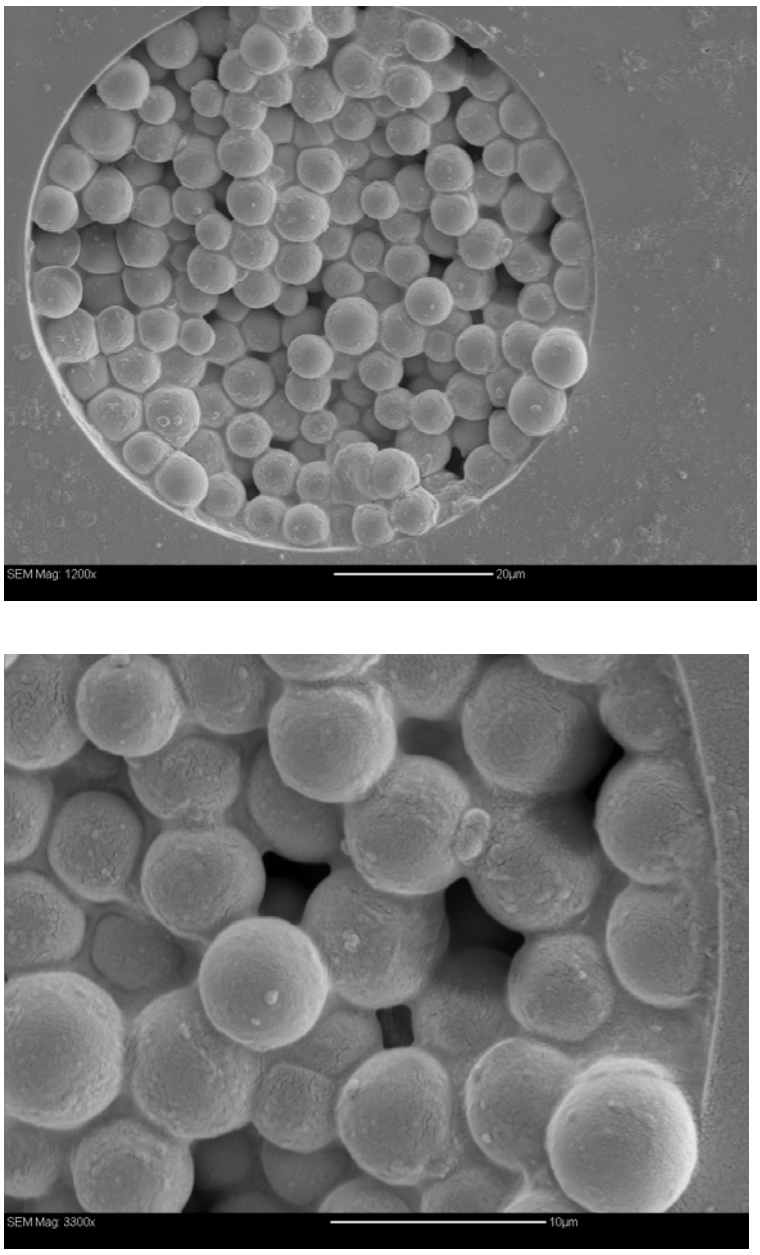

Figure 2.3: Representative images of the initial attempts at entrapping fluorous microspheres with the Shepodd-type polymerization mixture (90 s UV irradiation time). Polymer forms heterogeneously, coating the surface of the spheres and filling many of the interstitial spaces.

2.3.2 – Changes to Porogenic Solvent: To assess whether the same arguments about polarity that previously described the partitioning for polymer with C18 beads were also

true for the use of fluorous spheres, a series of tests were performed with porogens of differing composition while maintaining all other polymerization conditions the same. Choices ranged from a solvent that was relatively similar (methanol; Log *P* = -0.74) to the Shepodd porogen of 60% acetonitrile (Log *P* = -0.34), 20% ethanol (Log *P* = -0.30) and 20% water, to one that was substantially less polar (pentane; Log *P* = 3.45).[33] This analysis yielded the expected results (Figure 2.4), with solvents of decreasing polarity competing more strongly for the forming polymer such that it remained in solution longer and appeared more granular upon precipitation.

Tests with porogens of greater polarity (increased aqueous content) were also examined, but this often led to issues of miscibility with the monomers and cross-linker. This was unfortunate, because one of the easiest ways to improve the effectiveness of partitioning would be to use a porogen which is a comparatively poor solvent for the forming polymer such that phase separation occurs more quickly. This would likely encourage the production of the desired webbing by enhancing the underlying selectivity of the polymerization process, improving the quality of the material through a fairly simple procedure.

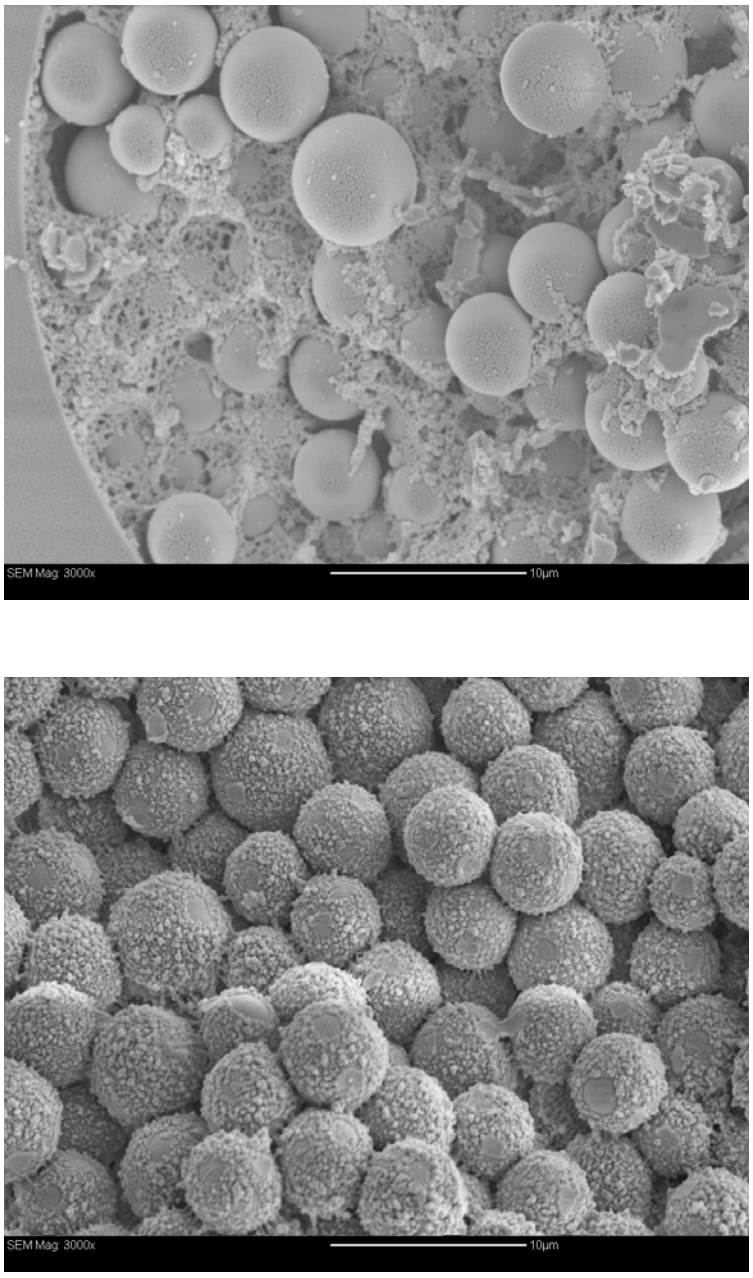

Figure 2.4: Representative images showing the effects of changing the polarity of the porogenic solvent while maintaining the use of butyl acrylate as the monomer. The upper panel shows methanol (Log *P* = -0.74) as the solvent, while the lower panel shows the result when pentane (Log *P* = 3.45) is used as the porogen.[33] The structure of the resultant polymer can be seen to change in the expected manner, with decreasing solvent polarities competing more strongly for the forming polymer such that it remains in solution for a longer time and appears more granular upon precipitation.

2.3.3 – Introduction of Fluorous Monomers: Because tailoring the composition of the porogen to force the desired partitioning proved to be a poor direction, a second option was chosen instead. The strong fluorous-fluorous interaction has already been discussed at great length (Chapter 1), so a logical application as applied to microsphere entrapping is the introduction of a fluorous monomer. Logically, it should follow that a polymer with fluorous character would greatly prefer the highly fluorous environment between the beads as opposed to essentially any organic porogen, forcing a very early phase separation and the desired partitioning in the system. To test this theory, a simple experiment was performed by substituting the butyl acrylate in the conventional Shepodd PPM solution with trifluoroethyl acrylate (TFEA) while leaving all other parameters (including irradiation time) equal. The results from this seemingly minor change were quite surprising, as the polymer that was produced was now much more selective, and the first evidence of the desired webbing was observed (Figure 2.5). This result boded well for the further use of fluorous acrylates, as even without optimizing the porogenic solvent, a TFEA monomer gave better results than any of those seen for the non-fluorous butyl acrylate monomers.

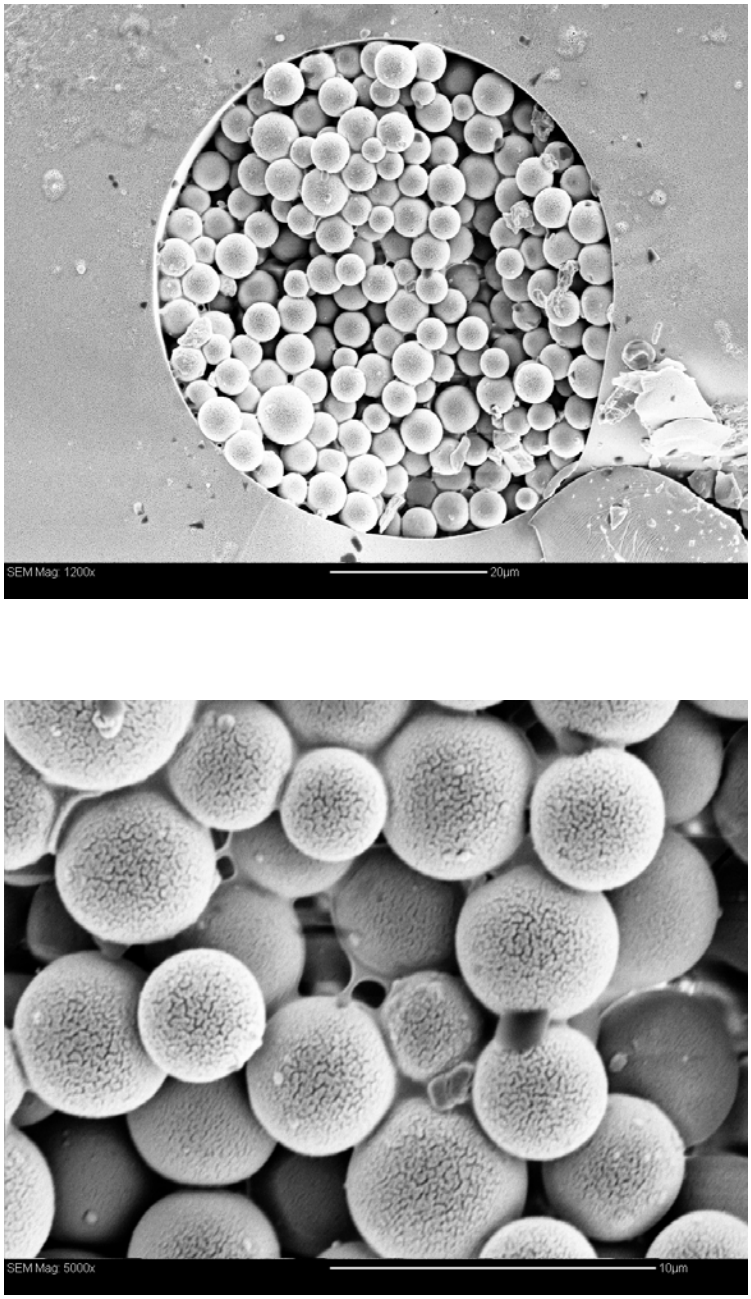

Figure 2.5: Shown above are representative images for the polymer that was achieved by substituting TFEA for BA in the Shepodd-type polymerization mixture. All other parameters were maintained, yet now the polymerization appeared to be much more selective, with traces of webbing visible in some of the spaces between the microspheres.

Based on monomer availability, these initial tests were unfortunately not perfectly analogous with the previous Shepodd method because those earlier examinations used butyl acrylate while the fluorous acrylate available here was ethyl. Consequently, to ensure that the improved results were derived from a fluorous effect rather than simply a decrease in the size of the monomer, ethyl acrylate was purchased and tested in the same manner. By substituting the butyl acrylate in the Shepodd PPM with ethyl, the polymer that resulted still lacked selectivity and coated the spheres much like the results from the initial tests (Figure 2.6). This reinforced the assertion that fluorous affinity was causing some of the improved selectivity in polymer formation, and helping lead to the improved entrapment chemistry.

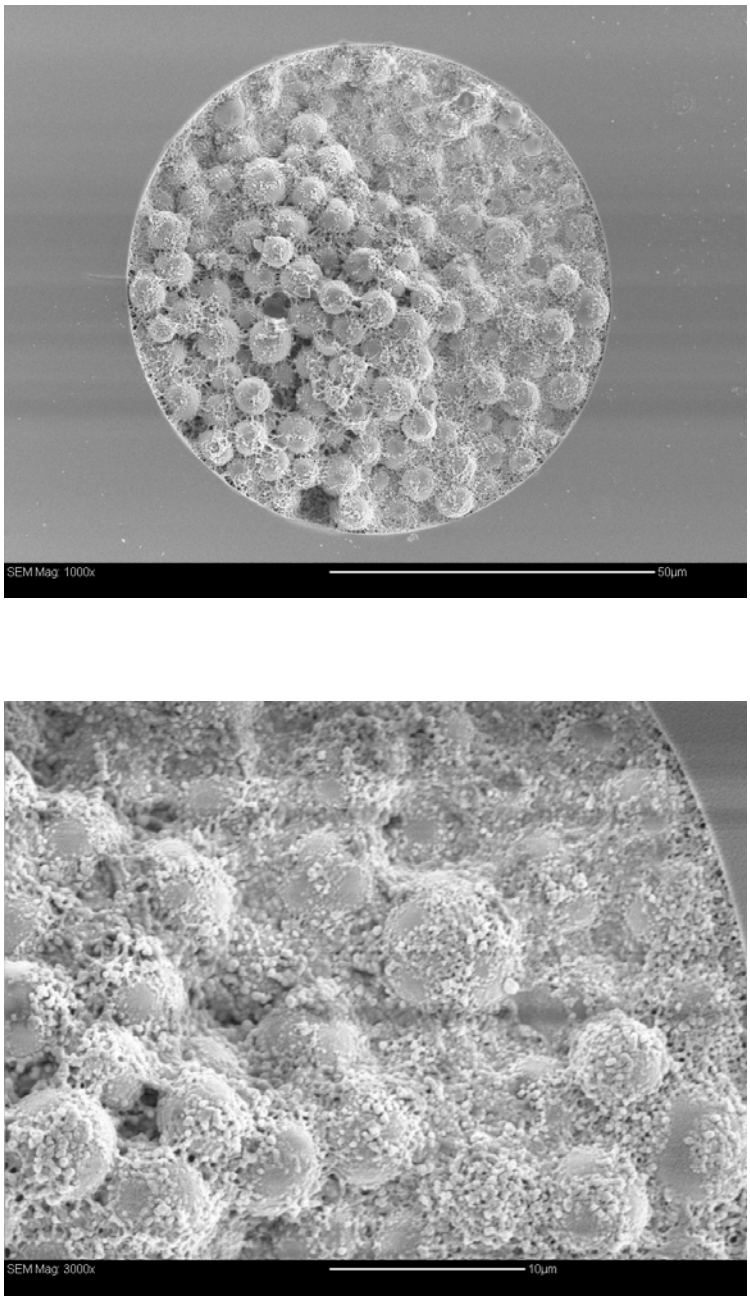

Figure 2.6: Shown above are representative images obtained using a Shepodd-type polymerization mixture that substitutes EA for BA (60 s UV exposure time used for entrapment). Although some evidence of web-like polymer can be observed, there is too much produced in a non-selective manner to be of any use (even with the reduced UV exposure time from normal 90 s preparations).

2.3.4 – Optimizing the Fluorous System: Once it had been established that using TFEA led to improved entrapment, the next step was to examine whether modifications to the porogenic solvent could further optimize the system. This involved changes on two different levels: broad changes to the entire composition of the porogenic mixture, as well as smaller changes designed to fine-tune the ratios of components in the system.

2.3.5 – Broad Changes to the Porogenic Solvent System: This series of tests was designed similarly to those that were previously performed with butyl acrylate, changing the composition of the porogen from the usual Shepodd system to a number of different polarities to examine the effect on the formation of polymer. Using both TFEA and ethyl acrylate (EA) as a comparator, the results that were observed mimicked those that were previously noted; decreased solvent polarity still led to formation of smaller polymer granules and increased coverage of the bead surfaces (Figure 2.7). Again, this was not the desired partitioning, and because it has already been established that increasing the aqueous content of the Shepodd PPM system (acetonitrile based) caused poor miscibility, a new variation was attempted here. Two other solvents with similar polarities to acetonitrile (Log *P* = -0.34) and good aqueous miscibility were chosen (acetone; Log *P* = -0.24, and THF; Log *P* = 0.46),[33, 34] and by changing their aqueous content, miscibility concerns could be further assessed.

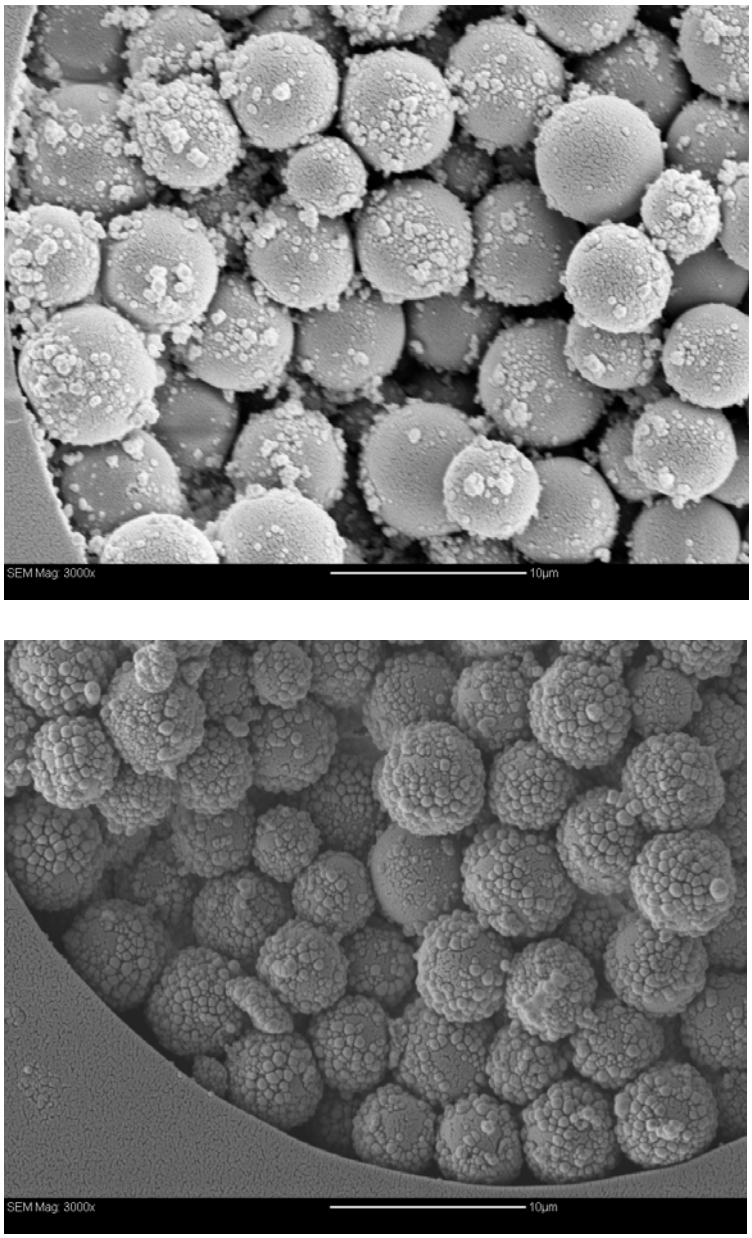

Figure 2.7: Shown above are characteristic images for the results obtained by changing the polarity of the porogenic solvent for EA and TFEA monomer mixtures. The upper panel used methanol as the porogen and EA as the monomer to produce a lightly granular polymer, while the lower panel shows a mixture with pentane and TFEA that produced a more highly granulated coating. Neither of these cases exhibits the desired partitioning, which was the underlying trend from all of the alterations to the porogenic solvent with EA and TFEA monomers.

The normal Shepodd solution is 80% organic (60% acetonitrile, 20% ethanol) and 20% aqueous, so the first step in changing the aqueous content of the acetone and THF systems was to increase this proportion to 30%. Just as with the Shepodd system this change led to the formation of two layers (this time for both TFEA and EA polymerization mixtures), indicating that the increased aqueous content was still causing problems. To fully determine the point at which miscibility returned, ethanol was added to the polymerization mixtures in a drop-wise manner to increase the organic content while also paralleling the third component of the Shepodd system. The point at which the mixture regained a single-phase character was noted, and the volume fractions of each component were recorded (Table 2.1). It was interesting to note that in each case the relative aqueous fraction remained close to 20%, indicating that that particular ratio is preferable for obtaining the needed miscibility of organic and aqueous phases in these types of polymerization mixtures.

Table 2.1: Composition of polymerization mixtures tested to assess aqueous miscibility.

Primary Component	Vol. % Primary Component	Vol. % Ethanol	Vol. % Aqueous
Acetonitrile	60	20	20
Acetone	60.5	13.5	26
THF	53	24	23

At this point, another option that was examined was the use of a fluorophobic solvent instead of one with increased polarity. It was suggested that because the area where the polymer is desired should be highly fluorous, a better option to force selective partitioning would be to use a solvent that has a high organic miscibility for the

monomers, but also a sufficient degree of fluorophobicity. This way, when the polymerization mixture is presented with a fluorous phase there should be a greater propensity for polymer to choose the fluorinated areas rather than the liquid phase, forcing selectivity onto the system. To this end, toluene was chosen as a reasonable option to meet the desired criteria,[35] and a series of tests were performed to examine the effect on partitioning.

Polymerization mixtures were prepared with a 70:30 mixture of monomer (TFEA or EA) to cross-linker (BDDA) as in the Shepodd system, and a ratio of this monomer solution to porogen (100% toluene) of 33:67 (again, as per the Shepodd ratio). Unlike all previous tests which used 254 nm UV light to initiate polymerization though, this situation forced the usage of 365 nm (the aromatic nature of toluene caused a strong absorption at the lower wavelength and hindered initiation). Fortunately, benzoin methyl ether has a broad window of effective initiation wavelengths,[36] making this change less of a problem. Using irradiation times of 60 and 90 s (the standard times tested), no flow through columns based on both EA and TFEA polymerization mixtures could be observed. When the materials were imaged by scanning electron microscopy (SEM), essentially all of the interstitial spaces were filled with polymer (Figure 2.8). This indicated that although partitioning was occurring with the fluorophobic solvent system, bead encapsulation might be a problem that needs to be seriously considered when it comes to microsphere entrapment mechanisms.

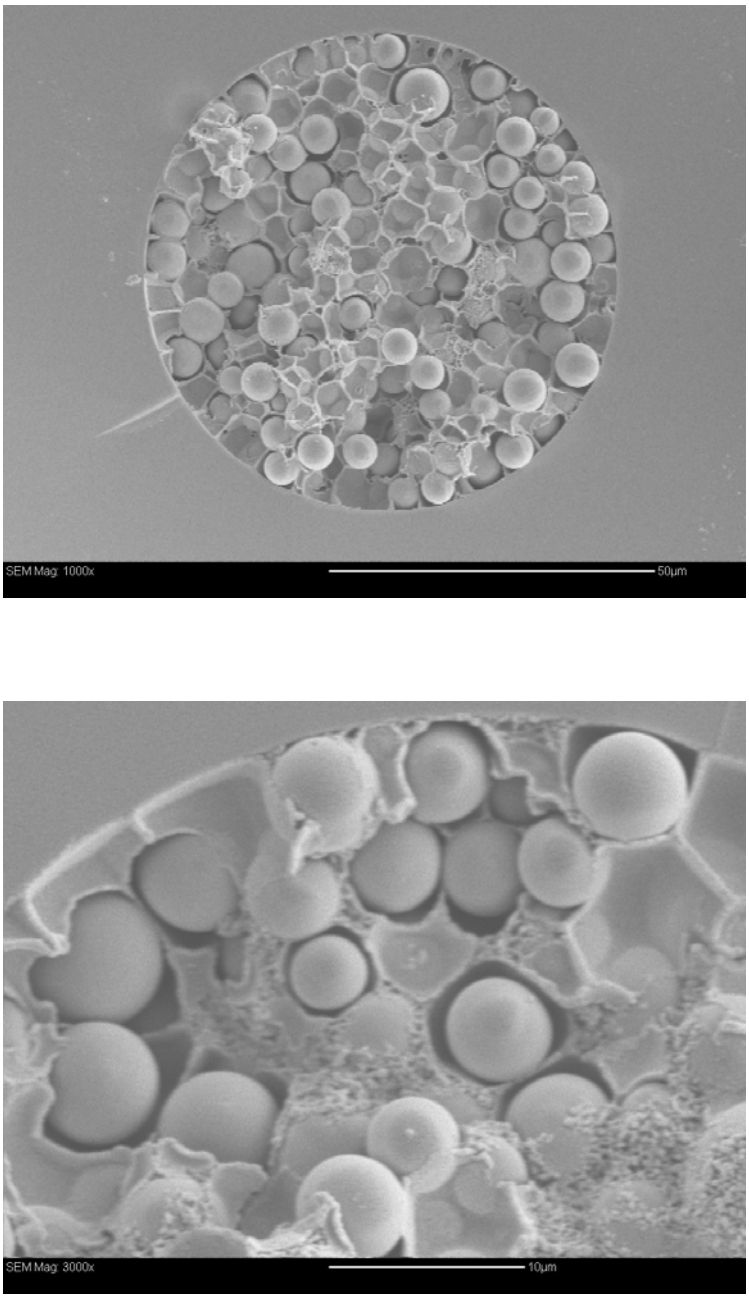

Figure 2.8: Shown here are representative images of the results obtained from polymerization mixtures of EA and TFEA with toluene as the porogenic solvent. Although the surfaces of the microspheres do not appear to be coated, the encapsulation, filling of interstices and subsequent reduction in column flow limit the usefulness of these materials.

2.3.6 – Porogen-to-Monomer Ratio: Since one of the most frequently observed concerns in all cases was an excess of polymer formation (regardless of porogen choice and composition), it was decided that fine-tuning the amount of monomer and cross-linker relative to the amount of porogen might be a reasonable option. The first test of this method involved a simple change to the Shepodd-type polymerization system, maintaining the same ratios for monomer (TFEA or EA) to cross-linker, and the same porogenic solvent (60% acetonitrile, 20% ethanol, 20% water), but decreasing the ratio of monomer mixture to porogen from 33:67 to 20:80. This still resulted in a system with excellent miscibility, but as compared to all of the previous tests where the polymerization mixture was varied, the changes in the observed polymer morphology under SEM were quite startling (Figure 2.9). Polymer now appeared to be highly selective, and there was evidence of substantial webbed character without excessive surface coating of the beads when using the same polymerization times and wavelengths as previously examined (60 and 90 s irradiations; 254 nm). While this could ultimately be said to be the expected result when a fluorous monomer like TFEA is employed, the reasons for the selective partitioning when a non-fluorous acrylate like EA is used are somewhat less clear. One potential argument might be with respect to the amount of polymer, as the excessive amounts of polymer seen in earlier systems of all types could simply overwhelm any potential partitioning. While selectivity may have actually been occurring initially in the desired regions, the excessive formation of subsequent polymer would simply obscure the amounts that were forming in the desired areas and render it impossible to differentiate the two cases.

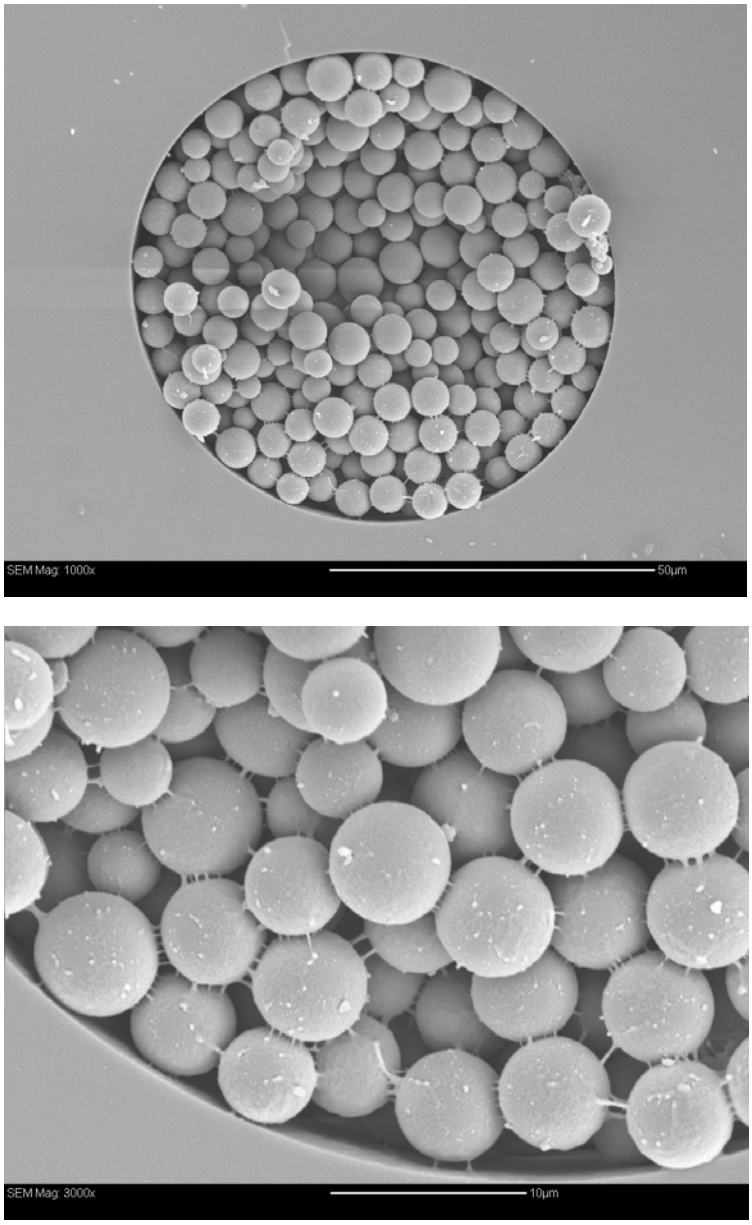

Figure 2.9: These images show the results from a modified polymerization mixture using EA. Webbing between the spheres is now clearly visible, while the surfaces seem relatively clean and unaltered by the entrapping (90 s UV exposure). Similar results were noted for the 20:80 mixture using TFEA rather than EA, with highly stable columns that should permit uninhibited flow.

Similar to the tests just described, the same process was also performed with toluene as the porogenic solvent instead of the Shepodd system. Here, the results that were obtained more closely matched those that would be expected from the partitioning arguments as they are currently defined. When EA was used as the monomer, visible coating of the beads was evident (Figure 2.10), while using TFEA as the monomer gave a slightly granular polymer with webbing and much less coating of the spheres (Figure 2.11). As before, this was with 365 nm irradiation to counteract absorbance of the toluene, but unlike all other cases, polymerization required more time with these solutions. Whereas previous studies used 60 and 90 s to assess polymer quality, the mixtures with 20% monomer mixture in toluene required two minutes of polymerization to produce a column capable of withstanding the pressures used for column flushing (~14 MPa). This difference aside (likely arising from the decreased amount of monomer taking longer to form a stable polymer), the introduction of a fluorophobic porogen along with decreased monomer concentration seemed to be the combination that provided the best polymer distribution.

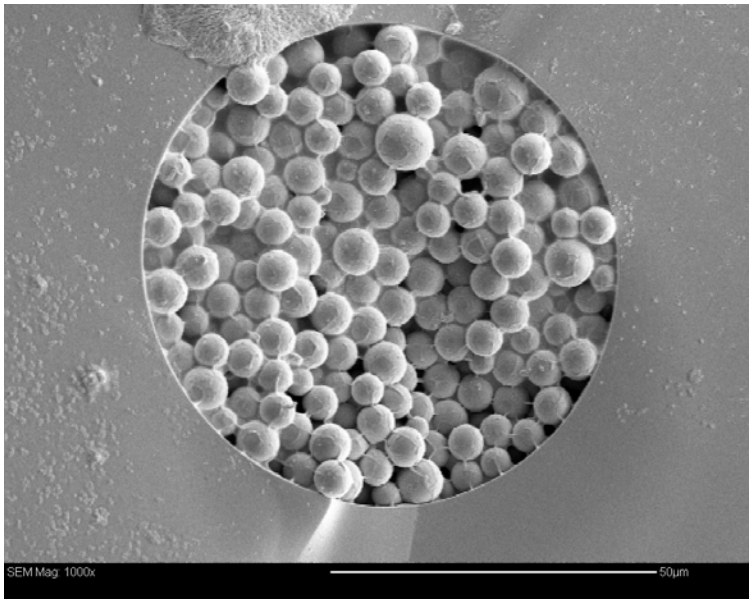

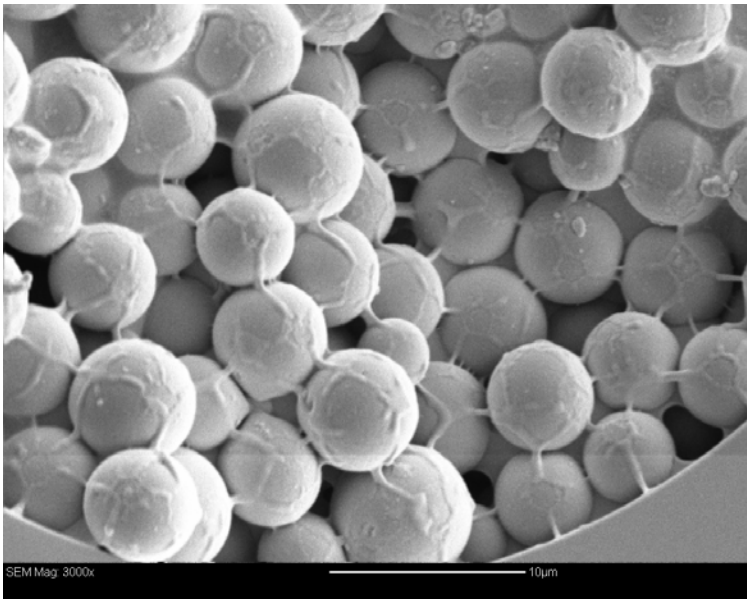

Figure 2.10: Shown here are representative results from 2 min irradiation at 365 nm of a 20:80 polymerization mixture of EA in toluene porogen. The spheres show evidence of polymer coating, with less of the selective webbing evident.

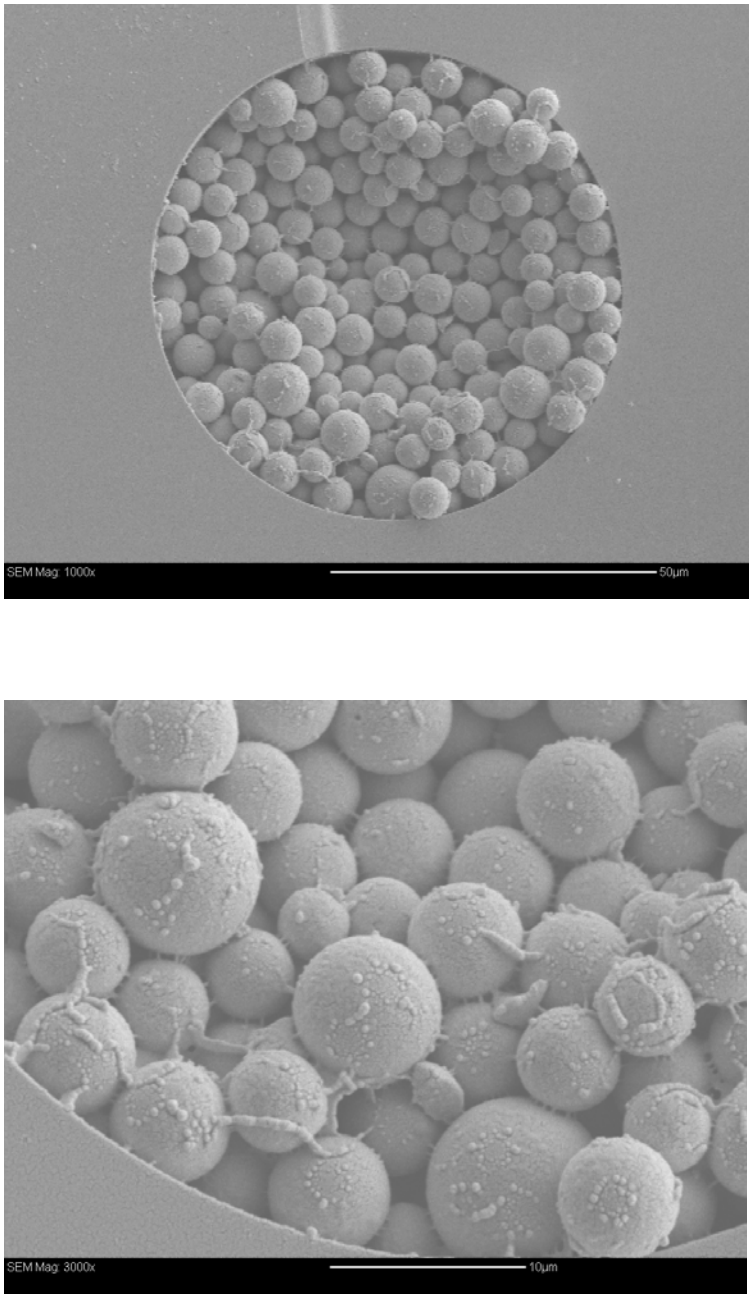

Figure 2.11: Pictured here are two images showing the typical result for 2 min UV irradiation at 365 nm of a 20:80 polymerization mixture consisting of TFEA in toluene. Unlike the EA case shown in Figure 2.10, there is less evidence of coating and more desired webbing in these images. This would seemingly indicate a greater degree of selectivity from this system.

2.3.7 – Backpressure Analysis of Entrapped Fluorous Columns: With a method in place that provided columns of reasonable quality based on visual assessment, the next step was a series of tests to evaluate their performance under analytical separation conditions. This was predominantly judged by flow induced backpressure as a measure of column potential, as this is a technique that has been previously discussed in the literature.[28, 37] In general, when a column is attached to an LC pump, the pressure at the head of that column can be measured and reported as an indicator of the quality of flow.[38] Large backpressures indicate that there is substantial resistance to flow, which can be interpreted here as non-specific polymerization (a column filled with heterogeneous polymer). Conversely, lower back pressures correspond to the desired case where polymer has formed selectively, allowing unhindered mobile-phase flow.

Initially, polymerization mixtures based on the modified Shepodd system using a 20:80 ratio of monomer mixture (TFEA or EA plus cross-linker) to porogen were selected for analysis. These were entrapped for 90 s at 254 nm, and cut such that the bed of entrapped spheres was only 1 cm in length. For analysis, two columns (90 s entrapped TFEA and EA) were compared to three reference materials (90 s entrapped 5 μm C18 beads with Shepodd PPM, a 1 cm Shepodd PPM frit irradiated for 5 min, and un-entrapped fluorous spheres packed against a Shepodd PPM frit), as well as a TFEA solution (20:80 polymerizable material to porogen) irradiated for 60 s at 254 nm to contrast the relative effectiveness of fluorinated materials. The results from these tests were somewhat surprising (Table 2.2), as compared to the two materials where flow should be the least inhibited (PPM and un-entrapped beads), the entrapped fluorous columns made with TFEA showed comparable back pressure readings at all of the tested flow rates. As well, when compared to a column with 5 μm C18 beads (Microsorb 100-5

C18; 5 μm particle, 100 Å pore size; Varian; Mississauga, ON) entrapped in a Shepodd PPM solution (a system which should show favourable partitioning of the polymer),[28] the entrapped fluorous spheres exhibited superior back pressure readings. In general, this data supports the earlier visual assessment that the columns have a localized polymer distribution, as they exhibit reasonable flow characteristics and pressure stabilities under a wide range of rates. This would also seem to support the assessment that the columns will have potential for chromatography, although it is worth noting that the unentrapped microspheres provided the optimal pressure profile of any of the materials tested (a factor that will be discussed shortly).

Table 2.2: Summary of the slopes of a series of plots of backpressure versus flow rate for varied column compositions.

Column Composition	Slope (kPa per nL/min) for 1 cm of Material
90 s Entrapped 20% EA	4.20 ± 0.87
90 s Entrapped 20% TFEA	1.48 ± 0.44
60 s Entrapped 20% TFEA	1.51 ± 0.08
90 s Entrapped 5 μm C18 Spheres	3.18
5 min Shepodd PPM Frit (1 cm)	1.56
Un-Entrapped 5 μm Fluorous Spheres	1.20

Given the excellent linearity of plots of back pressure versus flow rate for particle entrapped columns, the value of their slope can be used to compare their effectiveness. Lower values equate to less flow resistance, making those columns with the lowest slopes the best options for chromatography. Results for the entrapped columns of fluorous microspheres are an average of the data from 2 replicate columns.

Similar tests were also attempted with the 20:80 polymerization mixtures based on the toluene porogenic solvent, but the results there were never satisfactory. Using the same methods that produced columns for SEM analysis did not give stable columns for

back pressure measurements, as the introduction of prolonged pressure would always force the entrapped material out of the columns prior to completion. Presumably this is a result of both polymer quality and wall anchoring, which also suggests that these materials are not as reliable as those made with the 20:80 modified Shepodd PPM systems.

2.3.8 – Shortcomings With Entrapped Microspheres: Despite the results presented thus far that imply (through visual and pressure assessments) that entrapped microspheres have the potential to serve as substrates for fluorous solid-phase extractions or chromatography, it has ultimately been determined that their polymer-based nature is a hindrance to any potential success. In much the same way that attempts that were made to entrap particles within sol gels were found to result in encapsulation and a loss of surface functionality,[22-24] the same was also found to be true for organic polymer entrapment. Work in our group that was focused on trapping C18 particles in a BA + BDDA polymer matrix showed that even for irradiation times as low as 10 s, column efficiencies were reduced by at least 25% from a packed column without any entrapment.[39] Longer times resulted in even more polymer formation (and consequent surface occlusion), with up to a 50% loss in column efficiency observed after 30 s of polymerization. This would seem to correlate with the pressure results shown here (*vide supra*), where the optimal flow characteristics (and consequently best chromatographic potential) was shown by the unentrapped fluorous spheres as compared to any of the entrapment conditions (Table 2.2).

Despite the optimism surrounding the potential for organic polymer-entrapped columns, it is perhaps the logical conclusion that they should cause at least some degradation of chromatographic performance. Based on the presumed affinity mechanism

of the polymer for the microspheres (hydrophobic van der Waals interactions),[39] it is inevitable that at least a thin coating of any appropriately-tailored polymer will still cover the entire surface of a sphere. Even if a more significant accumulation at the points of the greatest interaction does still exist (the aforementioned webbing at bead-bead contact points), this will not be sufficient to overcome the losses in performance that are incurred by the accumulation of polymer over the rest of the microsphere surface. Interestingly, this is not to say that there are no benefits available through the formation of this polymer layer, as it is still a material that should have an affinity for analytes in much the same way that a polymeric monolith does. Additionally, entrapped spheres can actually provide greater mechanical stabilities than pure monoliths by reducing the impact of shrinking/swelling on the substrate,[21] although this comes at the obvious expense of increased difficulty in formation relative to a monolith on its own. Consequently then, the choice in material largely becomes an issue of the conditions to which your system will be subjected. If there will be forcing conditions then it may be a case that the stability imparted by microsphere entrapment with an appropriate polymer will be beneficial for chromatography (even with the concurrent decrease in performance). On the other hand, most conventional situations should simply be able to make use of an appropriately-chosen monolithic material (which tend to have excellent permeability, pressure profiles and chromatographic performance), making microsphere entrapment an excessive effort for comparatively little benefit relative to the other available stationary phase options.

2.4 – Conclusions and Future Directions

Despite the efforts here to optimize a fluorous system for microsphere entrapment, it was ultimately determined that it was not worthy of further investigation on account of the

limiting factors for chromatographic performance imparted by the thin polymer layers on the surface of the spheres.[39] Column efficiency is one of the most important factors in determining the viability of a new material,[40] so if it is inferior to either of the competing options (packed spheres or porous polymer monolith) in terms of performance, it is better to simply stick with those options. Additionally, with the difficulties that have already been noted with frit fabrication[2] and particle packing efficiency[1] for bead-based columns presenting reasons to look away from those areas, porous polymer monoliths seem like the most appealing option for further exploration of new fluorous phases.

As for the aforementioned issue of polymer monoliths potentially being inferior to microsphere entrapment due to the possibility of needing to introduce an affinity medium after creating the monolithic backbone (which is often the case for siliceous monoliths),[13] this becomes far less of an issue if the monolith is naturally a good substrate for the desired separation. Fortunately, this is frequently the case for many organic systems, meaning that no additional treatment outside of the polymer formation is necessary given an appropriate choice of monomer and cross-linker. Here (through the use of TFEA), it has already been demonstrated that acrylates containing fluorous character are commercially available, and based on their differential interaction with fluorous microspheres as compared to the entrapment mixtures without fluorination, they appear to be promising materials for fluorous affinity interactions (presumably their observed partitioning resulted from a fluorous effect rather than from polarity based on the results for EA under similar conditions). Consequently, directly forming monolithic materials from fluorous polymer precursors seems as though it should present a viable alternative to particle-entrapment or packing in terms of the creation of new fluorous stationary phases, as well as avoiding the issues with column performance that polymer coatings on

microspheres have been found to provide. These ideas will therefore be further explored in the following chapter, with the potential for fluorous, porous polymer monoliths in the realm of separations introduced and described.

2.5 – References

(1) Colon, L. A.; Maloney, T. D.; Fermier, A. M. *J. Chromatogr., A* **2000**, *887*, 43-53.

(2) Piraino, S. M.; Dorsey, J. G. *Anal. Chem.* **2003**, *75*, 4292-4296.

(3) Hench, L. L.; West, J. K. *Chem. Rev.* **1990**, *90*, 33-72.

(4) Buckley, A. M.; Greenblatt, M. *J. Chem. Educ.* **1994**, *71*, 599-602.

(5) Avnir, D. *Acc. Chem. Res.* **1995**, *28*, 328-334.

(6) Schmid, M.; Bauml, F.; Kohne, A. P.; Welsch, T. *J. High Resolut. Chromatogr.* **1999**, *22*, 438-442.

(7) Zhang, X.; Huang, S. *J. Chromatogr., A* **2001**, *910*, 13-18.

(8) Svec, F.; Frechet, J. M. J. *Chem. Mater.* **1995**, *7*, 707-715.

(9) Viklund, C.; Ponten, E.; Glad, B.; Irgum, K.; Hoerstedt, P.; Svec, F. *Chem. Mater.* **1997**, *9*, 463-471.

(10) Svec, F. *J. Chromatogr., A* **2010**, *1217*, 902-924.

(11) Gusev, I.; Huang, X.; Horvath, C. *J. Chromatogr., A* **1999**, *855*, 273-290.

(12) Dulay, M. T.; Quirino, J. P.; Bennett, B. D.; Zare, R. N. *J. Sep. Sci.* **2002**, *25*, 3-9.

(13) Kato, M.; Sakai-Kato, K.; Toyo'oka, T. *J. Sep. Sci.* **2005**, *28*, 1893-1908.

(14) Bedair, M.; Oleschuk, R. D. *Analyst* **2006**, *131*, 1316-1321.

(15) Asiaie, R.; Huang, X.; Farnan, D.; Horvath, C. *J. Chromatogr., A* **1998**, *806*, 251-263.

(16) Morris, C. A.; Anderson, M. L.; Stroud, R. M.; Merzbacher, C. I.; Rolison, D. R. *Science* **1999**, *284*, 622-624.

(17) Dulay, M. T.; Kulkarni, R. P.; Zare, R. N. *Anal. Chem.* **1998**, *70*, 5103-5107.

(18) Chirica, G.; Remcho, V. T. *Electrophoresis* **1999**, *20*, 50-56.

(19) Ratnayake, C. K.; Oh, C. S.; Henry, M. P. *J. Chromatogr., A* **2000**, *887*, 277-285.

(20) Ratnayake, C. K.; Oh, C. S.; Henry, M. P. *J. High Resolut. Chromatogr.* **2000**, *23*, 81-88.

(21) Gu, X.; Wang, Y.; Zhang, X. *J. Chromatogr., A* **2005**, *1072*, 223-232.

(22) Chirica, G. S.; Remcho, V. T. *Electrophoresis* **2000**, *21*, 3093-3101.

(23) Tang, Q.; Wu, N.; Lee, M. L. *J. Microcolumn Sep.* **2000**, *12*, 6-12.

(24) Karwa, M.; Hahn, D.; Mitra, S. *Anal. Chim. Acta* **2005**, *546*, 22-29.

(25) Chirica, G. S.; Remcho, V. T. *Anal. Chem.* **2000**, *72*, 3605-3610.

(26) Xie, R.; Oleschuk, R. *Electrophoresis* **2005**, *26*, 4225-4234.

(27) Xie, R.; Oleschuk, R. *Anal. Chem.* **2007**, *79*, 1529-1535.

(28) Gibson, G. T. T.; Koerner, T. B.; Xie, R.; Shah, K.; de Korompay, N.; Oleschuk, R. D. *J. Colloid Interface Sci.* **2008**, *320*, 82-90.

(29) Xie, R. Microsphere Entrapped Columns for Capillary Electrochromatography. Ph.D., Queen's University, Kingston, Ontario, 2006.

(30) Koerner, T.; Xie, R.; Sheng, F.; Oleschuk, R. *Anal. Chem.* **2007**, *79*, 3312-3319.

(31) Courtois, J.; Szumski, M.; Bystroem, E.; Iwasiewicz, A.; Shchukarev, A.; Irgum, K. *J. Sep. Sci.* **2006**, *29*, 14-24.

(32) Ngola, S. M.; Fintschenko, Y.; Choi, W.-Y.; Shepodd, T. J. *Anal. Chem.* **2001**, *73*, 849-856.

(33) Sangster, J. *J. Phys. Chem. Ref. Data* **1989**, *18*, 1111-1229.

(34) Freed, B. K.; Biesecker, J.; Middleton, W. J. *J. Fluorine Chem.* **1990**, *48*, 63-75.

(35) Gladysz, J. A.; Curran, D. P.; Horvath, I. T., Eds. *Handbook of Fluorous Chemistry*; Wiley-VCH: Weinheim, Germany, 2004.

(36) Clarke, S. R.; Shanks, R. A. *J. Macromol. Sci., Chem.* **1982**, *A17*, 77-85.

(37) Bakry, R.; Stoeggl, W. M.; Hochleitner, E. O.; Stecher, G.; Huck, C. W.; Bonn, G. K. *J. Chromatogr., A* **2006**, *1132*, 183-189.

(38) Geiser, L.; Eeltink, S.; Svec, F.; Frechet, J. M. J. *J. Chromatogr., A* **2007**, *1140*, 140-146.

(39) Gibson, G. T. T.; Marecak, D. M.; Oleschuk, R. D. *J. Sep. Sci.* **2009**, *32*, 4025-4032.

(40) Skoog, D. A.; Holler, F. J.; Nieman, T. A., Eds. *Principles of Instrumental Analysis*, 5th ed.; Harcourt Brace College Publishers: Orlando, Florida, 1998.

Chapter 3: Fluorous Porous Polymer Monolith Development

3.1 – Introduction

Although they are often thought of as predominantly being materials that are used as frits in microsphere-packed columns, a large body of work has also been devoted to the use of porous polymer monoliths (PPMs) as stationary phases for chromatography. Some of the earliest work in this field was proposed by Hjertén,[1] who suggested the possibility of using macroporous polymer plugs as novel separation media for liquid chromatography. This idea was later taken up by both Svec and Fréchet, who published an extensive series of papers examining these PPM materials and the factors affecting their formation.[2-6]

To begin, the mixture designed to generate a PPM typically contains a monomer (group with one vinyl functionality), cross-linking agent (group with multiple vinyl functionalities), polymerization initiator (UV or thermal based), and a porogenic solvent. Upon decomposition of the free-radical initiator, polymer begins to form in solution, with precipitation occurring when the solid reaches a point where it is no longer soluble in the reaction medium (either as a result of excessive cross-linking or poor solvating capacity of the porogenic species). This produces many individual granules of polymer, which will ultimately comprise the backbone of the PPM.[4] Since the porogen is chosen such that it is a comparatively poor solvent for the polymer as compared to the mixture of monomers and cross-linker, there is a preference for polymerization to selectively occur within the granules of polymer as opposed to in the bulk solution should this be possible. This results in the swelling of the polymer after precipitation, growing the size of the granules. Eventually, these granules become large enough that they can begin to associate into clusters, which in turn will become large enough to come in contact with other clusters

and become linked by the ongoing polymerization. This scaffolding is reinforced by further cross-linkage and the capture of any chains of polymer remaining in solution, leading to the ultimate formation of the PPM structure.[4] It is interesting to note that the porous structure that is imparted onto a PPM is a permanent feature arising from the granular nature by which it is formed, meaning that it remains in the dried state. This is unique as compared to many other polymeric species, which require solvent swelling to impart a degree of porosity.[7]

Porosity within a PPM can be classified in three levels: micropores (diameters less than 2 nm), mesopores (diameters from 2 to 50 nm), and macropores (any diameter over 50 nm).[4] The macroporous structure is generally accepted to arise from the volume fraction of porogenic solvent originally used for polymerization, since it is immiscible with the growing polymer granules and will therefore form voids in the growing PPM backbone.[4, 7, 8] The rest of the porous structure can be controlled by the choice of reaction conditions, with porogenic solvent composition playing one of the key roles.[9] When the solvent is sufficiently well matched that it can compete with the growing polymer granules for monomer and cross-linking units, phase separation is slow to occur since there is no preference between the two phases. This means that the polymer granules tend not to swell, which limits the formation of clusters that would otherwise form the backbone of the PPM. The result is a large number of very small polymer granules, shifting the porosity of the PPM to smaller values. Conversely, choosing a porogenic solvent that competes quite poorly with the growing polymer granules for monomer and cross-linker allows more of the swelling and interconnection to occur, leading to a backbone with relatively large individual units and larger pore sizes.[9]

Another factor that plays an important role in the porous structure of the PPM is the choice of free-radical initiator, as UV or thermal initiation give rise to different levels of control.[10] For example, when using a thermal initiator, the porosity of the PPM can be controlled by factors such as the extent and rate of heating,[5, 6, 11] while UV initiation presents similar controls in the length of exposure to light and the choice of experimental wavelength (different initiators have their efficiency dictated by the choice of UV light source).[9, 12, 13] These factors can be used in conjunction with the composition of the porogenic solvent to tailor the porosity of the resultant PPM, affecting its capacity and efficiency for separation in the process. Since monolithic columns are solid rods of polymer and not filled with chromatographic particles like many conventional columns, considerations of particle size are replaced by the size and extent of porosity when it comes to discussions of chromatographic efficiency.[14] In general, monolithic columns have the advantage of high permeability arising from their macroporous nature, as well as efficient mass-transfer resulting from the granular nature of the backbone (a series of small, porous structures permit rapid sample movement).[15] This makes them quite attractive as separation media, since they improve upon many of the important factors required for efficient chromatography.

In summary then, PPM as a separation medium has the advantages of facile formation (no difficult packing required), excellent control of porosity (and related separation efficiency), and a variety of system designs (choices of monomer, cross-linker, initiator and porogen).[16] It has seen uses in a variety of different areas, including studies on improved (versatile) chromatographic media,[17-22] specialized applications designed for protein separations,[23, 24] and novel use as an emitter for ESI (the inherent porosity provides multiple spray points to improve the electrospray process).[25-28] These

applications do an excellent job of showing the breadth of study PPM can be used to facilitate, as well as the growth of the field in recent years.

In previous chapters it has been noted that the predominant stationary phase option in fluorous chemistry is functionalized silica, with little attention paid to the suitability of fluoropolymers as a competing medium. This is somewhat unexpected, as given the benefits associated with PPM technologies relative to microsphere-packed columns (the elimination of discrete microspheres in favour of a continuous polymer rod eliminates sphere movement, void formation, and the subsequent reduction in chromatographic efficiency), it is expected that a fluorous PPM would already have been tested. As well, given the commercial availability of monomers and cross-linking agents with an inherent fluorous nature, it seems relatively facile to prepare and test materials of this type. This is not to imply that materials based on fluorous polymers are not already known, as microspheres formed from fluorous acrylates have been used for over 20 years,[29] and stationary phases based on fluoropolymers are not uncommon (even though they still pack these columns with the polymer rather than creating it as a monolith).[30, 31] Fluorous polymers have also seen use as valves in microfluidic devices,[32-35] and the superhydrophobic properties of fluorinated layers frequently appear in surface and materials publications.[36, 37]

Interestingly, work by Wang et al. on mesoporous carbon monoliths rendered superhydrophobic by treatment with a fluoroalkylsilane represents the closest analogue to a fluorous PPM that could be used as a stationary phase for fluorous chromatography,[37] and even then, it was never tested in this capacity. Consequently then, this is an area worthy of further exploration, as combining the versatility of monolithic materials with the potential inherent to fluorous separations seems beneficial. With the feasibility of

fluorous polymerization already briefly explored during my previous work with microsphere entrapment (Chapter 2), this is a logical extension of the ideas touched upon there. To this end, fluorous monoliths of differing compositions were formed and compared with their non-fluorous analogues, allowing an assessment of their relative structure, function and utility to be performed. Similarly, the specificity of the optimized monoliths for fluorous separations was explored and discussed, and the potential applications for materials of this type were detailed.

3.2 – Experimental

3.2.1 – Materials: Butyl acrylate (BA; Figure 3.1), 1,3-butanediol diacrylate (BDDA), benzoin methyl ether (BME), 3-(trimethoxysilyl)propyl methacrylate (TMSPMA), triphenylphosphine oxide (TPPO), ammonium formate, fluorene (zone-refined, 99%), phenanthrene (zone-refined, 99.5+%), pyrene (sublimated, 99%) and DL-dithiothreitol (99%) were obtained from Aldrich (Oakville, ON), while 1H,1H-heptafluorobutyl acrylate (FBA) and 2,2,3,3-tetrafluoro-1,4-butyl diacrylate (TFBDA) were purchased from Oakwood Products (West Columbia, SC, USA). Mixtures of fluorous-tagged carbamates with either an N-substituted 4-nitro-benzyl group ($C_{17+x}H_{17}F_{2x+1}N_2O_4$; x=3, 4, 6 and 8; named N1, N2, N3, N4, respectively, according to fluorous tag length; Figure 3.2) or 4-phenyl-benzyl group ($C_{23+x}H_{22}F_{2x+1}NO_2$; x=3, 4, 6 and 8; named P1, P2, P3, P4, respectively, according to fluorous tag length) were custom analytes synthesized by Fluorous Technologies (Pittsburgh, PA, USA), who also provided diphenyl-[4-(1H,1H,2H,2H-perfluorodecyl)phenyl]phosphine oxide (1F-PO), bis[4-(1H,1H,2H,2H- perfluorooctyl)phenyl]phenylphosphine oxide (2F-PO), and N-[(3-perfluorohexyl)propyl]iodoacetamide. Custom peptide (acetylated leucine-leucine-cystine-leucine-leucine; Figure 3.2) with purity greater than 90% was synthesized by JPT

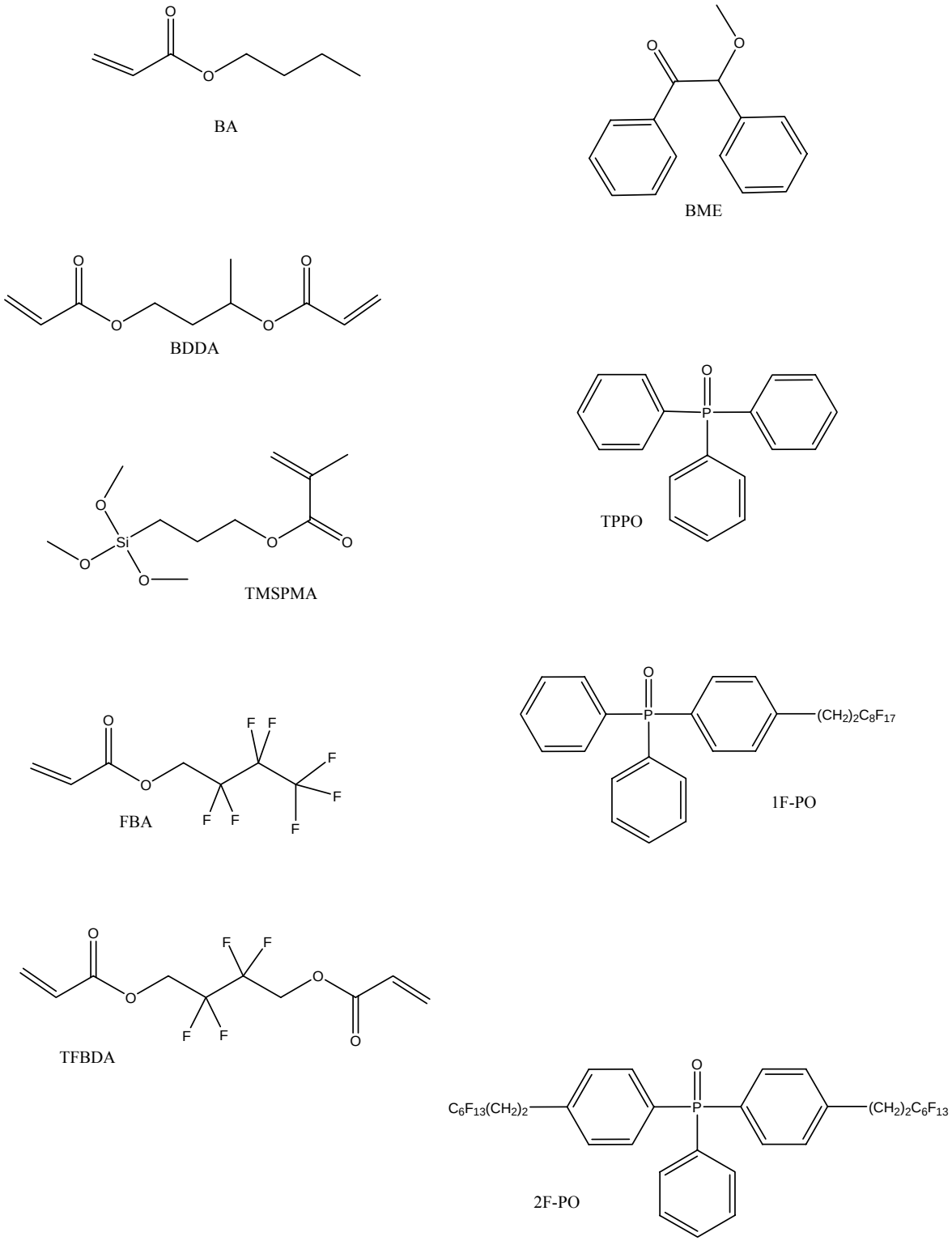

Figure 3.1: Structures of standard compounds employed.

Peptide Technologies GmbH (Berlin, Germany). Glacial acetic acid, acetonitrile (HPLC grade) and tetrahydrofuran (certified) were obtained from Fisher Scientific (Nepean, ON), formic acid (98%) was purchased from BDH Chemicals (Toronto, ON), and ethanol (95%) was acquired from Commercial Alcohols (Brampton, ON). Water for aqueous solutions was purified by a Milli-Q system (Millipore; Bedford, MA, USA) to a value of 18.2 MΩ. All reagents were used as received without further purification.

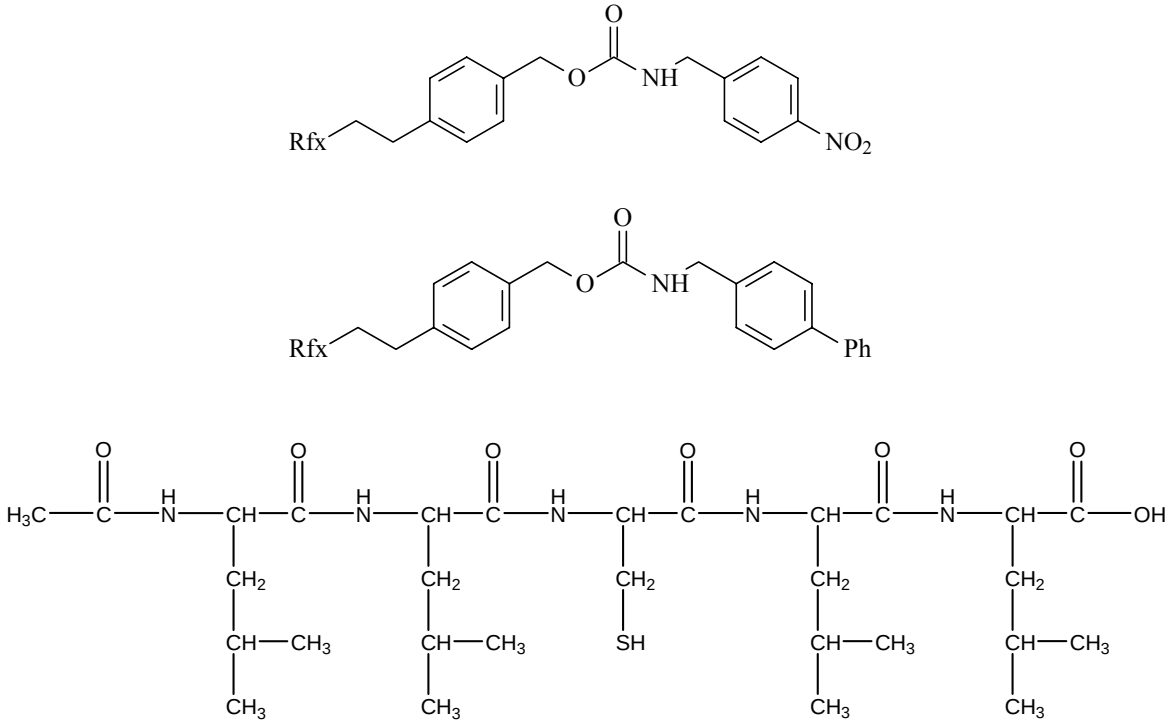

Figure 3.2: Structures of custom-synthesized analytes employed: 4-nitro-benzyl substituted carbamate mixture (top), 4-phenyl-benzyl substituted carbamate mixture (middle) and custom peptide (acetylated-LLCLL; bottom). For the carbamate mixtures, the fluorous tag (R_{fx}) can be any one of C_3F_7, C_4F_9, C_6F_{13} or C_8F_{17} for either structure.

3.2.2 – Monolith Formation: All monoliths were formed in fused silica capillaries (75 μm I.D., 363 μm O.D. with a UV-transparent coating; Polymicro Technologies; Phoenix, AZ, USA). Prior to use, the interior of the capillaries were functionalized with vinyl groups to facilitate monolith attachment using a pre-treatment procedure originally

described by Ngola et al.[38] Briefly, the capillary was first flushed with a solution of 3-(trimethoxysilyl)propyl methacrylate (20%, all quantities volume percent unless otherwise stated), purified water (50%) and glacial acetic acid (30%), then left filled with a static volume of this mixture overnight to react. Subsequently, the capillary was flushed with a mixture of acetonitrile (60%), ethanol (20%) and purified water (20%), and could then be used directly or stored (filled with the flushing solution) until needed.

The monoliths selected for study covered a variety of polymerization mixtures, comprising each of the available combinations of monomer and cross-linking agent, as well as a number of different densities (density here being defined as the amount of polymer-forming component relative to porogenic solvent). As an example, a density of 20% would represent a mixture that contained 20% (by volume) of a solution of monomer and cross-linker, with the remaining 80% of the mixture made up by the porogenic solvent. Finally, all mixtures were finished by adding 1 μL of 3-(trimethoxysilyl)propyl methacrylate per millilitre of polymerizable material to encourage polymer attachment to the capillary walls, as well as 2 mg/mL benzoin methyl ether to serve as radical initiator.

As a result of miscibility issues between the most heavily-fluorinated polymer mixture (FBA + TFBDA) and the porogen (60:20:20, acetonitrile:water:ethanol), it was necessary to keep the percentage of the monomer and cross-linker to 20% of the total volume when dealing with this solution. Similarly, other mixtures with a fluorous component were handled in the same manner for a number of tests so that their results would be comparable. Conversely, when mixtures of BA and BDDA were examined, it was found that percentages of monomer and cross-linker that amounted to less than 25% of the total volume resulted in monoliths that were highly unstable and irreproducible. As such, these solutions were prepared with slightly reduced porogen totals in the interest of

producing the most stable column possible. In an attempt to maintain consistency despite these necessary changes, the ratio of monomer to cross-linker was held consistent (70:30 v/v) for all solution types and in all studies regardless of porogen content.

Monolith formation was the result of UV-initiated radical polymerization, catalyzed by a Spectroline hand-held 8 W UV lamp (model ENF-280C; Fisher Scientific; Nepean, ON) emitting a wavelength of 254 nm at a distance of ~2 cm from the capillary being irradiated. After manual introduction of a polymer solution into a length of pre-treated capillary by syringe, any regions where polymer was undesirable were masked such that exposure to the UV source for 5 min produced a stable monolith of controllable length and location for all of the mixtures examined. Unfortunately, small amounts of heterogeneous polymer still tend to form at the boundaries between the masked and exposed regions, presumably due to leaching under the photomask. In these areas the monolith morphology is uncontrollable and unpredictable, meaning that they need to be eliminated prior to testing. This can easily be accomplished by forming a monolith that is slightly longer than the desired length and subsequently cutting off the two boundary regions to leave a material of the proper scale and without any structural concerns.

Following formation and trimming, monoliths were flushed with a solution of acetonitrile and purified water (95:5 v/v) using a Waters model 590 HPLC pump (Milford, MA, USA) for at least 30 min per cm of polymer at a flow rate of ~10 μL/min to remove any unreacted monomer or cross-linker prior to column storage or use.

3.2.3 – Scanning Electron Microscopy: Scanning electron microscopy (SEM) images were obtained using a Jeol JSM-840 scanning microscope (Tokyo, Japan). Small pieces of capillary were mounted on aluminum stubs using tape such that an unobstructed view of their cross-section was possible, permitting examination of the polymer contained

within. Prior to imaging, the stubs were coated with a thin layer of gold using a Hummer 6.2 Sputtering System (Anatech; Hayward, CA, USA).

3.2.4 – Backpressure Measurements: The flow-induced backpressure for each of the monoliths was assessed using an Eksigent NanoLC pump (Livermore, CA, USA) with a 1:1 acetonitrile/purified water solvent composition. For analysis, columns were cut to an exact length (either 1 or 10 cm), with a small amount of empty capillary also left prior to the monolithic bed for the purposes of fluidic connections. Each column was flushed for at least 20 min prior to the start of data collection, with measurements then taken at five different flow rates between 200 and 1000 nL/min. A total of 15 pressure readings were collected over a span of 45 s for a given flow rate, with their average then being taken as the representative pressure for that trial. This process was repeated twice for each of the five flow rates (with 5 min of waiting time between measurement sets) to determine all of the average pressures.

The resulting plots of observed pressure versus flow rate for all of the columns exhibited high degrees of linearity ($R^2 > 0.99$), so the slopes of their corresponding regression functions were taken as the best representations of the associated backpressure.[39, 40] In turn, these values were also used as a means of quantifying the relative porosities of the different monolith compositions.

3.2.5 – Sample Preparation for Chromatography: Samples of TPPO, 1F- and 2F-PO were prepared at varying concentrations in a solvent of methanol and 10 mM ammonium formate (60:40 v/v). This is a typical system for fluorous analyses, with benefits reported in terms of analyte retention and resolution.[41, 42] Injections of this same solvent acted as the blank for all of the associated chromatographic trials. For the polyaromatic hydrocarbons (PAHs), a solvent of 20% acetonitrile in water was selected. Fluorene and

phenanthrene were prepared at concentrations of 3 μM, while pyrene was prepared at 30 μM (chosen to help keep peak intensities similar despite differing molar absorptivities).[43]

The 4-nitro-benzyl substituted carbamate mixture was prepared at a concentration of 0.24 mg/mL in acetonitrile, while the 4-phenyl-benzyl substituted carbamate mixture was prepared at 0.167 mg/mL in acetonitrile. These concentrations were also maintained when mixtures of both sets of carbamates were prepared. For the fluorous tagging of the custom peptide, it was initially dissolved in acetonitrile to achieve a concentration of 125 μM, then combined with 4 μL of 45 mM dithiothreitol (in water) and 10 μL of 10 mM N-[(3-perfluorohexyl)propyl]iodoacetamide (in tetrahydrofuran). This mixture was shielded from light and allowed to react for 90 min at 37 °C, after which point it was diluted with 581 μL of water and subsequently analyzed.

3.2.6 – Liquid Chromatography: All chromatographic tests were performed using a Waters nanoAcquity UPLC system fitted with a tunable UV detector, and operated by the MassLynx software package (v 4.1). Columns were 10 cm monoliths of varying fluorous composition, coupled in-line with the detector using both a standard, transparent Teflon sleeve (detector side of capillary), as well as a high pressure fitting and capillary outfitted with a NanoTight union (P-779-01) and MicroTight Fittings (F-125X; sleeve F-185X) from Upchurch Scientific (Oak Harbor, WA, USA) to allow proper coupling of the PPM column with the high-pressure valve of the nanoAcquity.

The system was setup with a 2 μL sample loop, and used the full-loop injection method to introduce samples. No column heating was employed for any of the tests, while the autosampler compartment was maintained at 25 °C. Detection set the UV lamp at either 228 nm (the determined optimum for the fluorous analytes) or 254 nm (an

optimum for polyaromatic hydrocarbons). System flow was maintained at a steady rate of 400 nL/min.

Analysis made use of a gradient method, mixing an aqueous phase (99.9% purified water with 0.1% formic acid) with an organic (99.9% acetonitrile with 0.1% formic acid). Initial conditions were 99% aqueous, switching to 10% aqueous over 15 min. From there, the gradient changed to 1% aqueous over 5 min, and then finally back to 99% aqueous in 1 min to give a method time of 21 min. When injection and re-equilibration times for the system were also factored in, the total time for a single run was 40 min. System pressures at representative solvent compositions throughout this gradient profile were noted, allowing comparisons of different column responses.

3.2.7 – Determination of Void Volumes: Monolithic columns (10 cm) were initially run under isocratic conditions (98.9% purified water, 1% acetonitrile and 0.1% formic acid) on the nanoAcquity at a constant flow rate of 400 nL/min, followed by injection of a 2 μL plug of the solvent used for chromatography (60:40 v/v methanol and 10 mM ammonium formate). By monitoring the UV response at 228 nm it was possible to determine the point at which this solvent had passed entirely through the column, allowing it to serve as an unretained marker. If this same injection process was also performed without a column in place (system directly coupled to the UV detector), a shorter time between sample introduction and detection was observed. The difference between the times with and without a column in place (in minutes) represented the additional volume introduced by the monolith, so with the constant flow rate of 400 nL/min taken into consideration, a void volume for each PPM could be obtained.

3.2.8 – Electrospray Ionization Mass Spectrometry: Liquid chromatography with electrospray ionization mass spectrometry was performed on an API 3000 triple-

quadrupole mass spectrometer (MDS SCIEX; Concord, ON). A fluorous monolith (10 cm; 30% total polymerizable material) was first mounted between the pump (NLC-1DV-500; Eksigent) and a 54 hole, photonic fiber-based emitter of the type previously reported by our group[44] using a MicroTee union (Upchurch Scientific; Oak Harbor, WA, USA). Ionspray voltage was applied after the fluorous column (through the union), and maintained at 3.55 kV during gradient elution. The distance between the outlet of the fiber-based emitter and the orifice of the mass spectrometer was 8 mm. For the gradient, aqueous phase (A; 99% water, 1% acetonitrile, with 0.1% formic acid relative to the volume of water plus acetonitrile) and organic phase (B; 99% acetonitrile, 1% water, with 0.1% formic acid relative to the volume of acetonitrile plus water) were combined in differing ratios to comprise the mobile phase. The gradient employed was 90% to 10% A over 15 min, 10% A to 1% A over 10 min, back to 90% A in 1 min, and finally 90% A maintained for 10 min to give a total run time of 36 min. The flow rate was constant at 400 nL/min for all steps, with a sample loading time of 1 min.

3.3 – Results and Discussion

3.3.1 – Initial Assessment of Monolith Porosities: One of the primary concerns with varying the monomer or cross-linker in the different monoliths is the effect that this can have on the porosity of the resultant PPM. With the addition or subtraction of fluorine from the respective polymer components, there exists the possibility that this will produce monoliths of differing structure. In turn, this could alter the chromatographic properties through factors other than the chemical composition of the column. When determining the porosity of a PPM, the solubility of the resultant polymer in the porogenic solvent during its growth acts as a major contributor.[7] As such, it is reasonable to suspect that fluorous polymeric materials will behave differently than their non-fluorous equivalents

during formation given the literature that exists on the unique characteristics and solvent preferences of other types of fluorous materials.[45] While the porogenic solvent used here is assumed to be sufficiently polar that it should produce similar effects in both the fluorous and analogous, non-polar species, confirmation is required.

To this end, flow-induced backpressure in tandem with SEM imaging provides a combination of quantitative and visual evidence in concert with relative ease of use. Although a method such as mercury intrusion or gas sorption is more typically chosen as an absolute quantifier for the total sample porosity, these techniques do not provide realistic models for capillary-bound monoliths in that they require large quantities of material and cannot account for any swelling that occurs in the presence of solvent. In their place, a simple assessment that all of the monolithic materials possess similar flow permeabilities is desired such that effects on chromatography arising from factors other than the amount of fluorous substitution can be ruled out. It has already been shown that the slope of a calibration curve encompassing a range of backpressures resulting from different flow rates at a static solvent composition is an excellent predictor for total sample porosity,[39, 40] as well as providing a realistic model for the normal column conditions. Similarly, visual inspection of the dried monolithic structure by SEM can also be used to reinforce the assertion that all of the PPM materials are physically similar in terms of polymer morphology and comparable to the backpressure results.

For the initial tests, four main PPM compositions were examined (each of the combinations of monomer and cross-linker when FBA, TFBDA, BA and BDDA were the available options), with the slopes (units of kPa per nL/min) acquired for flow rates between 200 nL/min and 1 μL/min for 1 cm of PPM conforming to the expected linearity. Although only the results at 1 μL/min are shown in Table 3.1 for comparison purposes,

others would be equally valid given that the results scale linearly for all flow rates at the same solvent composition. From here, it can be noted that for the three PPM compositions with 20% of the monomer/cross-linker mixture, the results from the backpressure testing were all very similar. While the observed backpressures from column-to-column were not very reproducible for any of the three mixtures (as evidenced by standard deviations in the range of 50%), this variation can likely be attributed to the monolithic structures forming in an irreproducible fashion. With only 20% polymer-forming component relative to the porogen, it is expected that there will be a significant variation in the structure of monoliths that are formed from a particular solution. Interestingly, this inherent structural variation at lower polymer densities will mean that the standard deviation for pressure will not follow a Gaussian trend (explaining their magnitude here), but rather, a more complex fitting parameter would have to be used to properly address their distribution. Finally, it is worth noting the lower-than-average backpressure for the FBA + BDDA PPM that can be observed here, since this difference is also noticeable when dealing with the chromatographic results (*vide infra*).

Table 3.1: Flow-induced backpressure for a series of 1 cm monolithic columns at solvent flow rates of 1 μL/min.

PPM Composition	**Backpressure (kPa per nL/min) for 1 cm of material**
20% FBA + TFBDA	386 ± 131
20% FBA + BDDA	303 ± 186
20% BA + TFBDA	372 ± 179
25% BA + BDDA	462 ± 14

Each value reported is an average of the results from four replicate columns, along with the associated standard deviation (n = 4).

Looking next at the BA + BDDA mixture (containing 25% monomer/cross-linker by volume) the average backpressures were predictably higher than those at 20% owing to the greater percentage of monolith-forming components (and therefore less total pore volume). Despite this difference, it is doubtful that any serious effect on the chromatography will result given the degree of variability that is already inherent to the monoliths. Perhaps the more interesting result is how the change in composition managed to enhance the reproducibility of the resultant monoliths. The average results for four different BA + BDDA columns showed substantially less deviation than any of the other materials, as well as eliminating the column instability that was observed when a PPM of BA + BDDA with 20% of the monomer/cross-linking mixture was attempted. Although the fact that increases in the amount of polymerizable material can produce effects on the resultant monolithic structure has already been alluded to in the literature,[46] it was still surprising to note how suddenly the change can be observed for seemingly minute compositional differences such as those exhibited here.

As a second gauge of PPM porosity, images taken by SEM served to confirm the conclusions suggested by the backpressure readings. Visually, the sample porosities were quite consistent (as shown in Figure 3.3), although the mixture of 25% BA + BDDA was expectedly denser than all of the others. Additionally, as observed for the backpressure readings, columns made with 25% monomer mixture instead of 20% provided monoliths with better structural reproducibility both from cut-to-cut and batch-to-batch upon visual inspection. This is the result of increased amounts of polymer-forming components in solution (affecting solubility and nucleation during growth), which further explains and confirms the observed trends in deviation for the backpressure readings reported earlier.

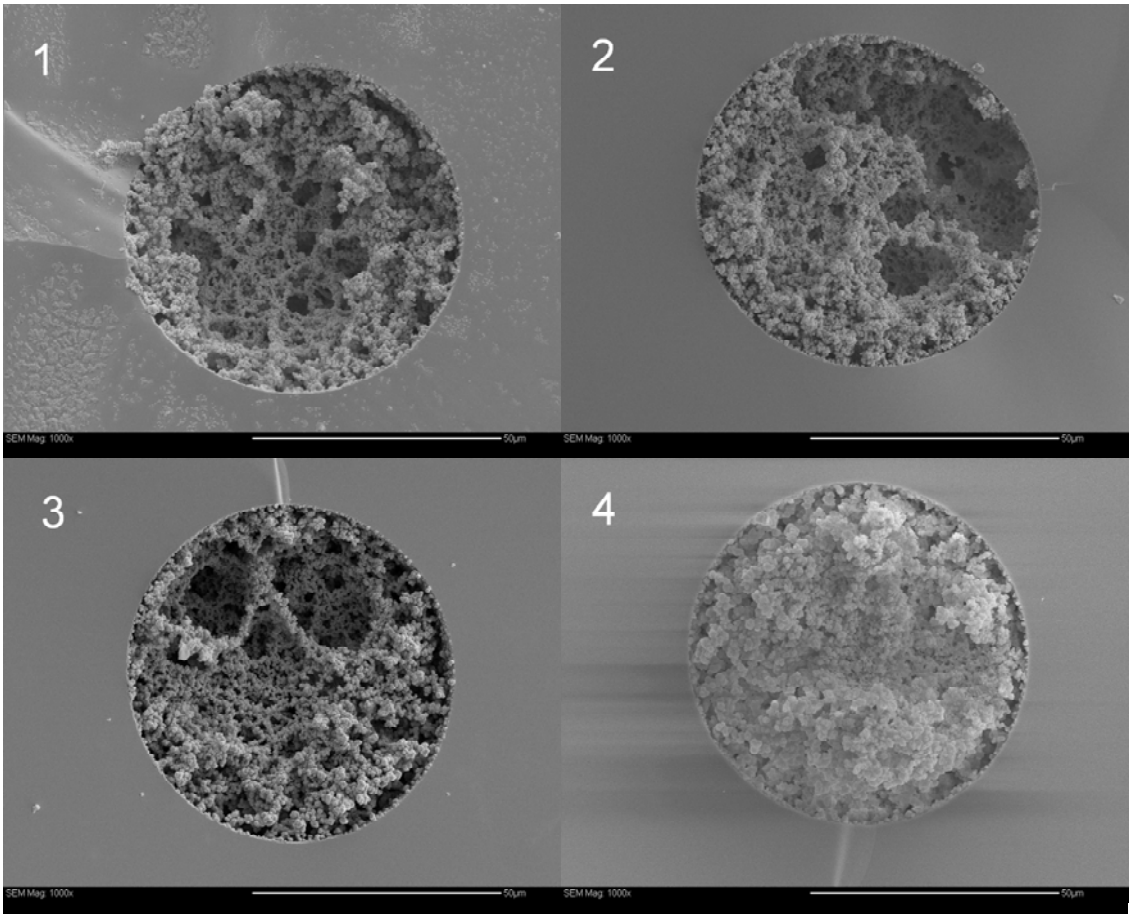

Figure 3.3: SEM images for the four PPM compositions: 1) FBA + TFBDA, 2) FBA + BDDA, 3) BA + TFBDA, and 4) 25% BA + BDDA. The structural similarities for the three mixtures with 20% monomer/cross-linker can be noted, as can the denser PPM resulting from the increase to 25%. While the individual polymer nodules remain structurally similar regardless of composition, monolith density increases or decreases depending on the particular mixture.

In addition to the assessment of backpressure, another factor that must also be considered with respect to the overall porosity of the columns is the void volume that is associated with each PPM composition. Should the voids be significantly different between any of the columns, the subsequent retention values that would be determined would not accurately express the true distinction that exists between the materials (capacity factors would instead need to be reported). To address this concern, the void

volumes for each of the monolith compositions were calculated and summarized in Table 3.2, where it can be seen that their magnitudes do not differ significantly for any of the columns under consideration. In turn, this implies that retention times will provide an accurate description of the separation efficiency for the monolithic materials, and because retention differences are also easier parameters to visualize than capacity factors, they will exclusively be presented when discussing the performance of the different columns.

Table 3.2: Observed void volumes for a series of columns comprising each of the PPM compositions.

Column		Void Volume (nL)
20% FBA + TFBDA	1	447 ± 9
	2	503 ± 7
20% FBA + BDDA	1	482 ± 9
	2	490 ± 19
20% BA + TFBDA	1	501 ± 14
	2	516 ± 12
25% BA + BDDA	1	510 ± 13
	2	522 ± 7

Two columns of each monolith composition were examined, with five different injections of unretained solvent on each column being averaged to determine the associated void volume (n = 5).

3.3.2 – Initial Monoliths Applied for Fluorous Chromatography: Given that the porosities as evaluated by backpressure and SEM were all of similar magnitude for the four different PPM compositions, it was determined that any differences in column performance during chromatography could safely be attributed to the fluorous character of the respective monoliths (keeping the inherent, physical difference of the 25% BA + BDDA mixture in mind). In terms of analytes for chromatographic testing, a series of triphenylphosphine oxides with differing fluorous tags (Figure 3.1) were selected not only

for their useful range of retention, but also because they represent analogues for targets in areas such as catalyst development where fluorous separations are frequently employed. The presence of a strong chromophore for UV detection was also desirable, allowing for a simple, online evaluation of different column characteristics using the nanoAcquity UPLC system.

In developing a gradient separation method, a packed Waters column (1.7 μm BEH130 C18, 75 μm x 100 mm; Part 186003542) was initially used to determine what conditions would be necessary for effective detection of the three analytes before final optimization on the monolithic columns. It is worth noting that although this initial test represented a reverse-phase (RP) separation rather than a fluorous one, in the absence of commercially-available fluorous columns for the nanoAcquity it served as an adequate starting point (similar conditions should promote retention and elution from both types of materials). Looking at the results from these preliminary gradient tests, it was determined that very high aqueous conditions (99%) were initially required if the TPPO was to be retained at all. When any amount of organic was used at the start of the flow profile TPPO would simply pass with the void volume, eluting without any noticeable retention on the RP column.

Although the lack of TPPO retention under the initial gradient conditions would not be a problem for fluorous chromatography (where a total lack of affinity for non-fluorinated species is desirable), because these were initially designed to be reverse-phase conditions (using a reverse-phase column), a strong selectivity for non-polar analytes like TPPO should have been observed (hence the subsequent optimization). Interestingly, since it has already been established that fluorinated columns should behave as excellent RP stationary phases when non-fluorous analytes are used,[47-49] ultimately selecting

optimized RP conditions for the subsequent analysis of the fluorous triphenylphosphine oxide series on the monolithic columns presented a useful avenue for characterization. Any differences in retention between these columns should be directly attributable to increasing fluorous character because the gradient is not biased towards fluorous retention, and factors that support reverse-phase separation mechanisms remain consistent from run-to-run. As such, this allows the PPM materials to be directly evaluated on the basis of only their fluorous character (i.e. it is the only parameter changing), and to determine how they apply to fluorous chromatographic separations.

Over the range of the gradient that was employed, pressure changes based on the solvent composition were noted for representative fluorous and non-fluorous columns, as well as the Waters column used early in the gradient optimization process (Figure 3.4). While these results show that the monolithic materials were very similar in terms of their pressures at any given solvent composition and a fixed flow rate, the conventional UPLC column packed with 1.7 μm particles gave responses that were significantly larger across all solvent compositions. Although this outcome was to be expected given the preferential pressure and flow characteristics of monolithic materials over packed columns with small particle sizes,[50, 51] the magnitude of the difference is still important given the relatively low flow rate of 400 nL/min.

For the chromatography tests, two 10 cm columns of each of the PPM compositions were fabricated in the manner previously discussed. To determine the average retention of each of the analytes, a series of injections were performed in the order of: blank, 5 μM TPPO, 5 μM 1F-PO, 5 μM 2F-PO, and finally a mixture containing 5 μM of each of the three different triphenylphosphine oxides. The retention times for each of the species were noted for the individual injections as well as the mixture, and

with two replicate columns for each PPM composition this gave four readings for each retention time. These values could then be averaged, with the results summarized in Table 3.3.

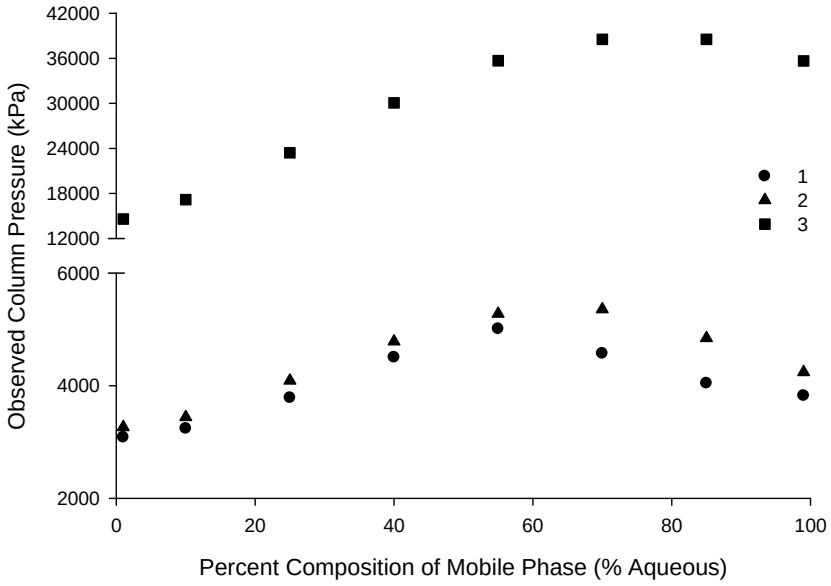

Figure 3.4: Plots of observed column pressure at varying mobile phase aqueous composition for three representative 10 cm columns of the following varieties: 1) 25% BA + BDDA, 2) 20% FBA + TFBDA and 3) packed Waters column (1.7 μm BEH130 C18). At a constant flow rate of 400 nL/min there was a significant difference between the pressures experienced by the monolithic materials relative to the column packed with microspheres. These observations are consistent over multiple trials of the same column.

Table 3.3: Average retention times for the three triphenylphosphine oxides on 10 cm columns of each of the PPM compositions.

Column (10 cm)	TPPO Retention (min)	1F-PO Retention (min)	2F-PO Retention (min)
20% FBA + TFBDA	5.87 ± 0.19	12.07 ± 0.09	14.54 ± 0.10
20% FBA + BDDA	6.14 ± 0.05	12.63 ± 0.03	15.12 ± 0.04
20% BA + TFBDA	6.77 ± 0.05	11.32 ± 0.01	12.80 ± 0.03
25% BA + BDDA	6.84 ± 0.18	11.31 ± 0.03	12.67 ± 0.01

Each value was calculated as the average of two replicate retentions for two different columns, giving four total readings (n = 4).

Looking at the results, a distinction can be observed between the columns made with fluorous (FBA) monomer and those without. While the FBA columns exhibited excellent retention for the two fluorous species, they performed less admirably for the non-fluorous TPPO which eluted relatively early and as a comparatively small signal (Figure 3.5).

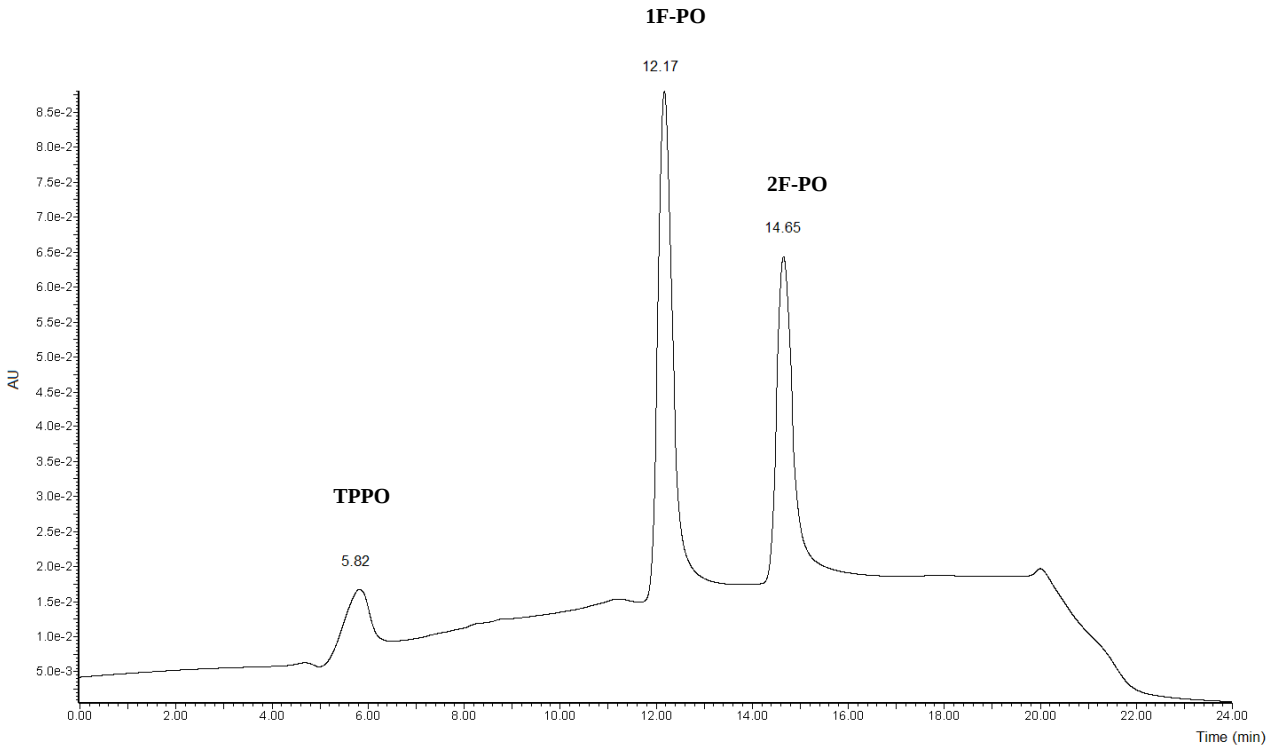

Figure 3.5: Chromatogram produced by a 10 cm FBA + TFBDA PPM column. The fluorous signals (5 µM 1F-PO at 12.17 min and 5 µM 2F-PO at 14.65 min) appear as well-resolved peaks (R_s = 4.03), while the non-fluorous compound (5 µM TPPO) elutes much earlier at 5.82 min.

Conversely, as the fluorous content of the monomer/cross-linker was decreased, columns began to exhibit more of a reverse-phase character as evidenced by their longer retentions for TPPO and concurrent decreases in selectivity towards fluorous analytes (1F- and 2F-

PO not retained as strongly; Figure 3.6). Interestingly, the two columns made with BA monomer were virtually indistinguishable in terms of analyte retention, suggesting that the interaction of analytes with the cross-linked component of the polymer was only a minor contributor to the total retention. Given the relatively small amount of cross-linker as compared to monomer this was not entirely unanticipated, although it was expected that the contribution of the fluorous TFBDA would provide slightly more of an increase in fluorous retention over BDDA than the minor improvement that was observed.

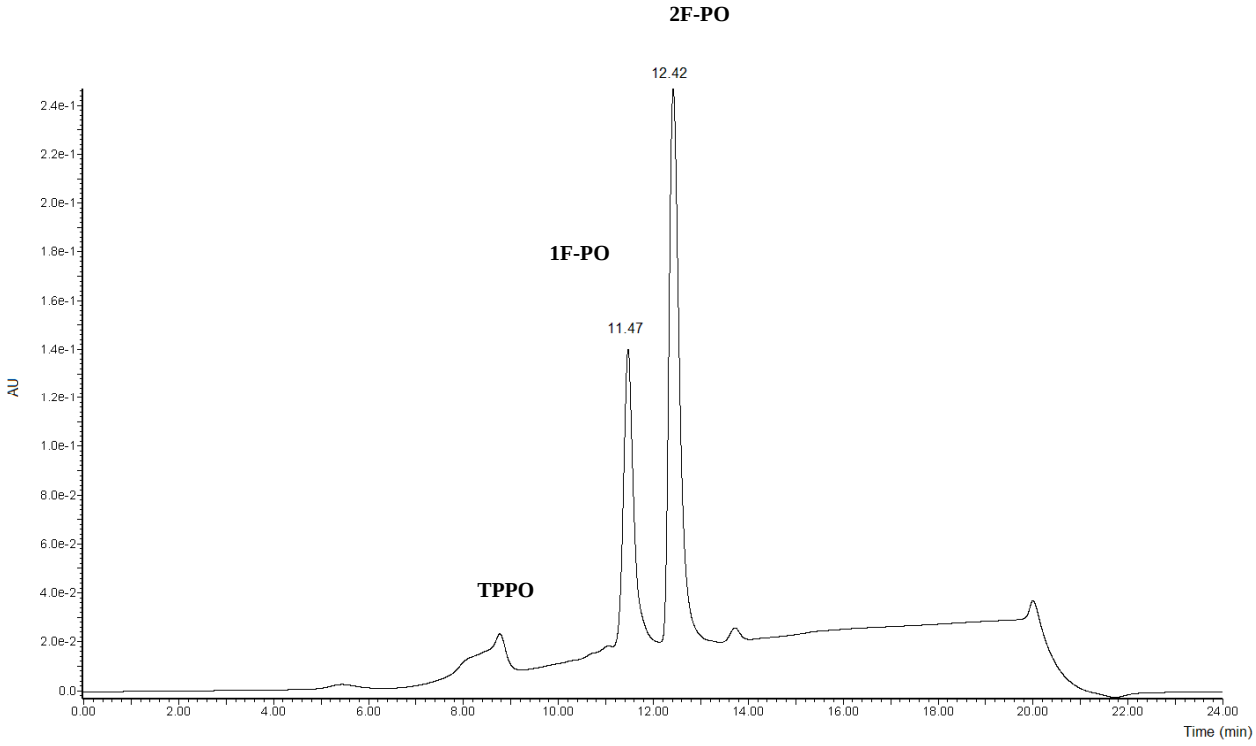

Figure 3.6: Chromatogram produced by a 10 cm, 25% BA + BDDA PPM column. Increased retention for the 5 µM TPPO signal (now at ~ 9 min) can be observed as compared to a fluorous column (Figure 3.5), while fluorous selectivity has been lessened as indicated by decreases in retention for the two fluorous-tagged peaks (5 µM 1F-PO at 11.47 min and 5 µM 2F-PO at 12.42 min) and a poorer resolution than for the FBA + TFBDA monolith (R_s = 3.72).

In terms of an absolute comparison between fluorinated and non-fluorinated monoliths, the percent difference in retention for both singly- and doubly-tagged analytes on the respective columns could be calculated. For example, looking at FBA + TFBDA versus 25% BA + BDDA, there was an increase of almost 7% in retention of the singly-tagged triphenylphosphine oxide from the non-fluorous to the fluorous column and an increase on the order of 15% for the doubly-tagged analyte. Even given the structural differences between these two monoliths, the fluorous column still provided a significant increase in retention over its non-fluorinated analogue under identical gradient conditions, which supports the idea of differential retention mechanisms for fluorous and RP materials.

As previously observed during the analysis of backpressure, the FBA + BDDA mixture was noted to behave differently than the other 20% PPM mixtures. This was again the case here, where the combination provided an unexpected result of fluorous retention that was somewhat greater than for an equivalent mixture with both a fluorinated monomer and cross-linker. It is difficult to say exactly why this is the case, although it is possible that the solubility of this particular mixture has a role during monolith formation, producing a material with greater surface area through the nature of its porosity (higher percentage of micro-/mesopores along with larger macropores). An increase in area such as this could provide enhanced retention even with the loss of fluorous groups for affinity, as well as the observed decrease in backpressure. Subsequently, the surprising performance of this particular mixture became a topic of interest, with further experiments devoted to its examination (*vide infra*).

To assess the relative performance of the four initial stationary phases, the numbers of theoretical plates as well as the plate heights were calculated for each of the

PPM types (Table 3.4). As with the retention times, both the individual injections of the fluorous analytes, as well as the mixture containing all of the triphenylphosphine oxides together were used in tabulating a result with associated uncertainty for two replicates of each PPM column (n=4). Although it is known to not be purely correct to deal with these parameters as calculated using peak widths and retention times for columns operated with a gradient (changing solvent conditions over the course of the run affect migration velocities),[52] because each column was the same length and experienced the same gradient for the same analytes it was decided that it was reasonable to use them here as absolute comparators between the different materials based purely on the simplicity of the method. This is not to say that these values could subsequently be used to compare the PPM columns with other results reported in the literature, but as a self-contained experiment they provide a valid assessment of differences in chromatography as provided by the different PPM compositions examined.

Table 3.4: Summary of pertinent column parameters for 10 cm lengths of each PPM composition.

Column (10 cm)	Number of Plates		Plate Height (μm)		Fluorous Resolution
	1F-PO	2F-PO	1F-PO	2F-PO	
20% FBA + TFBDA	5900 ± 900	9200 ± 700	17.13 ± 2.82	10.92 ± 0.81	4.07 ± 0.06
20% FBA + BDDA	5900 ± 600	10100 ± 500	17.09 ± 1.83	9.93 ± 0.52	3.93 ± 0.08
20% BA + TFBDA	9000 ± 1900	13800 ± 1800	11.47 ± 2.57	7.33 ± 0.84	3.13 ± 0.26
25% BA + BDDA	14100 ± 1500	21800 ± 3200	7.16 ± 0.77	4.66 ± 0.72	3.86 ± 0.20

The numbers of plates and plate heights were calculated as the average of two replicate retentions for two different columns, giving four total readings (n = 4). Resolution values were calculated only from injections of the mixture of triphenylphosphine oxides on each PPM column, resulting in two replicates for each (n = 2).

For the three monoliths made with 20% monomer mixtures, the numbers of theoretical plates were of similar magnitudes when deviation between columns was taken into consideration. Plate height was also found to behave in a similar manner, although the result for BA + TFBDA was somewhat low if only the 1F-PO peak was considered. This was actually a noticeable trend wherein the results as obtained from the 1F-PO peaks showed a greater spread than those for the 2F-PO, although in neither case was it so large as to say that any of the materials were substantially better or worse than the others in terms of chromatographic performance. A slightly larger change could be observed between the columns with 20% monomer mixture and the 25% BA + BDDA columns, but this can solely be attributed to differences in the surface area of a denser monolith improving the chromatography. Additionally, even with this difference in mind, the 25% BA + BDDA columns were still in the same range as the 20% columns for both parameters, suggesting that none of the four PPM compositions had a distinct advantage over the others.

In calculating the resolution that could be obtained between the two fluorous-tagged triphenylphosphine oxides during mixture injections on each of the PPM columns (Table 3.4), there was a distinct trend toward poorer resolving power as the amount of fluorination was decreased. While the 25% BA + BDDA column showed a slightly elevated resolution owing to its higher amount of polymer-forming components, it was still less effective than the most heavily-fluorinated column (20% FBA + TFBDA) at resolving the two tagged species. This in turn can be interpreted as an endorsement for the use of fluorous monoliths, as they improved the selectivity for the desirable, tagged

species without any concurrent loss in chromatographic performance over a denser and purely reverse-phase monolith.

3.3.3 – Assessment of Fluorous Monoliths in Reverse-Phase Mode: As has previously been suggested (both here and in the literature), fluorous materials should also behave as reverse-phase columns given their strongly non-polar nature. If this is the case, it remains a possibility that the retention that is being observed for the fluorous monoliths here is due to this type of interaction rather than the desired fluorous affinity (despite previous results indicating that this is not the case). This would clearly not be desirable, so to truly clarify this point, one possible avenue is to simply test the initial series of monoliths in a purely reverse-phase application to observe how they compare to their non-fluorous analogues. If the fluorous columns prove to be inferior to non-fluorinated ones for separations of non-polar analytes (lacking fluorination), it will be a strong indication that the previous affinity for fluorinated analytes was indeed due to an interaction other than simple reverse-phase chemistry (further confirming the assertions made thus far).

For the analytes in this reverse-phase testing, three polyaromatic hydrocarbons (fluorene, phenanthrene and pyrene; Figure 3.7) were selected. These species are excellent analytes for this type of validation given that they are readily-available, present distinctly non-polar structures, exist as a series with sequential changes in structure to separate, and require an effective stationary phase to be cleanly resolved.[53] If the fluorous materials outperform their competitors then, it will be a strong indication that they are powerful reverse-phase columns (a result that would potentially mitigate some of the conclusions with respect to fluorous specificity).

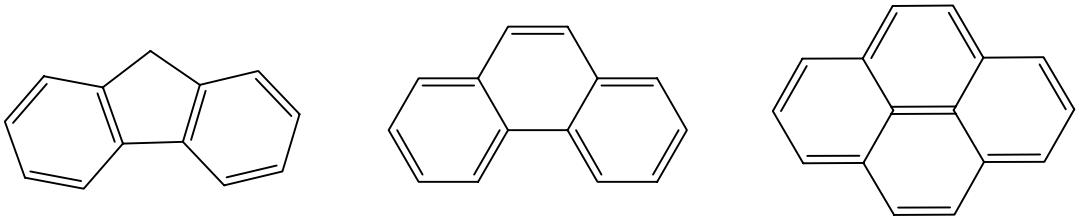

Fluorene Phenanthrene Pyrene

Figure 3.7: Structures of polyaromatic hydrocarbons examined.

For testing, the same 4 column compositions used in the initial fluorous analysis were again employed, as was the same gradient profile. Individual injections of each of the PAHs were first performed in sequence (to isolate the relevant peaks), followed by a final mixture injection to assess the resolution provided by each monolith. From the resultant chromatograms (Figure 3.8), it became clear that non-polar analytes without fluorination were poorly-resolved using a fluorous monolith. While the fluorous columns gave reasonable peak shapes during any individual injections of the PAHs, when mixtures were attempted there was always an excessive overlap of analytes that made resolution impossible. This was true for both materials made using FBA as the monomer (regardless of cross-linker), with each being outperformed by their BA analogue (Table 3.5). From these results then, it provided further evidence that the success attained earlier with the separation of the fluorous-tagged triphenylphosphine oxide samples was indeed due to a more specialized affinity. If only reverse-phase interactions were present the fluorous columns should have shown the same trends that were demonstrated with the PAHs, but since this was not the case it supports the suggestion that fluorous-fluorous interactions are a driving force in the selectivity of the new monolith compositions.

Table 3.5: PAH retention time summary on the initial monolith series.

Monolith Composition	Retention Time (min)		
	Fluorene	**Phenanthrene**	**Pyrene**
20% FBA + TFBDA	9.72 ± 0.25	9.88 ± 0.23	10.27 ± 0.22
20% FBA + BDDA	10.61 ± 0.12	10.90 ± 0.10	11.45 ± 0.08
20% BA + TFBDA	11.73 ± 0.31	12.21 ± 0.32	13.02 ± 0.31
25% BA + BDDA	12.83 ± 0.31	13.52 ± 0.30	14.54 ± 0.32

Results are expressed as the average of at least 2 runs using 2 replicate columns of each monolith composition.

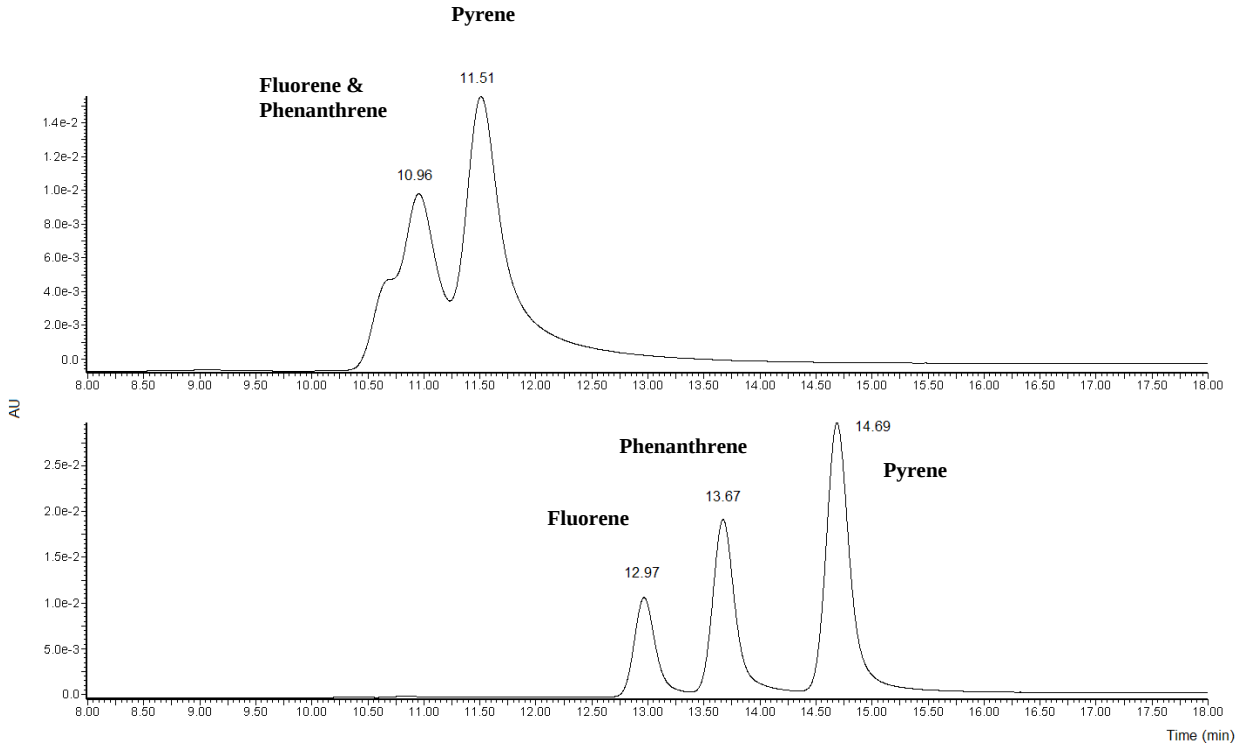

Figure 3.8: Chromatograms representing PAH mixture (3 µM fluorene and phenathrene; 30 µM pyrene) separations on a 20% FBA + BDDA column (upper panel) and a 25% BA + BDDA column (lower panel). Using a fluorous monomer meant that fluorene and phenanthrene could not be clearly resolved (they co-eluted at around 10.96 min), while the non-fluorous monolith allowed facile separation and resolution of all three PAH components.

3.3.4 – Expansion of Monolith Characterization: Through these previous tests on the four initial PPM compositions, it became evident that there was specificity inherent to the fluorous columns that was not attributable to a reverse-phase interaction. Additionally, with the superior performance of materials that eliminated the use of a fluorous cross-linker in favor of the non-fluorous analogue, it seemed that monolith structure and composition were significant contributors to the overall product. Although reducing the total amount of fluorine (by eliminating cross-linker fluorination) seems counterintuitive at first, it does make sense when further considering PPM formation. If a denser material can be formed through a more uniform polymerization reaction, this means that greater amounts of fluorine will be available in the resultant stationary phase. The cross-linker is already a relatively minor component of the polymerization mixture, and because it should therefore be less represented in any subsequent material relative to the monomer, its structure provides only minor (if any) impact on the selectivity. When considering this fact in conjunction with the issue of mixture solubility that was experienced when both fluorous monomers and cross-linkers were employed together, it becomes more plausible that eliminating the fluorous cross-linker could actually provide a superior fluorous monolith. If a denser material can be formed through better polymerization of an initially-homogeneous mixture, this should actually provide an increase in fluorine (more monolith backbone with predominantly fluorous monomer) relative to that which is lost by eliminating the negligible contribution of the fluorous cross-linker. Additionally, the improvements in solubility gained by switching exclusively to a BDDA cross-linker also mean that the total amount of polymerizable material (70:30 v/v monomer:cross-linker) relative to porogen can be increased from the limit of 20% previously imposed by the

poorly-soluble FBA + TFBDA mixture, meaning that a much more extensive series of monolith structures can be formed and tested. From here then, the next logical set of experiments involved creating a series of different monolith densities to explore (both structurally and chromatographically), with the goal ultimately being to assess the degree to which these factors actually impact the performance of the monoliths for fluorous chromatography.

3.3.5 – Assessment of Pressure Trends with Varying Monolith Density: Looking first at a plot of backpressure versus density (Figure 3.9) for a series of monoliths with densities ranging from 20% to 35% (see Experimental section 3.2.2 for formation methodology), there is an obvious trend toward higher pressures as the amounts of polymer-forming components are increased.

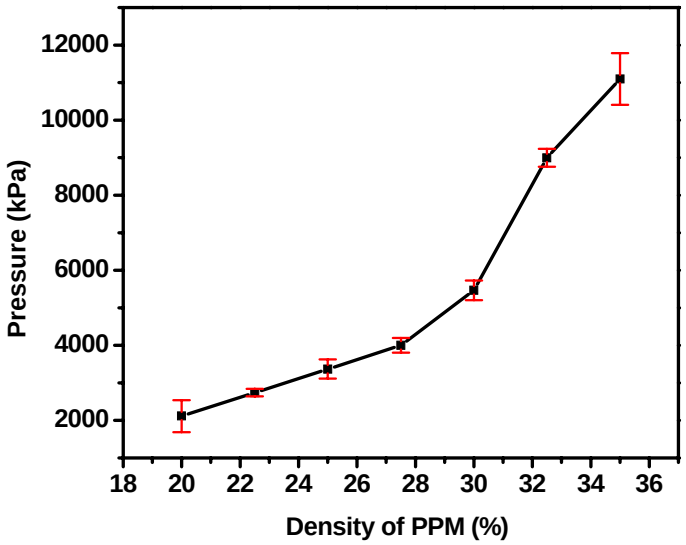

Figure 3.9: Backpressure for 10 cm of fluorous PPM with different densities. Each data point is the average of the results for three replicate columns. Error bars represent the associated standard deviations.

It should be noted that the errors for both the 20% and 35% formulations are relatively high (approximately 427 kPa and 689 kPa respectively) as compared to the other mixtures (which are all less than 276 kPa), although for entirely different reasons in each case. For

the column with 20% total polymerizable material, the small amount relative to a large porogenic solvent content results in significant, inhomogeneous macropores and poor PPM robustness (*vide supra*).[4] Conversely, for the column with 35% polymerizable material, the solubility of the fluorous monomer in the porogen becomes sufficiently poor such that heterogeneous polymerization and inconsistent porosity are the result (regions of both dense polymer and large, heterogeneous macropores coexist).

If the results from Figure 3.9 are compared to those obtained using SEM (Figure 3.10), the same basic trends can be observed. The reproducibility of the fluorous monoliths appears to be optimal at a composition of around 30%, with mixtures on either side of this point showing a greater propensity for void formation and irregularity. It was previously noted in the initial series of monoliths using FBA, TFBDA, BA and BDDA that no significant change in structure occurred in a PPM when switching between fluorous and non-fluorous components,[54] although those results did not have two exactly analogous mixtures to completely verify the point. Here, this previous assertion can indeed be confirmed, as looking at the physical structures of the 30% fluorous monolith and its non-fluorous analogue (replacing FBA with BA), there was no discernible visual difference between the polymeric networks that resulted (Figure 3.10, panels E and H).

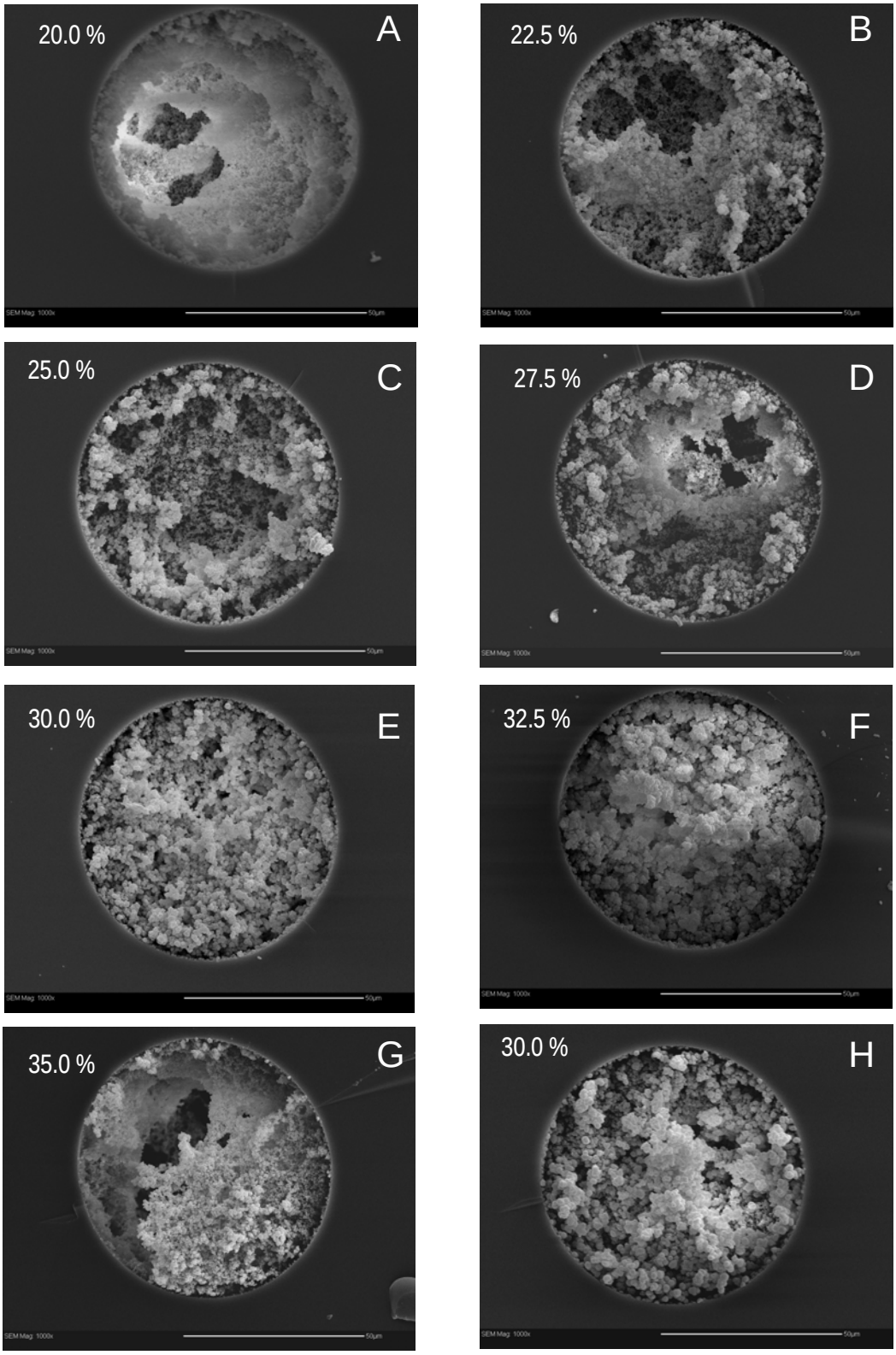

Figure 3.10: SEM images of PPM in capillary. Images A – G are for fluorous monoliths with different total concentrations of polymerizable material, while H is for a non-fluorous monolith (the direct analogue of column E).

One of the most useful conclusions drawn from the initial work with fluorous monoliths (and the basis for these tests) was that fluorous separations were not hindered by switching from fluorous to non-fluorous cross-linkers, but rather showed noticeable improvements in performance.[54] At the time it was hypothesized that the solubility gain incurred by eliminating the fluorous component yielded a more uniform polymerization, offsetting the loss in specificity that would accompany the removal of fluorine from some of the monolithic substrate and also allowing denser monoliths to be formed. These subsequent tests have now shown these assumptions to be accurate, forming a series of fluorous monoliths using solutions that would have been impossible to create if limited by the solubility of a fluorous cross-linker. The more saturated polymerization solutions subsequently allow the benefits of greater densities to be realized in fluorous monoliths,[50] meaning that truly optimized regimes (such as those seemingly around the 30% solution discussed here) can be further explored.

3.3.6 – Chromatographic Performance with Varying Monolith Density: Testing column performance for the various PPM formulations under chromatographic conditions was another important characterization step. Here, two series of analytes based on a carbamate backbone were selected: one with a non-polar phenyl-benzyl substituent, and the other with a more polar nitro-benzyl substituent (Figure 3.2). These compounds were ideal for these purposes as they both possessed a chromophore to make UV detection accessible (enabling online testing). Additionally, introducing identical fluorous groups into these series with either nitro-benzyl or phenyl-benzyl substituents also presented the option of exploring selectivity and the impact of "secondary effects" in the monolithic materials (separation differences between identically-tagged compounds with different inherent polarities could be noted during testing).

A number of groups have previously noted mixed specificity in analyses using fluorous columns,[55-58] referring to these so-called "secondary effects" that cause deviation from a purely fluorous interaction. Whether they arise from factors such as residual silanol activity in stationary phase particles, analyte character outside of an introduced fluorous tag or other possibilities, contributions such as these will clearly have an effect on the overall column performance. Additionally, when you consider that heavily-fluorinated stationary phases also have inherent non-polar natures that should be able to interact with analytes, it becomes quite likely that interactions on top of only the fluorous affinity will need to be considered in any retention mechanism. When considered in this light of fluorous specificity then, the acrylate-based fluorous monoliths to be explored here present a number of questions still to be addressed. In particular, it remains to be seen whether the concentration of fluorine at the surface of the monoliths gives rise to a high degree of specificity, or whether the hydrocarbonaceous nature of the rest of the substrate will cause an excess of secondary interactions that could otherwise hinder the selectivity.

Prior to these more complex analyses of monolith selectivity and specificity though, the first test that had to be undertaken was a comparison of the resolution for the fluorous analyte series that could be attained using a variety of monolithic densities. Using SEM and backpressure results (*vide supra*) it was previously suggested that a composition of 30% showed the best porosity characteristics. Comparing those initial results to what is observed during chromatography (Figure 3.11 and Table 3.6), an excellent correlation between the data sets can be found. Fluorous resolution for both the nitro-benzyl and phenyl-benzyl substituted series reaches a maximum at a monolith density of 30%; a result that is consistent with what the structural characteristics predicted

to be the most consistent material. These results also serve to reinforce the benefit of the fluorous interaction relative to a purely reverse-phase separation (in much the same way the earlier tests on PAH samples did), as monoliths made with FBA significantly outperformed their BA counterparts in terms of fluorous analyte resolution (a factor of 2-3 greater under identical conditions). Similar to resolution, peak shape for the fluorous series can also be seen to follow this same overall trend in quality (Table 3.6). Looking at the peaks for the most strongly-retained tagged species (N4 and P4; the compounds that should best exhibit fluorous interactions), the signals are narrowest when the monolithic composition is at 30% (which makes sense given that resolution is partially dependant on peak width). Finally, it is worth noting that the distribution and relative intensities of the observed peaks on the fluorous monoliths were consistent with the data obtained by the custom synthesis provider during their characterization of the analytes, reinforcing the identity of the peaks as they are labeled.

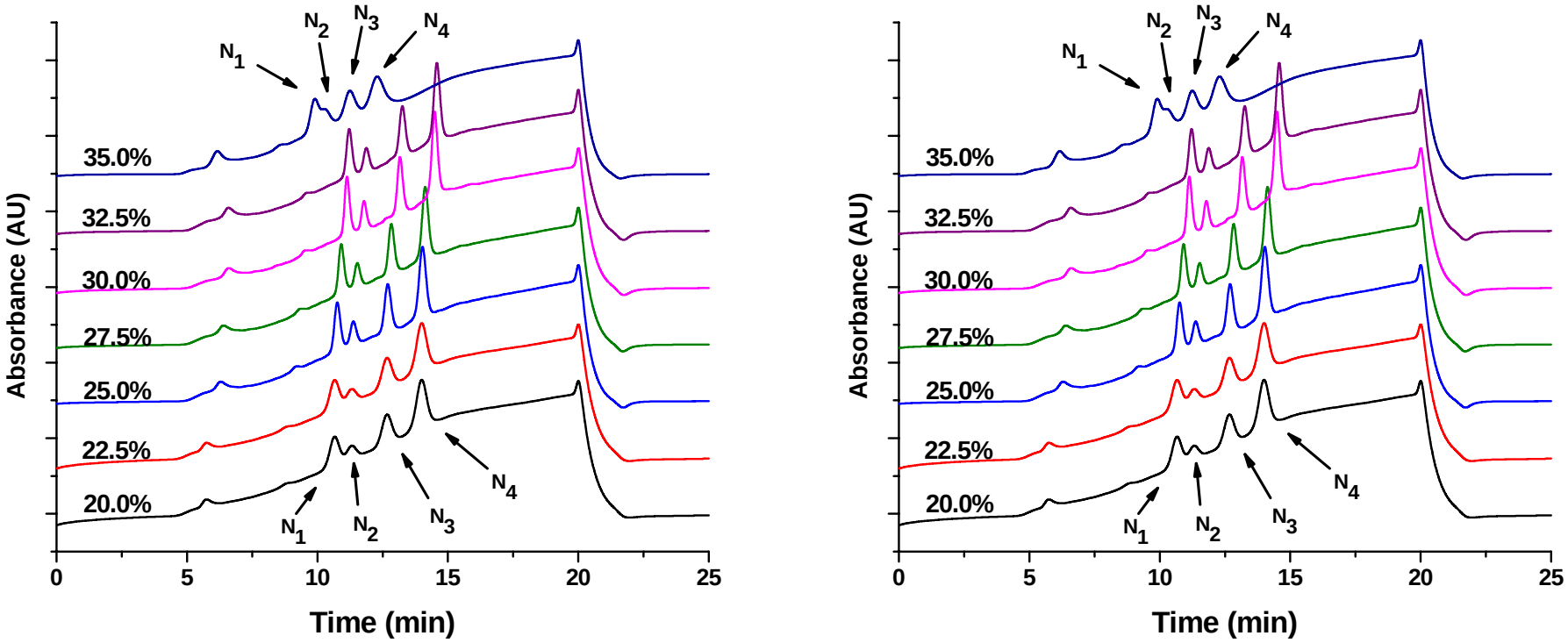

Figure 3.11: Chromatograms for N (left panel) and P (right panel) carbamate mixtures using columns with different fluorous PPM densities. The labels N1/P1 through N4/P4 indicate increasing fluorous tag lengths from C_3F_7 through C_8F_{17} (see Experimental section 3.2.1). Traces are offset for clarity.

Table 3.6: Resolution of fluorous analytes on columns with different PPM densities.

Column		Resolution				Peak Width (min)	
	Density (%)	**R(N1/N2)**	**R(N3/N4)**	**R(P1/P2)**	**R(P3/P4)**	**N4**	**P4**
Fluorous Column	**20.0**	0.86 ± 0.00	1.70 ± 0.02	1.02 ± 0.42	1.55 ± 0.02	0.81 ± 0.01	0.81 ± 0.03
	22.5	1.26 ± 0.09	2.29 ± 0.04	1.05 ± 0.02	2.16 ± 0.08	0.60 ± 0.02	0.54 ± 0.05
	25.0	1.39 ± 0.04	2.59 ± 0.05	1.16 ± 0.07	2.22 ± 0.04	0.54 ± 0.03	0.56 ± 0.02
	27.5	1.52 ± 0.03	2.81 ± 0.01	1.26 ± 0.03	2.43 ± 0.05	0.50 ± 0.04	0.50 ± 0.03
	30.0	1.68 ± 0.01	3.12 ± 0.05	1.46 ± 0.03	2.58 ± 0.01	0.44 ± 0.04	0.50 ± 0.01
	32.5	1.50 ± 0.02	2.84 ± 0.04	1.34 ± 0.00	2.39 ± 0.01	0.48 ± 0.00	0.50 ± 0.01
	35.0	0.54 ± 0.02	1.22 ± 0.02	--	0.96 ± 0.03	0.97 ± 0.00	1.34 ± 0.08
Non-Fluorous Column	**30.0**	0.74 ± 0.01	1.14 ± 0.01	0.48 ± 0.05	0.89 ± 0.00	--	--

Each value is reported as the average from two separate columns for each PPM composition. The labels N1/P1 through N4/P4 indicate increasing fluorous tag lengths from C_3F_7 through C_8F_{17} in either the nitro-benzyl or phenyl-benzyl substituted carbamate mixtures (see Experimental section 3.2.1).

Looking more closely at interaction specificity, it can be seen in the separate plots for the nitro-benzyl and phenyl-benzyl substituted carbamates (Figure 3.11) that compounds with identical fluorous tags (e.g. N1 and P1) do not exhibit identical retention times on the fluorous monoliths. Similar to earlier discussions then, this suggests that secondary effects causing deviation from a purely fluorous interaction must be present (separation based solely on fluorine content would show no difference between fluorous-tagged carbamates that differed only by a nitro-benzyl or phenyl-benzyl substituent). While it was expected that these types of secondary effects might occur in the compounds with smaller (C_3F_7 and C_4F_9) fluorous tags (where the amount of fluorine is less significant relative to the total molecular size), for them to also appear for the larger tags suggests that the secondary effects must be as much of a contributor here as they are in the commercial, silica particle-packed fluorous columns that have already been discussed.[55-58]

3.3.7 – Secondary Effects as Separation Utility: While it might initially be thought that the presence of secondary effects indicates a drawback of the monolithic materials, this does not have to be the case. As was seen with the commercial, microsphere-based fluorous columns, the inherent reverse-phase character of fluorous stationary phases coupled with only a partial fluorous character for analytes that have their fluorine introduced through tagging reactions allows other interactions and effects to provide a significant contribution to the retention that is observed. In trying to assess the quality of fluorous monoliths then, it is necessary to evaluate their performance in terms of the benefits that their fluorous character confers relative to equivalent phases that lack fluorination. Similarly, with secondary effects seemingly unavoidable, if it were possible

to find a way to use these deviations from purely fluorous separations as a tool for further analysis it would be highly beneficial.

In this vein, one way to highlight the power of the fluorous monoliths is to perform more complex separations (initially modeled here by combining the mixtures of both nitro-benzyl and phenyl-benzyl substituted carbamates). By comparing the performance of a fluorous column with an equivalent monolith that replaces the fluorinated monomer with its hydrocarbon analogue (Figure 3.12), the resultant chromatograms demonstrate the benefits arising from monolith fluorination. For the mixture separation on the fluorous substrate all 8 components can be identified, with only N2 and P1 showing a significant amount of overlap. Compare this to the non-fluorous column where N4, P1 and P2 all essentially coelute, and it is evident that the introduction of stationary phase fluorination has a positive impact on analysis. When separation is based solely on polarity (as it is in the reverse-phase column), there is not enough of a difference imparted by the fluorous tags to help differentiate the species outside of their nitro-benzyl or phenyl-benzyl composition. All of the nitro-benzyl substituted carbamates therefore elute before any of the phenyl-benzyl compounds do; a result of the additional fluorine content in longer tags not appreciably altering the polarity of the compounds. This is contrasted by the fluorous case, where the small additional amounts of fluorine in each subsequent tag produce a measurable difference in the overall fluorous character. This in turn results in a grouping of analytes based predominantly on tag choice rather than substrate polarity (N2 does still elute marginally before P1 in a polarity-based fashion due to a combination of the small fluorous tags and secondary effects), which is a totally different paradigm than for the reverse-phase column.

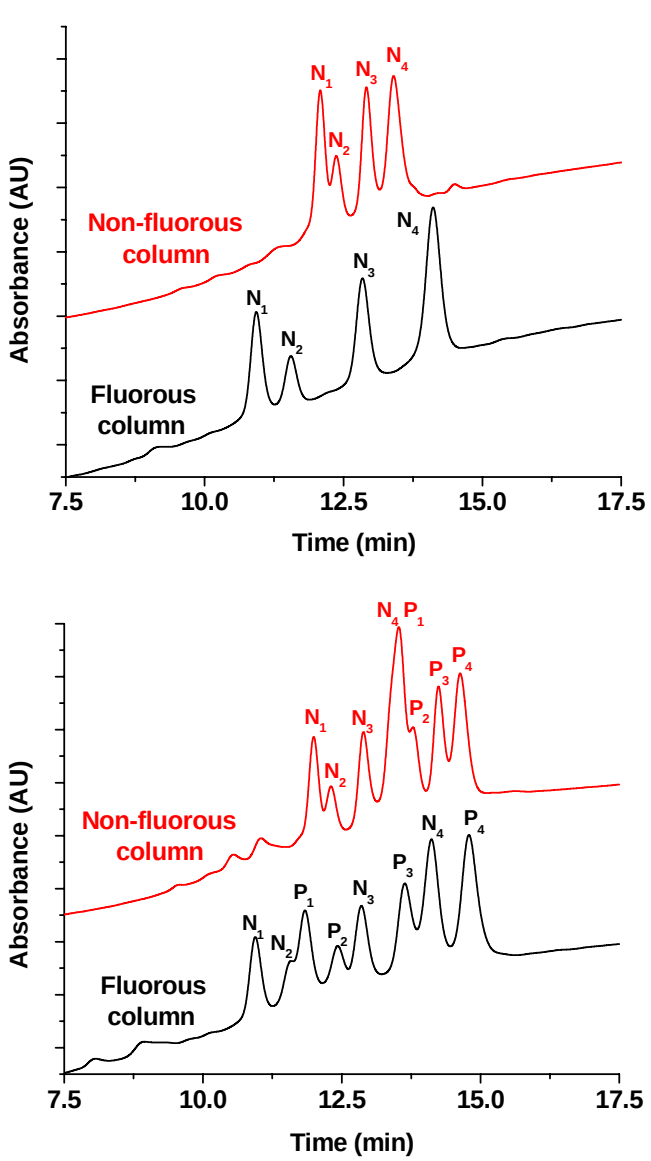

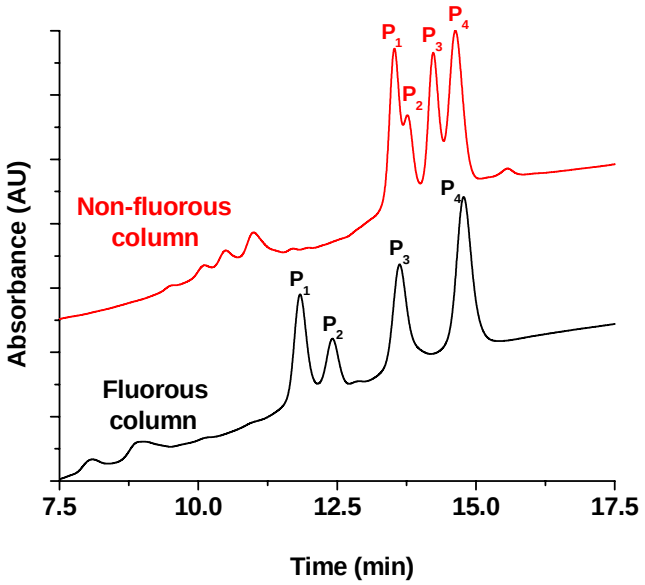

Figure 3.12: Chromatograms for individual N (above left) and P (above right) carbamate mixtures, as well as a combined sample with both N and P carbamates mixed together (below left). The labels N1/P1 through N4/P4 indicate increasing fluorous tag lengths from C_3F_7 through C_8F_{17} (see Experimental section 3.2.1). Each panel shows separations using a fluorous column (upper trace) and its non-fluorous analogue (lower trace). The PPM density is 30% in each case, with only the monomer choice being varied (FBA or BA). Traces are offset from each other for clarity.

Interestingly, it is worth noting here that while retention was shown to increase with the length of the fluorous tag, it is also evident that the fluorous-tagged compounds are sometimes retained for a longer time on the non-fluorous column (Figure 3.12). While this result is somewhat unexpected, the longer retention times for the fluorous species on the non-fluorous column can likely be attributed to the differences in retention mechanism that are present between the two materials. In each case, the exact same gradient was used, meaning that differences in elution strength for the same solvent on either fluorous or reverse-phase materials should be expected. The fluorous-eluting power of the solvent system will not be the same as its ability to elute species from a reverse-phase column (where different affinity interactions dominate), so this could lead to longer retention times for the reverse-phase column despite its poorer overall selectivity.

Looking more closely at the secondary effects, they can be seen to manifest in a predictable manner for the fluorous monoliths. The less-polar phenyl-benzyl substituted carbamates have uniformly longer retentions than their more polar nitro-benzyl counterparts, which is the expected result given the known, reverse-phase capabilities of fluorous monolithic substrates. This in turn leads to slight differences in retention between identically tagged species based on their inherent substrate polarity, although the vast majority of the retention character is still dictated by the choice of fluorous tag. Interestingly, these differences in retention for species with the same tag but different analyte character might actually be used as a benefit in fluorous analyses, serving as a second dimension for separation. This ability to differentiate between compounds of different polarity but identical tagging could become particularly useful in complex analyses like those often found in proteomics. Here, it is possible to imagine a situation

where there would be multiple peptides with similar post-translational modifications or other targets that could be labeled with fluorous groups to simplify the analysis of a digest. If it were further possible to identify these fragments based on their polarity after tagging (differences that would result from specific amino acid residues), that would be a huge benefit for further characterization. With that said, the secondary effects exhibited by fluorous monoliths coupled with their demonstrated tag specificity for fluorous analytes represent one such manner to potentially achieve these proteomic separations, making them an interesting area for further exploration.

3.3.8 – Applications for Fluorous Proteomics: As a step toward proving the utility of fluorous monoliths in proteomic applications, a tagging experiment using a custom-synthesized peptide (Figure 3.2) was initially used to explore the efficacy of fluorous separations. Using N-[(3-perfluorohexyl)propyl]iodoacetamide ($C_{11}H_9F_{13}INO$) to react with the lone cysteine residue in the custom peptide provided a handle for an affinity-based separation, theoretically allowing any tagged peptides to be resolved from their non-fluorous counterparts. Unlike previous experiments where LC separation followed by UV detection could be used to determine resolution though, the lack of a significant chromophore in the custom peptide meant that these tests required a change to a LC/MS system with electrospray ionization to achieve proper detection. Fortunately, maintenance of a similar gradient profile despite this change in system meant that the results should still allow a reasonable assessment of the monolith performance in terms of the achieved resolution for a proteomic separation to be made despite the change in equipment.

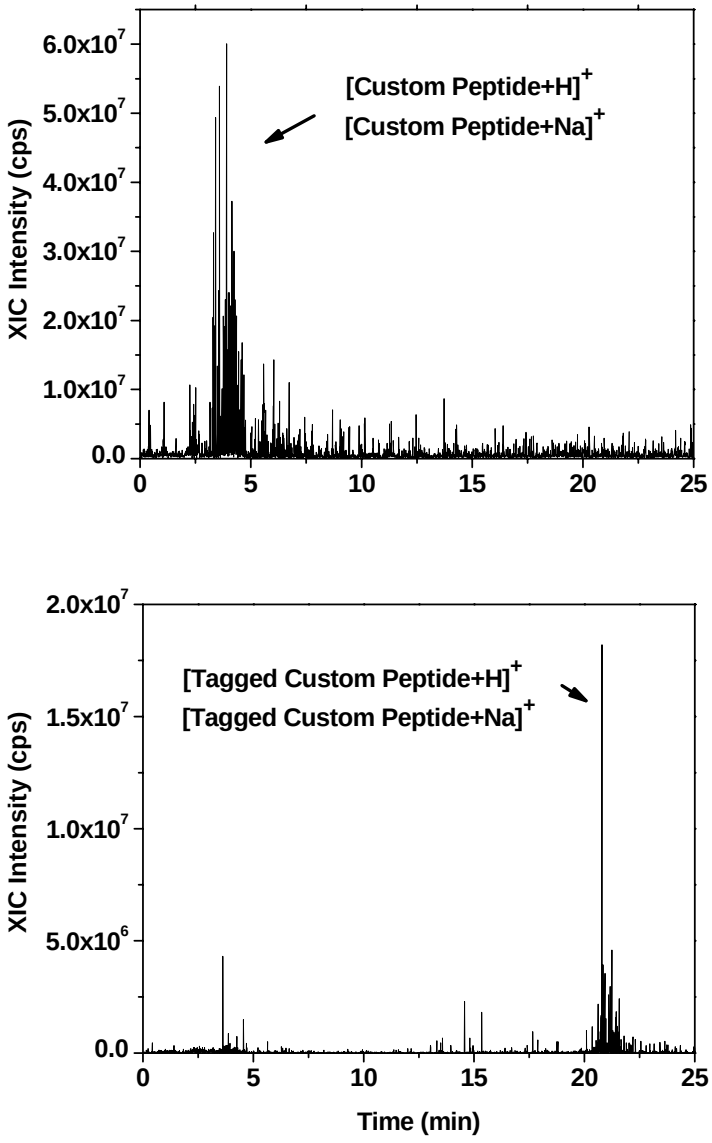

Figure 3.13: Extracted ion current (XIC) for custom peptide with both H^+ and Na^+ (top), as well as fluorous-tagged custom peptide with both H^+ and Na^+ (bottom). Mass spec conditions are not optimal for these trials (explaining the poor XIC quality), but rather are intended to serve as a demonstration of the viability of monoliths as a separation medium for fluorous-tagged biological samples.

Looking at some initial results from these tests (shown as extracted ion chromatograms; Figure 3.13), it can be seen that there is indeed a significant separation between tagged and untagged peptides when they are analyzed using the fluorous monolith. While the untagged peptide effectively elutes at the solvent front without any retention (immediately following the injection lag, at a solvent composition near 90% aqueous), the tagged analyte is retained quite strongly and requires a change in concentration to almost 90% acetonitrile before it elutes from the monolith and can be detected. Similarly, also of interest in these tests was the presence of a presumed dimer of fluorous iodoacetamide (a later eluting species than even the tagged custom peptide; mass confirmed by XIC), which with twice as much fluorine as the singly-tagged peptide should be retained longer by the fluorous column than the analyte with only one fluorous group. This is the result that would be predicted by fluorous affinity interactions, lending further support to the assertion that fluorous monoliths can effectively be used as substrates in fluorous proteomic and other labeling applications.

3.4 – Conclusions and Future Work

After a thorough analysis of fluorous monolith structure, density and composition, it has been shown that a 30% mixture of polymerizable material (FBA + BDDA) relative to the porogenic solvent produces the best results for fluorous separations. It was found that these materials have the greatest degree of reproducibility (a benefit partially conferred by eliminating the fluorous cross-linker), while also exhibiting superior resolving power as compared to their non-fluorous counterparts (BA + BDDA mixture). Analysis of a mixture of carbamates (both nitro-benzyl and phenyl-benzyl substituted) that were tagged with fluorous groups further expanded upon these results, as the optimal monolith composition could resolve the components in a manner that was otherwise not

possible with a non-fluorous column. Providing this totally different selectivity with no changes to the LC method or system other than the introduction of column fluorination demonstrates the power of the fluorous interaction for complex analyses, as it allows analyte grouping and detection that would otherwise be difficult on more conventional chromatographic substrates.

The presence of secondary effects in addition to the fluorous interaction were also observed for these optimized columns (identical to those noted for commercial fluorous silica gels). Despite this, there was no adverse effect on the performance of the monoliths. Analyte specificity was noted to primarily be a function of the choice of fluorous tag, with the secondary effects causing slight (predictable) deviations from ideal fluorous behavior (less polar analytes retained slightly longer than their more polar counterparts). These effects are suggested to have positive implications for the analysis of complex mixtures though, with the differentiation of components with different polarities but identical tagging potentially providing useful information in more complex separations with multiple dimensions.

Finally, it was shown that the optimized monolithic columns can effectively be used to separate labeled biological samples from their non-fluorous counterparts in a proteomic fashion. Expansion of this avenue to explore more complex mixtures should further demonstrate the proteomic ability of these monoliths, as well as allow a greater exploration of the proposed utility of their secondary interactions for complex biological separations. With their ease of fabrication, amenability to conventional LC systems, and potential for integration in microfluidics[27, 59] as additional benefits, there exists a great deal of potential for the further growth and wider implementation of fluorous monolithic substrates of this type in a number of applications.

3.5 – References

(1) Hjerten, S.; Liao, J. L.; Zhang, R. *J. Chromatogr.* **1989**, *473*, 273-275.

(2) Svec, F.; Frechet, J. M. J. *Anal. Chem.* **1992**, *64*, 820-822.

(3) Wang, Q. C.; Svec, F.; Frechet, J. M. J. *Anal. Chem.* **1993**, *65*, 2243-2248.

(4) Svec, F.; Frechet, J. M. J. *Chem. Mater.* **1995**, *7*, 707-715.

(5) Svec, F.; Frechet, J. M. J. *Macromolecules* **1995**, *28*, 7580-7582.

(6) Svec, F.; Frechet, M. J. *Science* **1996**, *273*, 205-211.

(7) Svec, F.; Frechet, J. M. J. *Ind. Eng. Chem. Res.* **1999**, *38*, 34-48.

(8) Gusev, I.; Huang, X.; Horvath, C. *J. Chromatogr., A* **1999**, *855*, 273-290.

(9) Viklund, C.; Ponten, E.; Glad, B.; Irgum, K.; Hoerstedt, P.; Svec, F. *Chem. Mater.* **1997**, *9*, 463-471.

(10) Geiser, L.; Eeltink, S.; Svec, F.; Frechet, J. M. J. *J. Chromatogr., A* **2007**, *1140*, 140-146.

(11) Viklund, C.; Svec, F.; Frechet, J. M. J.; Irgum, K. *Chem. Mater.* **1996**, *8*, 744-750.

(12) Clarke, S. R.; Shanks, R. A. *J. Macromol. Sci., Chem.* **1982**, *A17*, 77-85.

(13) Yu, C.; Xu, M.; Svec, F.; Frechet, J. M. J. *J. Polym. Sci., Part A: Polym. Chem.* **2002**, *40*, 755-769.

(14) Peters, E. C.; Petro, M.; Svec, F.; Frechet, J. M. J. *Anal. Chem.* **1998**, *70*, 2288-2295.

(15) Motokawa, M.; Kobayashi, H.; Ishizuka, N.; Minakuchi, H.; Nakanishi, K.; Jinnai, H.; Hosoya, K.; Ikegami, T.; Tanaka, N. *J. Chromatogr., A* **2002**, *961*, 53-63.

(16) Yu, C.; Svec, F.; Frechet, J. M. J. *Electrophoresis* **2000**, *21*, 120-127.

(17) Peters, E. C.; Petro, M.; Svec, F.; Frechet, J. M. J. *Anal. Chem.* **1997**, *69*, 3646-3649.

(18) Peters, E. C.; Petro, M.; Svec, F.; Frechet, J. M. J. *Anal. Chem.* **1998**, *70*, 2296-2302.

(19) Tanaka, N.; Nagayama, H.; Kobayashi, H.; Ikegami, T.; Hosoya, K.; Ishizuka, N.; Minakuchi, H.; Nakanishi, K.; Cabrera, K.; Lubda, D. *J. High Resolut. Chromatogr.* **2000**, *23*, 111-116.

(20) Dulay, M. T.; Quirino, J. P.; Bennett, B. D.; Zare, R. N. *J. Sep. Sci.* **2002**, *25*, 3-9.

(21) Kato, M.; Sakai-Kato, K.; Toyo'oka, T. *J. Sep. Sci.* **2005**, *28*, 1893-1908.

(22) Szumski, M.; Buszewski, B. *J. Sep. Sci.* **2007**, *30*, 55-66.

(23) Lee, D.; Svec, F.; Frechet, J. M. J. *J. Chromatogr., A* **2004**, *1051*, 53-60.

(24) Marcus, K.; Schaefer, H.; Klaus, S.; Bunse, C.; Swart, R.; Meyer, H. E. *J. Proteome Res.* **2007**, *6*, 636-643.

(25) Koerner, T.; Turck, K.; Brown, L.; Oleschuk, R. D. *Anal. Chem.* **2004**, *76*, 6456-6460.

(26) Lee, S. S. H.; Douma, M.; Koerner, T.; Oleschuk, R. D. *Rapid Commun. Mass Spectrom.* **2005**, *19*, 2671-2680.

(27) Bedair, M. F.; Oleschuk, R. D. *Anal. Chem.* **2006**, *78*, 1130-1138.

(28) Bedair, M.; Oleschuk, R. D. *Analyst* **2006**, *131*, 1316-1321.

(29) Hirayama, C.; Ihara, H.; Nagaoka, S.; Hamada, K. *J. Chromatogr.* **1989**, *465*, 241-248.

(30) Danielson, N. D.; Beaver, L. G.; Wangsa, J. *J. Chromatogr.* **1991**, *544*, 187-199.

(31) Alicea-Maldonado, R.; Colon, L. A. *Electrophoresis* **1999**, *20*, 37-42.

(32) Reichmuth, D. S.; Shepodd, T. J.; Kirby, B. J. *Anal. Chem.* **2004**, *76*, 5063-5068.

(33) Kirby, B. J.; Reichmuth, D. S.; Renzi, R. F.; Shepodd, T. J.; Wiedenman, B. J. *Lab Chip* **2005**, *5*, 184-190.

(34) Maltezos, G.; Garcia, E.; Hanrahan, G.; Gomez, F. A.; Vyawhare, S.; van Dam, R. M.; Chen, Y.; Scherer, A. *Lab Chip* **2007**, *7*, 1209-1211.

(35) Grover, W. H.; von Muhlen, M. G.; Manalis, S. R. *Lab Chip* **2008**, *8*, 913-918.

(36) Yabu, H.; Shimomura, M. *Chem. Mater.* **2005**, *17*, 5231-5234.

(37) Wang, L.; Zhao, Y.; Lin, K.; Zhao, X.; Shan, Z.; Di, Y.; Sun, Z.; Cao, X.; Zou, Y.; Jiang, D.; Jiang, L.; Xiao, F.-S. *Carbon* **2006**, *44*, 1336-1339.

(38) Ngola, S. M.; Fintschenko, Y.; Choi, W.-Y.; Shepodd, T. J. *Anal. Chem.* **2001**, *73*, 849-856.

(39) Bakry, R.; Stoeggl, W. M.; Hochleitner, E. O.; Stecher, G.; Huck, C. W.; Bonn, G. K. *J. Chromatogr., A* **2006**, *1132*, 183-189.

(40) Gibson, G. T. T.; Koerner, T. B.; Xie, R.; Shah, K.; de Korompay, N.; Oleschuk, R. D. *J. Colloid Interface Sci.* **2008**, *320*, 82-90.

(41) Brittain, S. M.; Ficarro, S. B.; Brock, A.; Peters, E. C. *Nat. Biotechnol.* **2005**, *23*, 463-468.

(42) Benskin, J. P.; Bataineh, M.; Martin, J. W. *Anal. Chem.* **2007**, *79*, 6455-6464.

(43) Kuppithayanant, N.; Rayanakorn, M.; Wongpornchai, S.; Prapamontol, T.; Deming, R. L. *Talanta* **2003**, *61*, 879-888.

(44) Su, S.; Gibson, G. T. T.; Mugo, S. M.; Marecak, D. M.; Oleschuk, R. D. *Anal. Chem.* **2009**, *81*, 7281-7287.

(45) Kiss, L. E.; Kovesdi, I.; Rabai, J. *J. Fluorine Chem.* **2001**, *108*, 95-109.

(46) Hebb, A. K.; Senoo, K.; Cooper, A. I. *Compos. Sci. Technol.* **2003**, *63*, 2379-2387.

(47) Itoh, H.; Kinoshita, T.; Nimura, N. *J. Chromatogr., A* **1994**, *662*, 95-99.

(48) Jinno, K.; Nakamura, H. *Chromatographia* **1994**, *39*, 285-293.

(49) Euerby, M. R.; McKeown, A. P.; Petersson, P. *J. Sep. Sci.* **2003**, *26*, 295-306.

(50) Guiochon, G. *J. Chromatogr., A* **2007**, *1168*, 101-168.

(51) Vlakh, E. G.; Tennikova, T. B. *J. Sep. Sci.* **2007**, *30*, 2801-2813.

(52) Neue, U. D. *HPLC Columns: Theory, Technology and Practice*; Wiley-VCH: New York, 1997.

(53) Moret, S.; Conte, L. S. *J. Chromatogr., A* **2000**, *882*, 245-253.

(54) Daley, A. B.; Oleschuk, R. D. *J. Chromatogr., A* **2009**, *1216*, 772-780.

(55) Yamamoto, F. M.; Rokushika, S. *J. Chromatogr., A* **2000**, *898*, 141-151.

(56) Turowski, M.; Morimoto, T.; Kimata, K.; Monde, H.; Ikegami, T.; Hosoya, K.; Tanaka, N. *J. Chromatogr., A* **2001**, *911*, 177-190.

(57) Poole, C. F.; Ahmed, H.; Kiridena, W.; DeKay, C.; Koziol, W. W. *Chromatographia* **2007**, *65*, 127-139.

(58) Sakaguchi, Y.; Yoshida, H.; Todoroki, K.; Nohta, H.; Yamaguchi, M. *Anal. Chem.* **2009**, *81*, 5039-5045.

(59) Koerner, T.; Oleschuk, R. D. *Rapid Commun. Mass Spectrom.* **2005**, *19*, 3279-3286.

Chapter 4: Fluorous Open-Tubular Chromatography

4.1 – Introduction

Frequently used in gas chromatography (GC),[1] open-tubular chromatographic columns are popular for their greater degree of permeability and overall superior efficiency as compared to other GC columns. While these columns can come in a variety of forms (including both wall- and support-coated open tubes), they are all ultimately designed with the purpose of sequestering a stationary phase to only the outer rim of a channel. This has the dual effect of reducing resistance for mobile phase flow while also allowing rapid partitioning of the analyte between the mobile and stationary phases, subsequently generating excellent efficiencies and eliminating many of the concerns seen in packed GC columns. To help quantify the efficiency of these open-tubular columns under pressure-driven separations, the Golay equation[2] can be cited as:

$$\begin{aligned} H &= \frac{B}{u} + C_m u + C_s u \\ &= \frac{2D_m}{u} + \frac{1 + 6k + 11k^2 d_c^2}{96(1+k)^2 D_m} u + \frac{2k}{3(1+k)^2} \frac{d_f^2}{D_s} u \end{aligned} \tag{1}$$

Here, the efficiency (expressed as H; the height equivalent to a theoretical plate) is shown to be determined by three separate components: the longitudinal diffusion (B), the mass transfer for analyte in the mobile phase (C_m), and the mass transfer for analyte in/on the stationary phase (C_s). While all three terms can also be seen to rely in varying degrees on the flow rate (u), it is interesting to note that the effects of eddy diffusion (the "A" term in the more classic van Deemter equation) are not significant when there is only a single open channel and are therefore omitted in the Golay equation.

If the terms of the Golay equation are more closely examined,[2] another fact that becomes apparent is that the diameter of the column (d_c) is a primary contributor to the C_m term. As such, it means that to optimize efficiencies through the reduction of plate heights, smaller column diameters should theoretically be used. Unfortunately, with the walls of the open tube serving as the only anchor for stationary phase, reducing the column diameter means that there is a concurrent decrease in the amount of stationary phase that can be present, which will limit the loading capacity of the column. This in turn means that longer columns and specialized sample introduction methods must be employed to ensure that satisfactory results are attained.

For all of the attention that open-tubular GC columns have received, applications in liquid chromatography (LC) have been comparatively less noteworthy. Although the idea was certainly considered over forty years ago,[3, 4] there have always been a number of lingering issues (both theoretical and practical) that have kept it from becoming a widely-applicable method.[5-7] Foremost amongst these issues has been the necessity for columns with very narrow diameters,[8-10] although the selection of stationary phase materials[5, 8, 11-15] and implementation of detection systems that can deal with the limited amount of sample that is introduced into a narrow column with minimal stationary phase are also frequently discussed.[16-18] In general, it has been suggested that to optimize an open-tubular liquid chromatography (OTLC) system that the inner diameter of the channel should be on the order of 1-3 μm.[8] With radii that are outside of this range factors such as diffusion and mass transfer can become problematic,[8] leading to lower numbers of theoretical plates and rendering the benefit of an OTLC column negligible relative to the effort that would go into preparing it. The challenge in recent years has therefore been to come up with columns that present adequate diameters in conjunction with sufficient

lengths to provide enough stationary phase to effect a proper separation in a reasonable time and without generating excessive backpressures.[17] Unfortunately, other than with the proponents of porous layer open-tubular (PLOT) columns[15] this type of OTLC development has been a largely neglected topic,[19, 20] leaving many avenues yet to be explored.

Recently, the use of photonic crystal fibers (alternatively termed microstructured fibers, or MSFs) in optics has given rise to many novel designs and applications.[21] Comprising a periodic array of parallel channels within a silica matrix, these fibers were predominantly designed as light guides that take advantage of the unique refractive properties of their arrangement of holes. Interestingly, despite this original application, one can envision a number of other uses that exploit the design of the MSF. Recent publications have used them as channels with excellent heat dissipation properties for electrophoresis,[22-24] a sensor for gasses when the walls are treated with a sol-gel to modify their spectral properties,[25] and even as multiplexed emitter arrays for improved electrospray performance.[26] In terms of OTLC, microstructured fibers hold great potential as they are essentially an array of seemingly ideal-sized open silica channels held together with a diameter equal to that of a conventional capillary column. In theory then, if they could be properly functionalized with stationary phase they would have the potential to revitalize the field of open-tubular liquid chromatography. Their multiple parallel paths would eliminate issues with limited stationary phase loading and excessive backpressure that are observed in singular channels of a similar size, allowing new applications that were otherwise impossible to be realized.

Although the application of microstructured fibers as substrate materials for LC is relatively new, the concept of an array of capillary columns for liquid chromatography is

not. A publication by Meyer et al.[27] examining the benefits and limitations of bundling capillaries to form a stationary phase highlighted many of the key points and equations for consideration in a multiplexed LC system over 27 years ago, and still remains useful even with the development of newer materials. In fact, their determination that arrays of capillaries must possess flow variations less than 1% (corresponding to holes in the array having diameter variations of no more than 0.5% from the mean) to produce column efficiencies that are competitive with packed columns of 5 μm particles remains a benchmark that is yet to be achieved. Interestingly, one of the main omissions in their paper was an examination of the effects of stationary phase on the performance of a capillary array (all of their tests were conducted on bare silica), as this is a factor that is also integral to OTLC column fabrication and performance. While these types of effects have been briefly explored for arrays of solid glass capillaries (where flow channels are formed by the inter-fiber spaces),[28] large (3-6 mm outer diameter) polycapillary arrays with millions of channels,[29] and polymer fibers,[30-33] they are virtually unknown for arrays of hollow silica fibers with smaller (on the order of hundreds of microns) outer diameters such as those presented by a MSF. Although in the past this could likely be attributed to poor hole diameter tolerances during MSF fabrication preventing reasonable results from being attained (a major issue that also plagued the large diameter polycapillary arrays with millions of heterogeneous channels),[29] rapid improvements in optics design in recent years would suggest that this is an area that is now worth revisiting. Consequently then, my work has focused on microstructured fibers modified to contain a fluorous stationary phase for open-tubular liquid chromatography. Research encompassed the development and characterization of these functionalized OTLC columns, as well as an exploration of

their potential for further development, improvement, integration and use in the greater analytical community.

4.2 Experimental

4.2.1 – Materials: All aqueous solutions were prepared using water purified by a Milli-Q system (Millipore; Bedford, MA, USA). Trichloro(1H,1H,2H,2H-perfluoroctyl)silane (**1**; Figure 4.1), ammonium formate and triphenylphosphine oxide (**2**) were obtained from Aldrich (Oakville, ON). Diphenyl-[4-(1H,1H,2H,2H-perfluorodecyl)phenyl]phosphine oxide (**3**) and bis[4-(1H,1H,2H,2H-perfluorooctyl)phenyl]phenylphosphine oxide (**4**) were purchased from Fluorous Technologies (Pittsburgh, PA, USA), while (tridecafluoro-1,1,2,2-tetrahydrooctyl)dimethylchlorosilane (**5**) and (heptadecafluoro-1,1,2,2-tetrahydrodecyl)dimethylchlorosilane (**6**) were acquired from Gelest (Morrisville, PA, USA). Toluene (A.C.S. Grade), hydrochloric acid, sodium hydroxide, HPLC grade acetonitrile and reagent grade methanol were obtained from Fisher Scientific (Nepean, ON), while formic acid (98%) was purchased from BDH Chemicals (Toronto, ON). With the exception of toluene (which was additionally dried with magnesium sulphate to remove residual traces of water), all chemicals were used as-received.

Microstructured fibers of four main varieties were purchased from Crystal Fibre (Birkerød, Denmark): 30 hole (LMA-PM-16; no longer available), two versions of 54 hole (LMA-PM-16 and LMA-PM-15; the former no longer available and replaced by the latter) and 168 hole (LMA-20). These holes are aligned in regular, hexagonal patterns emanating from the center of the fiber, with consistent channel diameters and spacing (Figure 4.2). Currently, MSF fibers of this type cost about 8 to 10 times more than single-bore fused silica capillary of similar dimensions. It is also worth noting that during

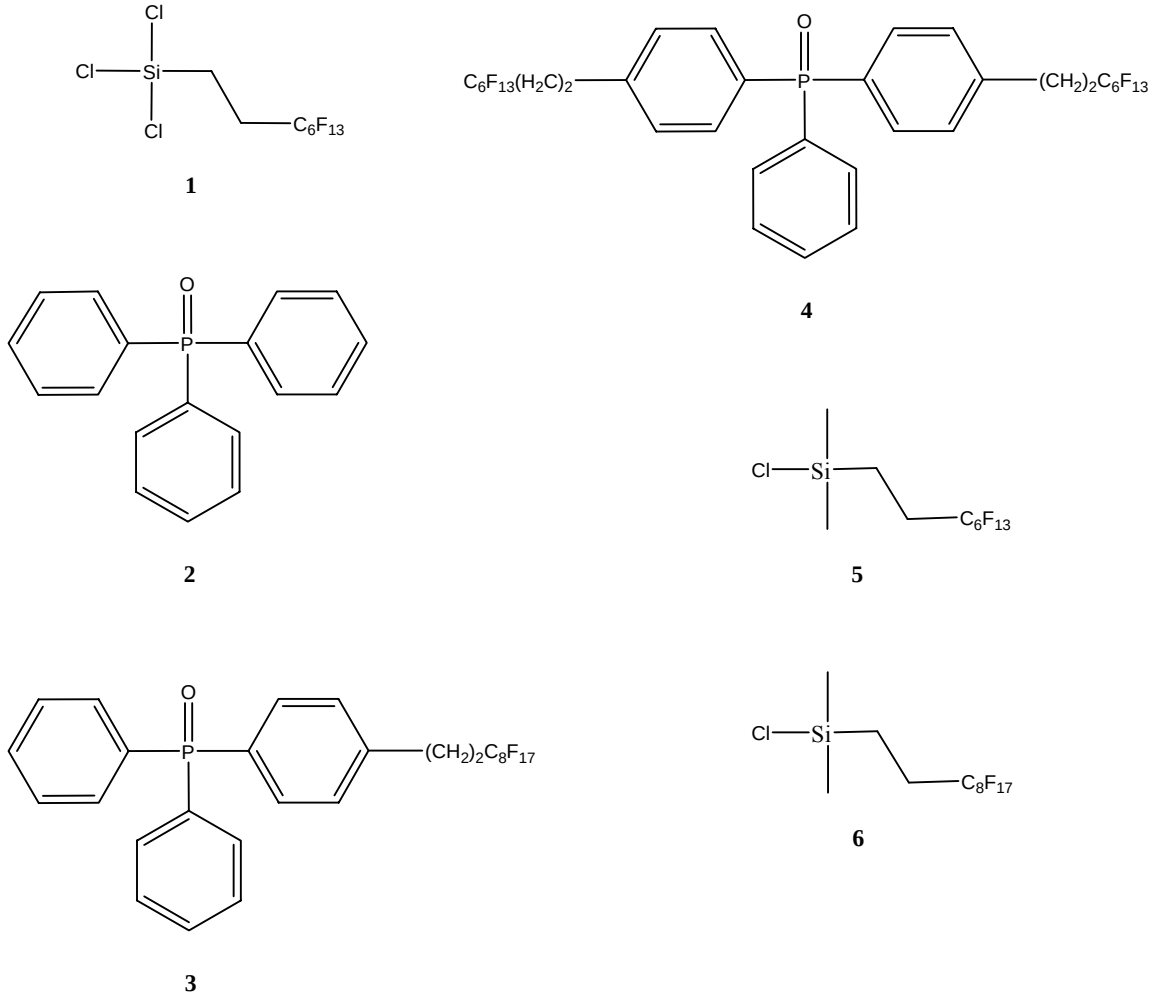

Figure 4.1: Structures of relevant compounds.

the time of these experiments, the 54 hole fiber was introduced as a replacement for the 30 hole variety with Crystal Fibre citing superior optical properties as the reason for the switch (also why both varieties have identical product numbers). Subsequently, this 54 hole fiber was itself replaced by a superior iteration (LMA-PM-15), introducing a smaller core size and further improvements to the optical properties. In turn, these switches necessitated a number of changes to the analysis of the fibers as OTLC columns, with the

flow properties changing considerably on account of the new numbers of holes and alterations to their tolerance in the newer generations.

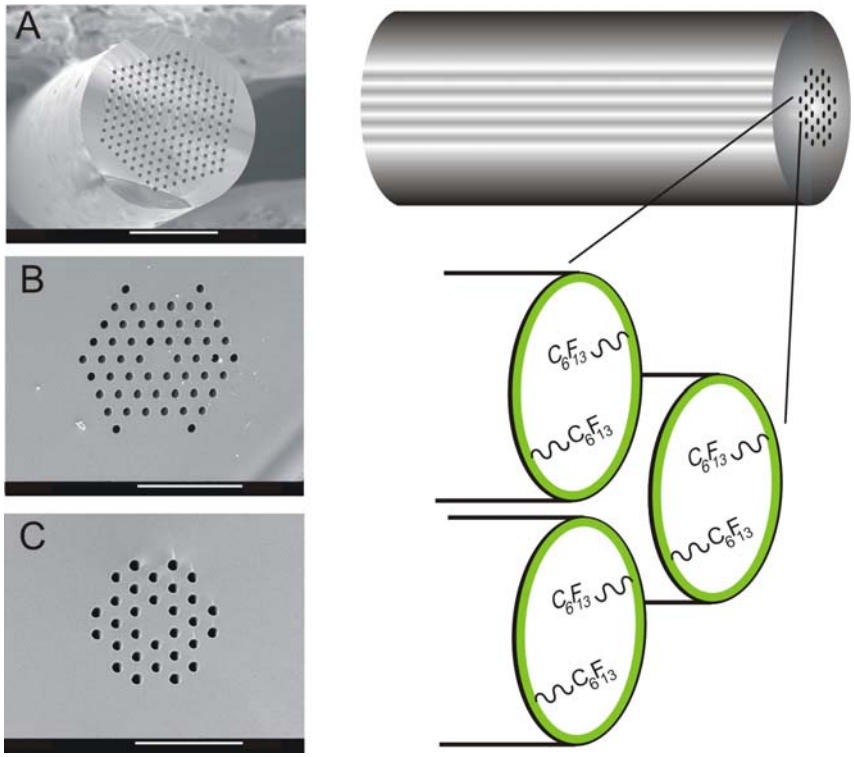

Figure 4.2: Scanning electron micrographs of (A) 168, (B) 54 and (C) 30 holed microstructured fibers. The schematic diagram depicts a covalently attached fluorous stationary phase coating within each of the microchannels.

4.2.2 – Column Preparation: Columns were prepared using one of two different reagent protocols. In each case, a 30 cm length of fiber was initially cut (using a ceramic cutter) to be subsequently treated with a silane solution to form a stationary phase for OTLC. Unfortunately, during the treatment procedure the acrylate coating on the exterior of the MSF can easily be damaged or stripped, requiring that the column be trimmed from its starting length to allow for proper fluidic connections. As a result, all of the OTLC columns were cut to, and used at lengths of 20 cm (down from the starting 30 cm),

ensuring reproducibility of results over all samples and columns regardless of the total amount of fiber that needed to be trimmed during any individual fabrication.

4.2.2.1: For the first method, a solution of trichloro(1H,1H,2H,2H-perfluoroctyl)silane (5% v/v) in toluene was loaded into a 500 μL gastight Hamilton syringe (Reno, NV, USA) and then driven through the length of fiber at 500 nL/min using a syringe pump (Harvard Apparatus; Holliston, MA, USA). Following 90 min of this treatment, the syringe was flushed and filled with acetonitrile, which was subsequently pumped through the fiber for 120 min at 500 nL/min to remove any residual treatment mixture before the column was used for chromatography. Fibers with both 30 and 168 holes were treated in this manner.

4.2.2.2: For the second method, a sequential etching and functionalization procedure was used to try and improve the surface coverage of silanes within the MSF channels. In series, 0.1 M NaOH (1 h), water (2 h), 0.1 M HCl (1 h), water (2 h), silane mixture (a 5% v/v solution of monochlorosilane **5** or **6** in toluene; 17 h) and finally acetonitrile (4 h) were introduced into the fibers via gastight syringe and driven by syringe pump in a treatment protocol similar to one previously discussed by Gottschlich et al.[34] Flow rates for this method were 300 nL/min for the acid, base and water steps, the final acetonitrile flush, and the first hour of silanization. For the remaining 16 hours of silanization, flow was reduced to 200 nL/min for the duration of the overnight treatment step. Fibers with both 54 and 168 holes were treated in this more intensive manner.

It should also be noted that control columns were fabricated using this same method by simply leaving out the silane and instead flushing the columns with only toluene during the 17 h step. Fibers with both 54 and 168 holes were treated in this manner.

4.2.3 – Scanning Electron Microscopy: Scanning electron microscope (SEM) images were obtained using a Jeol JSM-840 scanning microscope (Tokyo, Japan). Small pieces of fiber were mounted on aluminum stubs using tape such that an unobstructed view of their cross-section was possible. Prior to imaging, the stubs were coated with a thin layer of gold using a Hummer 6.2 Sputtering System (Anatech; Hayward, CA, USA).

4.2.4 – Backpressure Measurements: It has previously been shown that there is a linear dependence between backpressure and flow rate when solvent composition is held constant,[35-37] allowing the slope of the corresponding plot of observed pressure versus flow rate to serve as an indicator of the backpressure on the column under chromatographic operating conditions. As such, flow-induced backpressures were measured with an Eksigent NanoLC pump (Livermore, CA, USA) at a constant solvent composition of 1:1 acetonitrile/water and flow rates between 50 and 1000 nL/min. Columns were allowed to flush for several minutes at 1 μL/min prior to data collection, after which replicate data points could be collected and averaged to determine the slope (and associated backpressure) of each column type. Data here is compiled from three previous experiments within our group, encompassing results for MSF emitters,[26] porous polymer monoliths[37] and microsphere-packed columns.[38]

4.2.5 – Sample Preparation for Chromatography: Triphenylphosphine oxides **2**, **3** and **4** (Figure 4.1) were selected as targets based on previous success using them in fluorous chromatography.[37] Samples were prepared in one of two different solvent systems: a mixture of methanol and 10 mM ammonium formate (60:40 v/v; previously shown to have benefits in terms of sample retention and resolution in fluorous applications),[39, 40] or a solvent of 5% methanol in water. Sample concentrations ranged from 1 to 25 μM, with specific values detailed in the appropriate Figure captions.

4.2.6 – Chromatography: Tests were predominantly performed using a Waters nanoAcquity UPLC system fitted with a tunable UV detector (Milford, MA, USA), and operated by the MassLynx software package (v 4.1). Columns were coupled in-line with the detector using both a standard, transparent Teflon sleeve (detector side of capillary), as well as a high pressure fitting and capillary outfitted with a NanoTight union (P-779-01) and MicroTight Fittings (F-125X; sleeve F-185X) from Upchurch Scientific (Oak Harbor, WA, USA) to allow proper coupling of the column with the high-pressure valve of the nanoAcquity.

The system was setup with a 2 μL sample loop, and used the full-loop injection method to introduce samples. One of the initial concerns with respect to this injection protocol was with the associated sample loading, as the total volume within the 20 cm MSF columns (assuming perfectly cylindrical, uniform channels with diameters as shown in Table 4.1) would be 107 nL for 30 hole columns, ~ 139 nL for the 54 hole columns and 804 nL for the 168 hole columns. While these values are clearly exceeded by the volumes that were being injected, when the amounts of sample were calculated (with concentrations from 1 to 25 μM, between 2 and 50 pmol or approximately 0.5 to 50 ng of analyte was used) these values were found to be comparable to other publications that required trace analysis.[41, 42] Additionally, with the impact of the total injection volume on band broadening also found to be negligible relative to other factors (*vide infra*), it was established that the injection protocol was reasonable despite the seemingly limited column volumes. No column heating was employed for any of these tests, while the autosampler compartment was maintained at 25 °C. All detection set the UV lamp at 228 nm (λ_{max} previously determined to be optimal for the fluorous-tagged triphenylphosphine oxides).

Table 4.1: Observed variation in MSF properties related to hole diameter.

Number of Holes	Diameter of Hole Region (µm)	Average Hole Diameter (µm)	Coefficient of Variation (%)	Average Flow Rate (m/s)	Spread in Flow Rate at 1 SD (m/s)
30	61	4.8 ± 0.2	5.0	1.27E-05	1.32E-06
54 (LMA-PM-16)	75	4.0 ± 0.2	4.9	9.20E-06	9.52E-07
54 (LMA-PM-15)	75	3.8 ± 0.1	1.2	8.03E-06	1.93E-07
168	185	5.5 ± 0.2	3.3	1.71E-05	1.13E-06

The average diameter of 20 different holes in each of 10 cuts from a piece of fiber were used to determine the variation in diameter of holes across the MSF. Modelling of flow rates and their spread at one standard deviation (SD) used the Hagen-Poiseuille simplification to Bernoulli's equation (shown later as Equation 3).

Analyses primarily made use of a gradient method, mixing an aqueous phase (99.9% water with 0.1% formic acid) with an organic (99.9% acetonitrile with 0.1% formic acid). Initial conditions were 99% aqueous, switching to 10% aqueous over 15 min. From there, the gradient changed to 1% aqueous over 5 min, and then finally back to 99% aqueous in 1 min to give a method time of 21 min. With all necessary injection and re-equilibration times for the system also considered, the total time for a single run was 40 min. An isocratic method was also used in some tests, running at a constant 50:50 composition of aqueous and organic solvents for 37.5 min, followed by a final 5 min at 99% organic to ensure that all compounds had been eluted. Flow rates in all of these tests (gradient and isocratic) were a constant 400 nL/min.

To assess column performance, *pseudo* van Deemter plots were also constructed based on literature procedures.[43, 44] Briefly, it has been shown that if a constant gradient slope is maintained over a variety of flow rates, that a plot of the square of peak width (expressed as a volume) versus flow rate will be analogous to the results of a conventional van Deemter plot (which would require isocratic conditions and provide poorer peak shapes). For my tests, flow rates were varied between 100 nL/min and 1 μL/min, while the gradient spanned solvent compositions from 99% to 10% aqueous. To keep the slope constant (B_g; Equation 2), gradient time (t_G) was changed accordingly with the flow rate (F) while the span of the gradient ($\Delta\Phi$) was held as a constant.

$$B_g = \frac{\Delta\Phi}{Ft_G} \tag{2}$$

In addition to the experiments performed using the nanoAcquity system, an Eksigent NanoLC-1D Plus was also used for testing the effects of injection volume variations on peak shape. The Eksigent system offered better control of partial-loop

injection volumes less than the 2 μL, full-loop method offered by the nanoAcquity, making it a more reliable option for this subsection of tests. The same gradient profile previously discussed for the nanoAcquity was maintained for use on the Eksigent system.

4.3 – Results and Discussion

4.3.1 – Assessment of MSF Channel Uniformity: One of the primary concerns in dealing with MSFs is the distribution of hole diameters throughout the length of a column. While it has already been established that there is an optimal diameter range for OTLC channels that these fibers should ideally possess,[8] of equal importance for chromatography is the consistency of the diameter of each channel throughout the length of the MSF. If there is considerable variation, the result will be flow rates that can be significantly different for each channel and contribute to unwanted band broadening.[27] Although the process of fiber drawing is sufficiently refined that each of the distinct channels in a MSF should be relatively uniform,[21] it is still desirable to quantify the degree of difference in each of the main varieties tested such that the beneficial (hole diameter) and detrimental (channel variance) effects on chromatography can be properly identified.

To this end, hole diameters were quantified using scanning electron microscopy, and their uniformity over a fixed length of column assessed. Starting with a 10 cm piece of fiber (all four fiber types were tested), 1 cm intervals were cut and coated with gold for SEM analysis. Examining each of these cross-sections allowed two main factors to be quantified: the coefficient of variation for diameter across all of the holes on the head of a particular fiber type, and the coefficient of variation for the diameter of an individual hole throughout the length of a MSF. The results from these tests were twofold: they first showed that the variation of an individual hole over the length of a column is actually

quite good (uniformly on the order of 2%), while the diameter of all of the holes in a cross-section of fiber is somewhat less reliable (reaching up to 5% variation depending on the hole pattern; Table 4.1). Since the speed of flow in each channel for OTLC depends largely upon these hole diameters,[27] the observed degree of difference will mean that variation in flow velocity across each channel based on path heterogeneity should be expected during chromatographic tests.

Although previous work has used differences in diameter such as those reported in Table 4.1 as the sole means of determining the associated differences in flow velocity,[27] in those cases the diameter of the channels being compared from column-to-column were always the same. Unfortunately, as it pertains to MSFs, since each variety has channels of a different diameter (Table 4.1) it is impossible to use only their tolerances to properly assess the resultant differences in flow. Instead, it should be possible to use Bernoulli's equation in conjunction with the average hole diameters and their associated standard deviations to approximate the normal distribution of velocity profiles across the channels of a MSF under a specific set of conditions. By assuming that liquid flow is incompressible, laminar, and through a circular cross-section that is much longer than its radius, we can then apply the Hagen-Poiseuille simplification to Bernoulli's equation:[45]

$$Q = \frac{\pi d^4 \Delta P}{128 \mu L} \tag{3}$$

Here, Q is the volumetric flow rate, d is channel diameter, ΔP is the backpressure, μ is the liquid viscosity and L is the channel length. Using data gathered for the channel diameter tolerances, and properties for liquid flow in a cylindrical pipe, an expected range of flow rates can be calculated that will model MSF column performance (presented in the final two columns of Table 4.1).

Although this data is predicted using a very specific set of conditions (including constant pressure), the results are still diagnostic of the manner in which generalized flow will occur in MSF OTLC columns. While it was initially determined that the average flow rate generally increases in tandem with the total number of holes (assuming hole diameters were all uniform; a result of the constant pressure), of greater interest is the subsequent prediction that of the four MSFs tested, the 54-hole arrays have the smallest variation in flow rate over one standard deviation (accounting for 68% of the expected range of velocities assuming a normal distribution of hole sizes). This tighter distribution of flow velocities suggests that the 54 hole MSFs will suffer the least band broadening derived from hole diameter heterogeneity, which is known to be one of the greatest issues with columns derived from multiple channels.[27]

Interestingly, even with these flow characteristics in mind, at this time the theory and models proposed by Meyer et al.[27] still suggest that the number of plates that can be expected for multicapillary columns of the type described here will be prohibitively small. Hole diameter tolerance can therefore still be seen to represent a serious concern that will limit results, although it is expected that the manufacturing of fibers will soon be improved such that the standard materials will fall within the range of tolerances deemed as being competitive with packed columns.[27] This in turn will greatly enhance the effectiveness of MSF OTLC columns, and build upon the preliminary base that is being set out here.

4.3.2 – Backpressure Comparison: When using stationary phases other than packed microspheres for chromatography, one of the main benefits of the change is a reduction in flow-induced backpressure. Materials such as porous polymer monoliths[46] and OTLC columns have far less resistance to flow than do packed columns, allowing pumps with

much lower pressure ratings to be used. Additionally, their fabrication is usually much simpler and more versatile than that which is required during particle packing, making these new column varieties desirable for a number of different applications.

To assess the degree of difference between MSF OTLC columns and other chromatographic media, results from three separate publications within our group were consulted and summarized in Table 4.2.[26, 37, 38] Looking at MSF emitters, a monolith comprised of butyl acrylate (BA) monomer and 1,3-butanediol diacrylate (BDDA) cross-linker, and packed 3 μm Microsorb particles (Varian; Mississauga, ON), it is evident that there are significant differences in backpressure between the packed spheres and the more open media such as fibers and monoliths.

Table 4.2: Summary of previously observed flow-induced backpressures for different column varieties, as well as their associated permeability.

Column	MSF [26]		25% BA + BDDA Monolith [37]	Packed Microspheres [38]
Backpressure (kPa)	30 Holes	2200 ± 30	3900 ± 200	21700 ± 300
	54 Holes	1840 ± 90		
	168 Holes	160 ± 40		
Permeability (m^2 x 10^{-15})	30 Holes	126	47	8.5
	54 Holes	100		
	168 Holes	188		

Data is presented for a 10 cm column of each variety, using a flow rate of 600 nL/min. If these were not the given parameters in the original data, the known linear relationship for backpressure results in this format was used to convert the length and flow rate by the appropriate factor. Permeability is a transformation of these associated backpressures,[46] using the diameter of the hole region for an MSF (Table 4.1) as the required inner column diameter when appropriate (monoliths and packed columns were formed in 75 μm I.D. capillary). A solvent viscosity of 0.00081 Pa•s (corresponding to the 50% solution of acetonitrile used during testing) was also used for these permeability calculations.

Similarly, backpressures can also be used to calculate a permeability value assuming that the diameter of the hole-filled region in a MSF (Table 4.1) is used as the

column inner diameter that the necessary equations require.[46] This is a reasonable assumption to make given that permeability is calculated for a porous medium that fills a particular channel diameter; much the same way that the holes in a MSF cover a particular cross-section of fiber. From these results, of particular interest for the OTLC work is that despite the hole diameters for the 54-hole MSFs being smaller than those of the 30-hole column (Table 4.1), the associated backpressure is still lower when the total number of holes in the column is increased (although permeability decreases slightly for the 54-hole columns, this can be attributed to their smaller holes and larger diameters for the hole-filled regions as compared to 30-hole fiber, so it is not related to the total number of holes). This improvement with hole number should prove beneficial in the construction of OTLC columns, as greater numbers of homogeneous channels (with diameters within the ideal range)[8] will allow more stationary phase to be introduced than in a single-channel of similar size, increasing column capacity and alleviating some of the concerns with detector sensitivity.

4.3.3 – Column Preparation and Chromatography: To prepare OTLC columns, two different techniques were employed. For the first method, column functionalization was performed in a simplified manner as a proof of concept. Using a solution of fluorous trichlorosilane **1** (Figure 4.1) in toluene, this mixture was flowed through fibers with both 30 and 168 holes for 90 minutes at 500 nL/min to functionalize their walls. Silanol groups such as those on the surface of the MSF channels are known to react with a silanizing agent such as **1** through a well-defined pathway, introducing a covalently-bonded phase onto the walls through a condensation reaction.[47] Depending on the number of leaving groups available on the silanizing agent, the network that is formed can be either a monolayer (one leaving group) or a more complex cross-linked structure

(multiple leaving groups), with fewer points of attachment leading to simpler stationary phase networks.

Samples of triphenylphosphine oxides **2**, **3** and **4** (Figure 4.1) were prepared in a solvent of methanol and 10 mM ammonium formate, and analyzed both individually and in mixtures to assess the effects on chromatography produced by MSF functionalization. Representative chromatograms from these analyses are presented in Figure 4.3, showing a comparison of separations for all three triphenylphosphine oxides on the 168 and 30 hole MSF OTLC columns. From these results it can be seen that the triphenylphosphine oxides are being retained on the introduced stationary phase, and also that the components are being split into multiplets rather than eluting as single, Gaussian peaks.

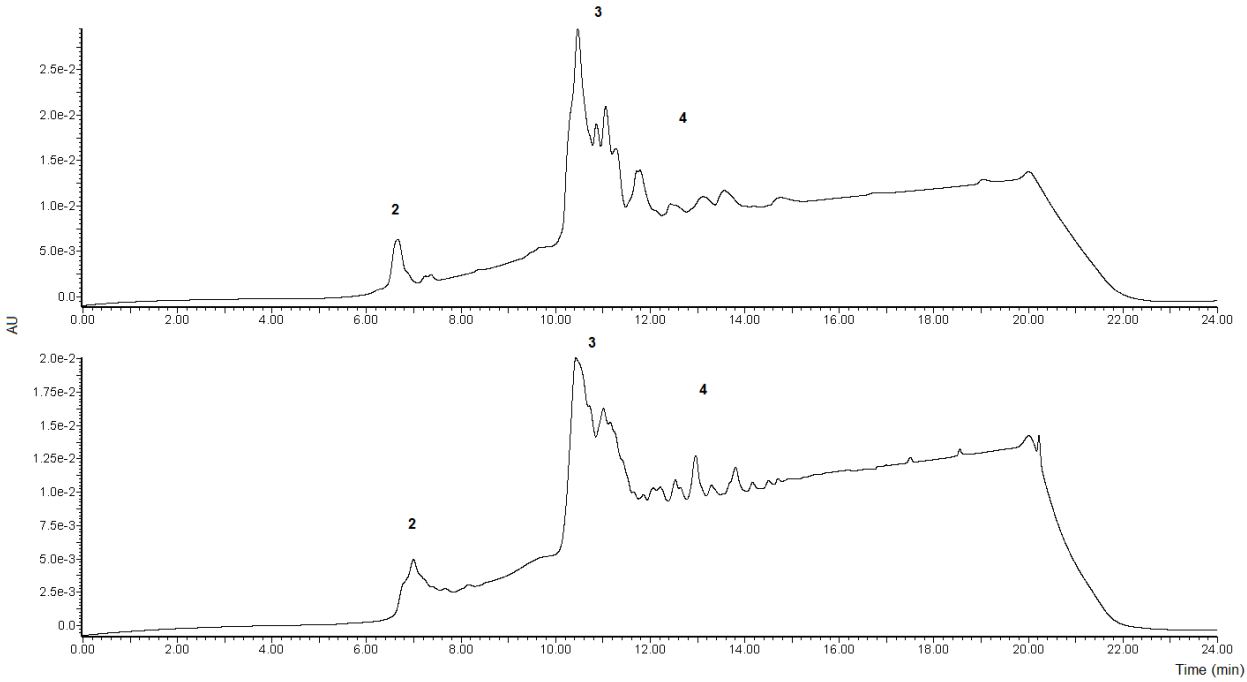

Figure 4.3: Chromatograms resulting from 30 (top) and 168 hole (bottom) MSF columns functionalized with trichlorosilane **1**. Triphenylphosphine oxide (**2**; 25 μM) is the peak around 6.75 min, the singly-tagged compound **3** (15 μM) produces the first multiplet of peaks centered around 11 min, and the doubly-tagged compound **4** (25 μM) yields the second set of multiplets centered around 13 min. All samples are prepared in a solvent of 60:40 methanol/10 mM ammonium formate.

While the observation of analyte retention suggests that the methods used for column functionalization through silanization are indeed applicable to MSFs (generating stationary phases that will interact with analytes of the proper functionality), a concern that remained was the possibility that the observed retention might be the result of mobile phase composition and relative analyte solubility rather than the desired preferential retention on the newly-introduced stationary phase. This was initially probed by preparing analytes **2**, **3** and **4** (Figure 4.1) in a solvent of 5% methanol to closely approximate the starting conditions of the gradient and allowing any changes in

chromatography to be examined, but no distinct difference in analyte retention from the equivalent runs using 60:40 methanol/10 mM ammonium formate as the solvent was observed. Consequently, control columns were fabricated in a manner analogous to that used for the introduction of stationary phase, but instead of including a silanization step there was instead only a toluene flush in its place (see Experimental section 4.2.2.2).

While these columns were initially tested under gradient conditions, it was found that an isocratic method was more diagnostic in terms of demonstrating the difference between the columns with and without stationary phase (Figure 4.4). While the control column showed essentially no resolving or retaining power in these tests (all samples eluted following the 10 min injection region produced by the nanoAcquity), the column with fluorous stationary phase successfully identified 3 distinct samples for compounds **2**, **3** and **4** (Figure 4.1) respectively. This is a very significant difference in column performance under identical operating conditions, which reinforces the assertion that the introduction of a stationary phase (regardless of quality) is essential for generating specificity in a MSF OTLC column.

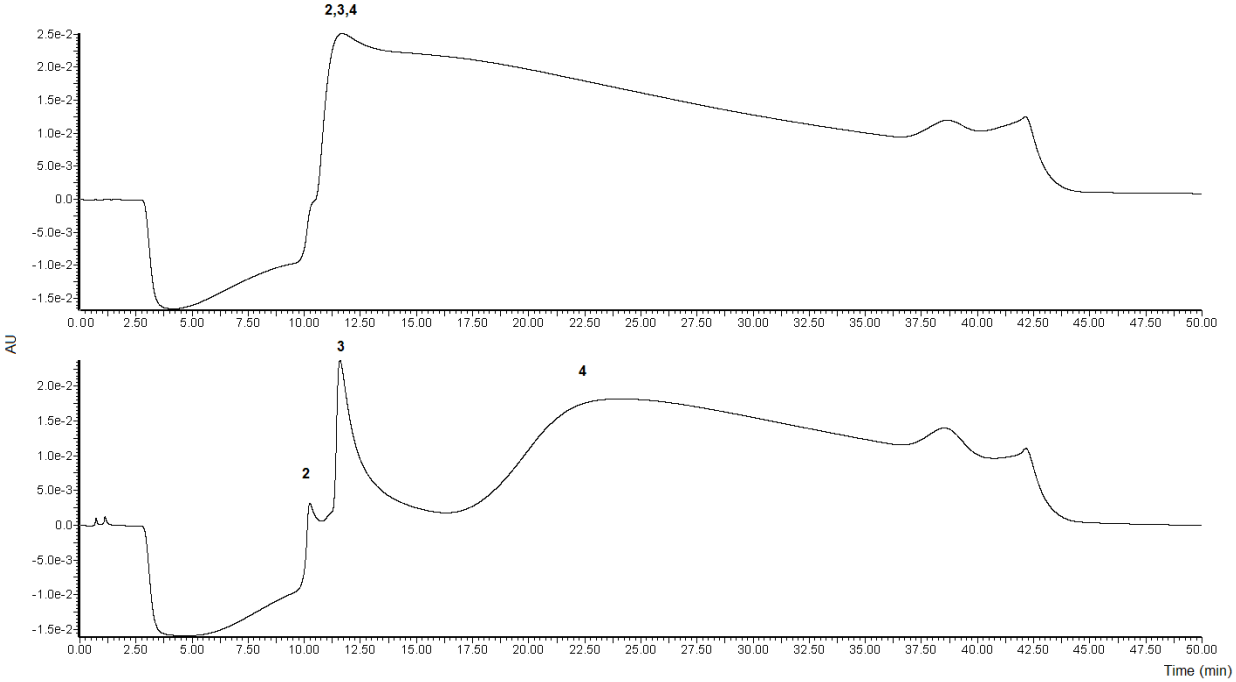

Figure 4.4: Isocratic runs on a control column (top) and a 54 hole MSF column (LMA-PM-16) treated with monochlorosilane **5** (bottom). Analysis is of a mixture containing 5 μM concentrations of each of compounds **2**, **3** and **4** in a solvent of 5% methanol. The signal at ~38.5 min in each case is an artifact produced by the introduction of a high organic flush following the isocratic run to ensure that nothing is retained on-column prior to subsequent injections.

As for the issue of peak multiplicity, this was not entirely unexpected given the nature of the MSF. The disparity in flow velocities for columns with different numbers of holes has already been detailed (Table 4.1), meaning that analytes in each channel are experiencing varied flow characteristics during chromatography (a factor that will only be exacerbated by the introduction of stationary phase). Additionally, in using a trichlorosilane reagent, the resultant network produced through silanization has the added potential to be highly cross-linked and complex on account of the three chlorine leaving

groups. When you consider that there is no way to predict the nature of the silane network that will be formed in each of the distinct MSF channels in conjunction with this unpredictable cross-linked structure, there are a significant number of factors that could be contributing to the poor peak shapes. One way to assess these effects is to simplify the silanization reaction, forming a monolayer instead of a cross-linked network to examine the results.

To explore whether better stationary phase homogeneity could improve the resultant chromatography, two factors were introduced to alter the column treatment in subsequent iterations. First, a more involved column treatment protocol adapted from the literature was employed,[34] adding both hydroxide and acid etching steps prior to silane introduction. These pre-treatment steps are known to help expose more silanol groups at a silica surface,[48] subsequently increasing the surface coverage of the stationary phase produced through silanization. Second, trichlorosilane **1** was also replaced with a monochloro- version (**5** or **6**; Figure 4.1) to prevent cross-linking. This should ideally yield a monolayer coating within each of the MSF channels, which if successful, will greatly simplify the network structure and eliminate much of the previously-noted band broadening and peak splitting due to stationary phase heterogeneity. It should also be noted that for these (and all subsequent) tests, fiber selection was limited to the 54 and 168 hole varieties as the 30 hole version that was initially used had been discontinued by the supplier and replaced by the 54 hole materials. Concurrently, since the average hole diameters of the 54 hole fibers were approximately 4 μm (where the 30 and 168 were nearer to 5 μm; Table 4.1), the flow rate of the treatment steps were reduced to 200 or 300 nL/min from the initial rate of 500 nL/min to minimize any difficulty in backpressure arising from the syringe-driven flow. Interestingly, despite the changes to the treatment

protocol necessitated by the supplier changing the fiber types, the move to the 54 hole varieties was actually fortuitous given that they were found to possess the smallest average hole diameters of all of the fibers tested (putting them closest to the 1-3 μm "ideal" diameter hypothesized for OTLC columns).[8]

In examining representative chromatograms that are produced by MSF columns using the direct monochloro- analogue of trichlorosilane **1** (Figure 4.5), it is evident that switching from a trichloro- to a monochlorosilane produces a marked improvement. For the 168 hole fiber, the peak multiplicity as seen in Figure 4.3 was essentially eliminated using the new method, leaving only some band broadening in the desired peaks. Perhaps more impressive than this are the results for the 54 hole fiber, which gives discrete peaks with improved peak shapes and conclusive resolution for the fluorous analytes ($R_s \approx 1.6$). The signal reproducibility from these columns is also very good (Table 4.3), with intra-column results over a number of trials maintaining a high degree of consistency in all cases. Also of particular interest here, compound **2** (Figure 4.1), which should exhibit virtually no retention on any fluorous column, does indeed elute at essentially the same time in every one of the columns tested (the only analyte without noticeable variation in its retention between column replicates and types).

Table 4.3: Summary of retention times on 20 cm MSF columns treated with fluorous monochlorosilane **5**.

Column		Retention Time (min)		
		Compound **2**	Compound **3**	Compound **4**
54 Hole MSF (LMA-PM-16)	Column 1	5.77 ± 0.17	9.54 ± 0.25	11.91 ± 0.24
	Column 2	6.06 ± 0.04	9.30 ± 0.03	11.53 ± 0.37
168 Hole MSF	Column 1	6.03 ± 0.08	10.42 ± 0.17	12.29 ± 0.10
	Column 2	6.14 ± 0.14	9.10 ± 0.04	11.18 ± 0.12

All retention times are presented as the average of 4 runs of each analyte for two replicate columns of each variety. For the 168 hole MSF (where some residual peak broadening and multiplicity can still exist), the retention time used is at the center of the peak cluster.

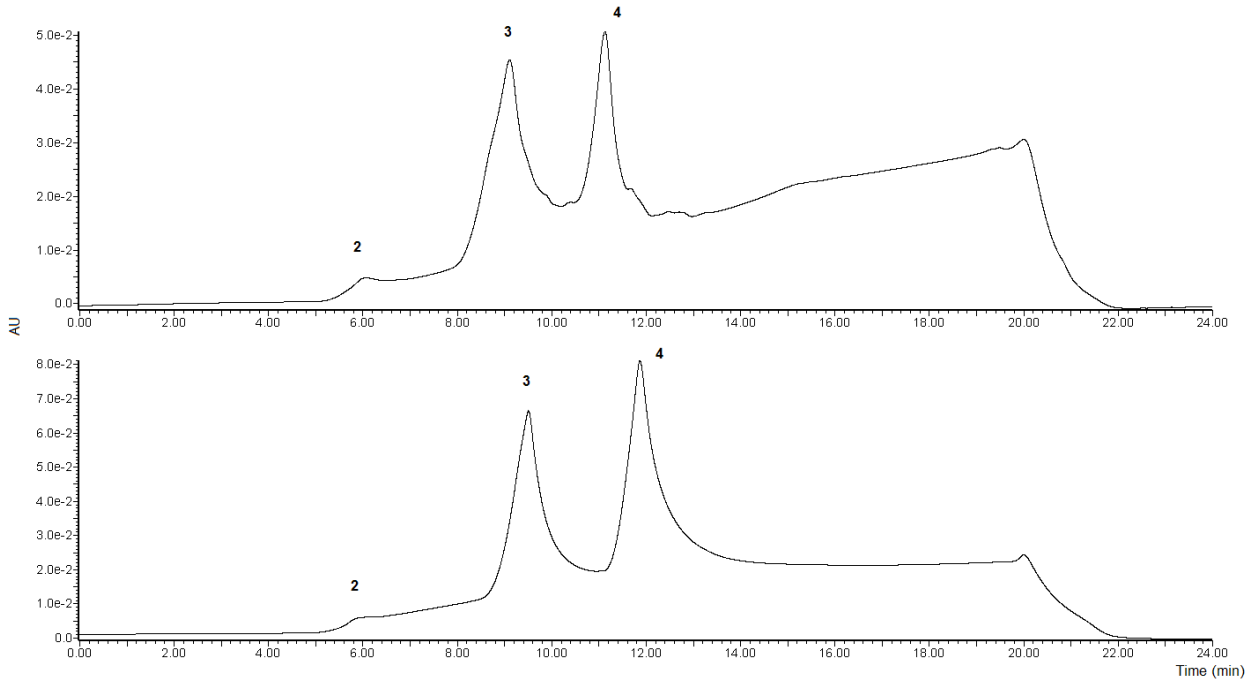

Figure 4.5: Chromatograms of 168 hole (top) and 54 hole fibers (LMA-PM-16; bottom) treated with fluorous monochlorosilane **5**. Triphenylphosphine oxide (**2**; 25 μM) is the small peak around 6 min, the singly-tagged compound **3** (15 μM) produces the signal between 9 and 10 min, and the doubly-tagged compound **4** (25 μM) produces the signal from 11 min onward. All samples are prepared in a solvent of 60:40 methanol/10 mM ammonium formate.

The variation in the inter-column results, while somewhat disappointing, can be explained by some of the factors that are inherent to the fabrication process. For example, despite possessing the same 20 cm length, two columns can still be significantly different based on the relative success of silanization within each of the independent channels. Certainly, the fact that the retention time of an "unretained" analyte (triphenylphosphine oxide) does not vary significantly suggests that the introduction of stationary phase is a significant cause of irreproducibility. Although the switch to a monochlorosilane helps to minimize these effects, it is still possible for different degrees of functionalization to occur based on the accumulation of factors such as differential flow velocities and the relative surface coverage of silanol groups produced in the distinct channels during pre-treatment. The results of these types of effects will be inconsistent stationary phase coatings, leading to peak broadening and retention irregularity in otherwise similar columns. Similarly, another factor that can produce this type of variation is the amount of etching that arises from the initial column treatment. The walls between each of the MSF channels are relatively thin, which means that it may be possible to etch entirely through them in some instances. Should this happen, it can lead to unpredictable (and inconsistent) flow in columns that are seemingly prepared identically in terms of the methods and materials used.

4.3.4 – Investigation of Effects Derived From Injection Volume Variation: As stated earlier, concerns with the limited internal volume presented by MSF OTLC columns might suggest that injection volumes of 2 μL (used for my chromatographic tests) could lead to column overloading and subsequently poorer chromatography. Although literature sources suggest that the sample concentrations (and concurrent absolute amounts) used here were consistent with other trace analyses,[41, 42] validation was still

necessary. Using an Eksigent NanoLC system with metered injections then, it was possible to introduce volumes from 100 nL up to the usual 2 µL of a mixture containing 10 µM of compound **3** and 20 µM of compound **4** (Figure 4.1). This mixture was prepared in a solvent of methanol and 10 mM ammonium formate (60:40 v/v), and the gradient was identical to all of the other runs (see Experimental Section 4.2.6). In doing this, the high aqueous content (99%) at the beginning of the gradient helped to ensure that the samples were properly focused on the open-tubular column, as well as ensuring compatible results.

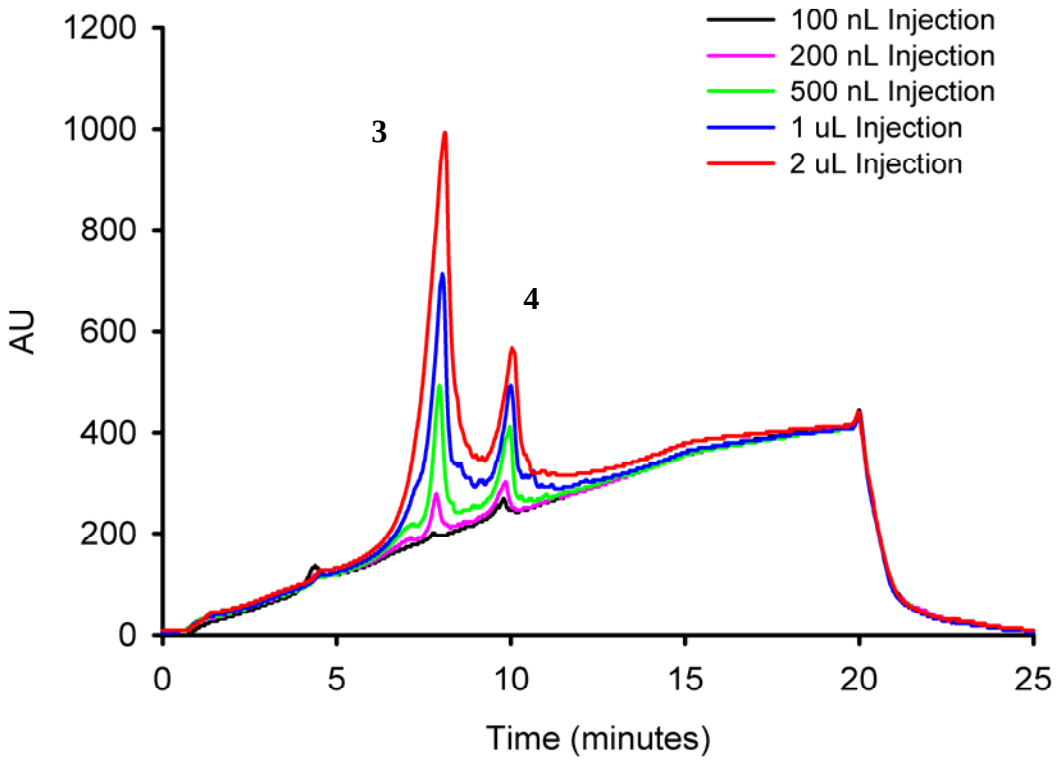

Figure 4.6: Traces showing the change in peak shape and intensity with reductions to the injection volume. Peaks depict 10 µM samples of compound **3,** and 20 µM samples of compound **4** (in order of elution)**.**

In looking at the results from these tests (performed on a 54-hole, LMA-PM-16 column functionalized with (tridecafluoro-1,1,2,2-tetrahydrooctyl)dimethylchlorosilane; Figure 4.6), a steady decrease in signal intensity as sample volume was reduced could be observed. Interestingly, slight improvements in peak shape and resolution also arising from this reduction in sample volume were noticeable. From this result, it could be concluded that band broadening as a result of column overloading was likely occurring (hence the improvement in baseline separation of the peaks with decreased injection volumes), although relative to the issues of hole diameter variation and stationary phase heterogeneity its impact was not yet of significant concern. Conversely, if more reliable fibers become available, it will eventually be necessary to re-examine the issue of column overloading as it will become a much more significant source of band broadening when flow variations are not the primary problem.

4.3.5 – Methods to Improve MSF OTLC Column Performance: One avenue that is frequently discussed with respect to OTLC column improvement is in the area of hole tolerance, with variations of 0.5% or less supposedly required to obtain performance that can compete with packed spheres.[27] With greater numbers of holes and poor manufacturing techniques, the concurrent increase in irreproducibility between channels in arrays has lead to significant issues with column performance,[29] limiting the results of the vast majority of multiplexed OTLC columns that have previously been attempted. Interestingly, with the frequent manufacturing changes to the 54 hole fiber that occurred during my testing, it actually became possible to examine some of the effects of these hole tolerance changes on column performance (subsequent iterations of fiber had better hole reproducibility than the generation they replaced). This degree of control in fabrication presented by the MSF relative to other, similar capillary arrays is actually one

of the greatest incentives for its use, as given sufficient interest by manufacturers to improve hole tolerance, they present a reasonable possibility for obtaining commercially-competitive OTLC substrates.

Similarly, another method that can be used to improve separations is to increase the affinity of the stationary phase for the analyte. A better quality stationary phase will yield better column efficiencies, which in the case of MSF OTLC columns should in turn minimize the impact of the channel velocity heterogeneity. If peaks can be made discrete enough, then even if there is a distribution of hole sizes in a fiber, these should still lead to a distinct distribution of responses and eliminate some of the uncertainty in peak identity that arises when broad clusters run together as seen in the poorer-quality MSF materials (Figure 4.3). Additionally, a better stationary phase will also improve sample resolution, which will further help identification by providing more space between analytes with different degrees of retention regardless of column flow character or heterogeneity.

As a preliminary examination of the experimental impact of these two factors (hole tolerance and stationary phase affinity) on chromatography, a series of columns using the newest-generation 54 hole fiber (LMA-PM-15) and monochlorosilane **6** were prepared using the more intensive treatment protocol detailed in Experimental section 4.2.2.2. The results found through this initial testing were striking (Figure 4.7), with significant improvements in peak shape over anything that had previously been observed. In many cases it was possible to identify a clear distribution of signals (peaks split, but identically and reproducibly for both singly- and doubly-tagged fluorous species), suggesting that a very reproducible and selective stationary phase coating must be resulting. If widespread heterogeneity arising from both channel diameter and stationary

phase quality were still interacting, it would not be possible to accurately differentiate distinct flow regions for channels in the manner seen here.

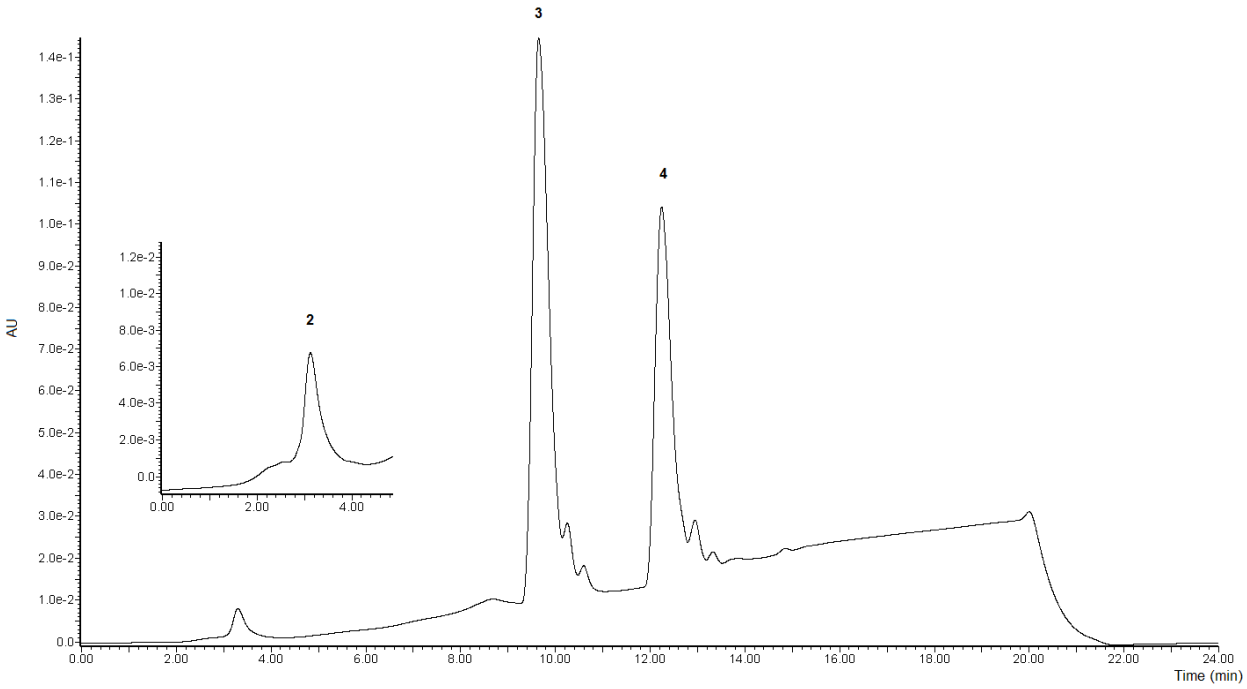

Figure 4.7: Chromatogram resulting from the new-generation (LMA-PM-15) 54 hole fiber functionalized with monochlorosilane **6**. Triphenylphosphine (**2**; 20 μM), the singly-tagged fluorous triphenylphosphine oxide (**3**; 10 μM) and the doubly-tagged fluorous triphenylphosphine oxide (**4**; 20 μM) can all be clearly identified and resolved (sample prepared in a solvent of 60:40 methanol/10 mM ammonium formate). For the two fluorous analytes, a distribution of hole sizes is believed to give rise to the regular pattern of peak spacing that is observed for each species (noticeable due to the improved specificity of the F_{17} silane).

While this result still suggests that diameter tolerances are not perfectly uniform (confirmed by the values shown in Table 4.1), the fact that their differences can be distinctly identified rather than manifesting in a completely random manner is encouraging. Not only does it suggest that using a silane possessing a more specific interaction with the analyte gives rise to better OTLC results (columns made with

fluorous silane **5** in the newest generation of fiber were not as effective as those using the longer fluorous chain of silane **6**), it also appears that the theoretical observations of the importance of hole tolerance on column performance are indeed accurate. The new generation fiber gave sharper peaks and with less unpredictable splitting than anything noted previously, which is the expected result when hole tolerance (and subsequent flow velocity) is more uniform. Although the materials are still not quite at the level that would make them competitive with the best monolithic or packed columns available today in their current form (diameter variation has still not reached the desirable tolerance of ~ 0.5%), it is still clear that things are trending that way (a positive indicator for their future viability).

Ultimately, no matter the substrate, the goal in developing MSF OTLC columns is for them to provide discernable benefits over the competing materials that are currently in use. One way that this can be quantified is to assess column performance, which is traditionally represented by the column efficiency. Unfortunately, to do things this way, one must also perform separations under isocratic conditions which was not the case for the systems tested here (although isocratic runs were performed, gradient methods were preferred for their vastly improved peak shapes). Alternatively then, for gradient separations a *pseudo* van Deemter plot[43, 44] can instead be used to approximate the results that would be found under analogous isocratic conditions. This has the benefit of not only allowing a reasonable assessment of column performance to be made, but also maintains the separation quality and sample injection focusing attained through the use of gradient conditions.

As discussed previously, open-tubular columns are normally treated with the Golay equation rather than the van Deemter equation since OTLC columns lack the band

broadening associated with a traditional "A" term. However, when using MSFs as a substrate for OTLC, the differential flow velocities arising from factors such as the variation in hole diameters gives rise to a similar type of "multipath" term that needs to be considered. As a result then, it seems more logical to form an assessment of column performance using the van Deemter equation with a "pseudo-A" term arising from the flow velocity variations instead of the Golay equation (which would totally neglect the contribution of these effects on the observed column efficiency).

In results for tests of this type (Figure 4.8), it was found that changes in flow rate had little effect on the column efficiency as predicted by a *pseudo* van Deemter plot (with the most significant band broadening contribution coming from a velocity-independent pseudo-A term). The difference in plate height between flow at 100 nL/min and 1 μL/min (averaged over 3 separate trials) was only 35%, meaning that separations in OTLC columns could be pushed to greater flow rates without significant degradation of performance (flow-induced backpressure at these greater flow rates should not be an issue given the multiple channels). This is confirmed experimentally in Figure 4.9, where separation ($R_s \approx 1.3$) of compounds **3** and **4** (Figure 4.1) was achieved in less than 5 min at a gradient flow of 1 μL/min. Ideally I would have liked to push this even further to assess the potential for faster flow rates to produce separations (one of the greatest benefits of MSF OTLC columns as compared to other media is that their relative performance increases with higher linear velocities),[27, 33] but things are currently limited by the durability of the fiber coating. The coating currently used on the MSFs is an acrylate-based polymer, and can easily be damaged when exposed to repeated pressure and solvent changes. This means that even though the columns themselves function under the conditions discussed here, material limitations are the primary factor standing

in the way of the further development of superior MSF columns for rapid, open-tubular liquid chromatography.

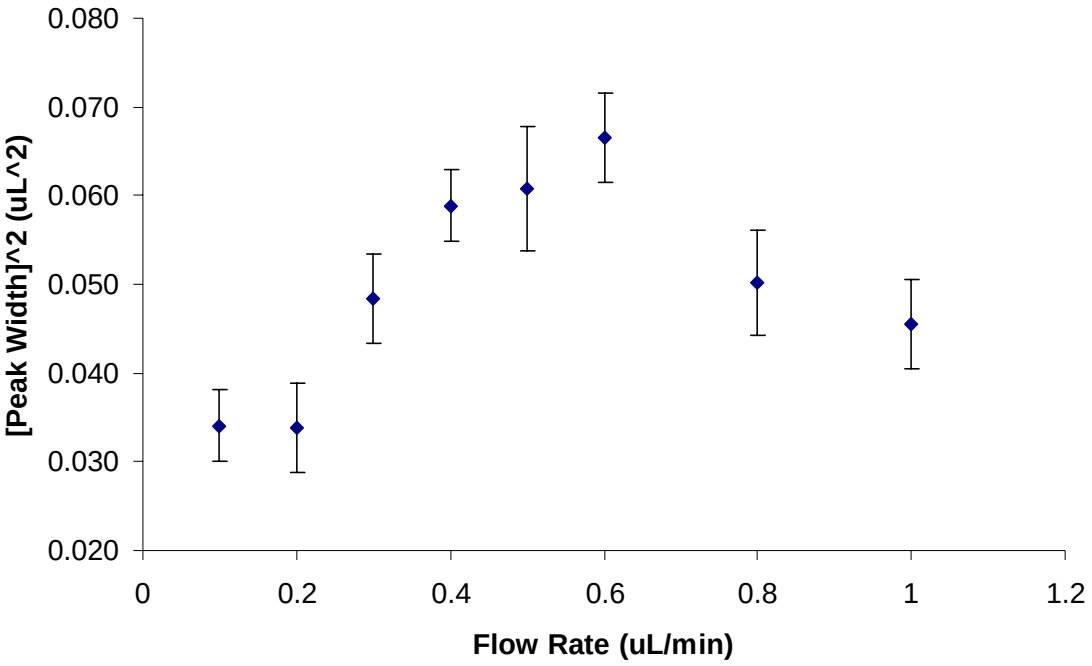

Figure 4.8: Representative *pseudo* van Deemter plot for MSF OTLC. Data is shown for a 54 hole fiber (LMA-PM-16) functionalized with monochlorosilane **5**, and running 3 replicate injections of the singly-tagged fluorous triphenylphosphine oxide (**3**) at a concentration of 25 μM to determine the necessary peak widths for calculation.

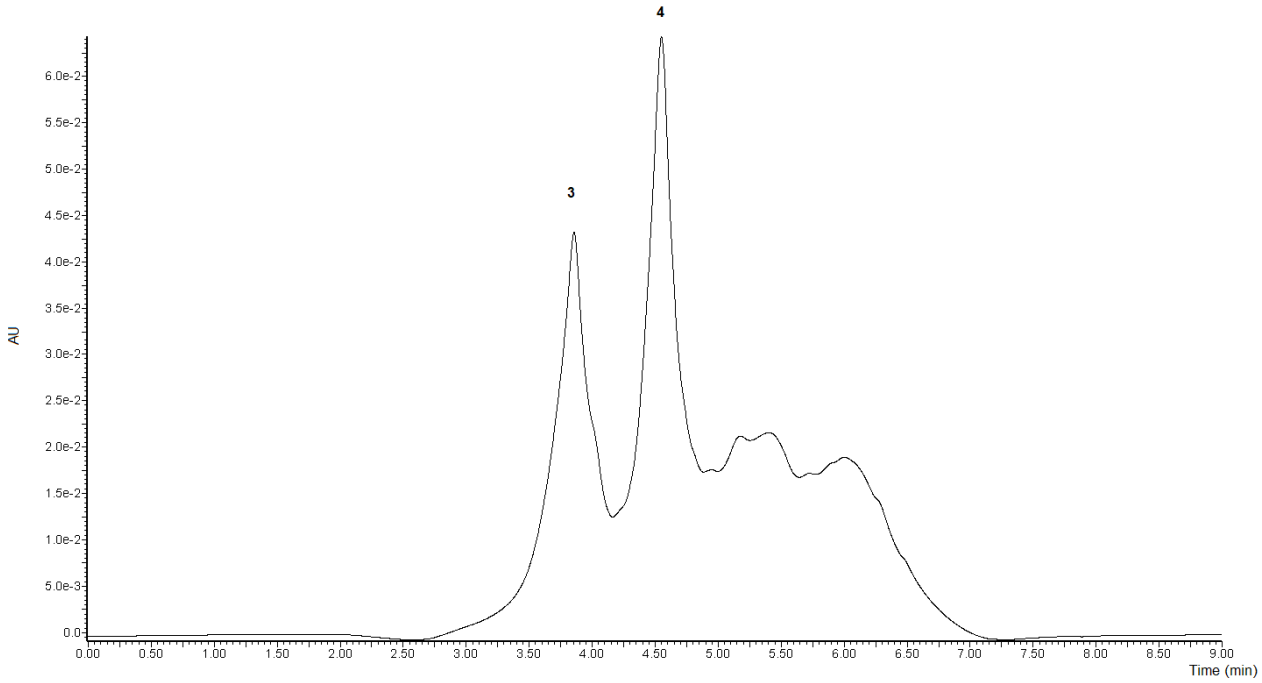

Figure 4.9: Chromatogram showing the separation of fluorous-tagged triphenylphosphine oxides **3** (1 μM) and **4** (2 μM) on a fluorous-treated 54 hole MSF column (LMA-PM-16) using monochlorosilane **5**. Gradient flow rate was 1 μL/min, which yielded separation in less than 5 min. Samples were prepared in a solvent of 60:40 methanol/10 mM ammonium formate.

4.4 Conclusions and Future Work

Through these experiments, it has been shown that it is possible to use a straightforward silanization process to create open-tubular chromatographic columns in microstructured fibers. In conjunction with their simple fabrication, these columns have been demonstrated to possess flow and pressure properties that are comparable to conventional chromatographic media such as packed spheres and monoliths, and possess similar column diameters (in a fused silica substrate) as many commercially-available products.

The sum of these properties should allow MSF OTLC columns to be used in a wide variety of existing LC systems without the need for any alterations or other specialized equipment. Interestingly, this move away from specialized equipment actually solves one of the greatest problems that had previously limited the development of OTLC systems, since on-column detection for small sample volumes are no longer necessary. With their many parallel channels MSF OTLC columns can easily be operated with parameters and setups that permit standard UV or MS detection, improving their versatility. Similarly, their numerous channels provide MSF columns with a much greater loading capacity than conventional, narrow-bore open-tubular columns. When the possibility for different stationary phase chemistries based on varied silanization protocols are also considered, one can envision a bright future for MSF-based OTLC columns. Additionally, an added benefit of many of these suggested protocols are that they are also believed to lead to more reproducible and complete (monolayer) stationary phase coatings;[49-52] factors that would further improve the performance of any MSF-based chromatography column.

As for some of the difficulties noted during the developmental stages, many of these issues can be attributed to the fact that microstructured fibers, in their current state, are designed with optics (and not fluidic) applications in mind. Things such as hole patterns, sizes and diameter tolerances, as well as the durability of the fiber coating have all been optimized for uses that are completely different than those that have been proposed and tested here. Fortunately though, the development of microstructured fibers is a field that is undergoing rapid expansion; something that could be seen even during the limited timeframe explored here. With both the 30 and 54 hole fibers being sequentially replaced by superior products in such short order, it is clear that there is a willingness and desire from manufacturers to improve these materials as applications

demand. As such, it is entirely possible that with an increased interest in fibers designed to act as fluidic channels rather than light guides that the materials will be appropriately adapted to meet the unique needs of new applications and further improve upon the level of results achieved here. In particular, if diameter tolerances can be sufficiently reduced through better manufacturing, it should be possible for MSF OTLC columns of the type presented here to directly compete with other conventional LC materials. Even now, these values have already reached levels where MSF OTLC columns easily outperform other substrates that have been tested for open-tubular liquid separations,[29] which bodes well for their future use as unique LC substrates in a variety of applications.

4.5 – References

(1) Bartle, K. D.; Myers, P. *Trends Anal. Chem.* **2002**, *21*, 547-557.

(2) Francotte, E.; Jung, M. *Chromatographia* **1996**, *42*, 521-527.

(3) Horvath, C. G.; Preiss, B. A.; Lipsky, S. R. *Anal. Chem.* **1967**, *39*, 1422-1428.

(4) Nota, G.; Marino, G.; Buonocore, V.; Ballio, A. *J. Chromatogr.* **1970**, *46*, 103-106.

(5) Tsuda, T.; Hibi, K.; Nakanishi, T.; Takeuchi, T.; Ishii, D. *J. Chromatogr.* **1978**, *158*, 227-232.

(6) Knox, J. H.; Gilbert, M. T. *J. Chromatogr.* **1979**, *186*, 405-418.

(7) Guiochon, G. *Anal. Chem.* **1981**, *53*, 1318-1325.

(8) Jorgenson, J. W.; Guthrie, E. J. *J. Chromatogr.* **1983**, *255*, 335-348.

(9) Tsuda, T.; Nakagawa, G. *J. Chromatogr.* **1983**, *268*, 369-374.

(10) Maskarinec, M. P.; Sepaniak, M. J.; Balchunas, A. T.; Vargo, J. D. *Clin. Chem.* **1984**, *30*, 1473-1476.

(11) Tock, P. P. H.; Stegeman, G.; Peerboom, R.; Poppe, H.; Kraak, J. C.; Unger, K. K. *Chromatographia* **1987**, *24*, 617-624.

(12) Eguchi, S.; Kloosterboer, J. G.; Zegers, C. P. G.; Schoenmakers, P. J.; Tock, P. P. H.; Kraak, J. C.; Poppe, H. *J. Chromatogr.* **1990**, *516*, 301-312.

(13) Guo, Y.; Colon, L. A. *Anal. Chem.* **1995**, *67*, 2511-2516.

(14) Guo, Y.; Colon, L. A. *Chromatographia* **1996**, *43*, 477-483.

(15) Yue, G.; Luo, Q.; Zhang, J.; Wu, S.-L.; Karger, B. L. *Anal. Chem.* **2007**, *79*, 938-946.

(16) Guthrie, E. J.; Jorgenson, J. W. *Anal. Chem.* **1984**, *56*, 483-486.

(17) Swart, R.; Kraak, J. C.; Poppe, H. *Trends Anal. Chem.* **1997**, *16*, 332-342.

(18) Hulthe, G.; Petersson, M. A.; Fogelqvist, E. *Anal. Chem.* **1999**, *71*, 2915-2921.

(19) Kuban, P.; Dasgupta, P. K.; Pohl, C. A. *Anal. Chem.* **2007**, *79*, 5462-5467.

(20) Wang, X.; Cheng, C.; Wang, S.; Zhao, M.; Dasgupta, P. K.; Liu, S. *Anal. Chem.* **2009**, *81*, 7428-7435.

(21) Russell, P. *Science* **2003**, *299*, 358-362.

(22) Sun, Y.; Kwok, Y. C.; Nguyen, N. T. *Electrophoresis* **2007**, *28*, 4765-4768.

(23) Sun, Y.; Nguyen, N.-T.; Kwok, Y. C. *Anal. Bioanal. Chem.* **2009**, *394*, 1707-1710.

(24) Nguyen, N. T.; Kwok, Y. C.; Sun, Y. Capillary Sample Separation Apparatus. International Patent WO 2009/005476 A1, January 8, 2009.

(25) Matejec, V.; Podrazky, O.; Hayer, M.; Pospisilova, M.; Berkova, D. *Proceedings of SPIE* **2008**, *7138*, 713806/713801-713806/713809.

(26) Su, S.; Gibson, G. T. T.; Mugo, S. M.; Marecak, D. M.; Oleschuk, R. D. *Anal. Chem.* **2009**, *81*, 7281-7287.

(27) Meyer, R. F.; Champlin, P. B.; Hartwick, R. A. *J. Chromatogr. Sci.* **1983**, *21*, 433-438.

(28) Czok, M.; Guiochon, G. *J. Chromatogr.* **1990**, *506*, 303-317.

(29) Naida, O. O.; Rudenko, B. A.; Khamizov, R. K.; Kumakhov, M. A. *J. Anal. Chem.* **2009**, *64*, 721-724.

(30) Saito, Y.; Kawazoe, M.; Imaizumi, M.; Morishima, Y.; Nakao, Y.; Hatano, K.; Hayashida, M.; Jinno, K. *Anal. Sci.* **2002**, *18*, 7-17.

(31) Marcus, R. K.; Davis, W. C.; Knippel, B. C.; LaMotte, L.; Hill, T. A.; Perahia, D.; Jenkins, J. D. *J. Chromatogr., A* **2003**, *986*, 17-31.

(32) Stanelle, R. D.; Mignanelli, M.; Brown, P.; Marcus, R. K. *Anal. Bioanal. Chem.* **2006**, *384*, 250-258.

(33) Marcus, R. K. *J. Sep. Sci.* **2008**, *31*, 1923-1935.

(34) Gottschlich, N.; Jacobson, S. C.; Culbertson, C. T.; Ramsey, J. M. *Anal. Chem.* **2001**, *73*, 2669-2674.

(35) Bakry, R.; Stoeggl, W. M.; Hochleitner, E. O.; Stecher, G.; Huck, C. W.; Bonn, G. K. *J. Chromatogr., A* **2006**, *1132*, 183-189.

(36) Gibson, G. T. T.; Koerner, T. B.; Xie, R.; Shah, K.; de Korompay, N.; Oleschuk, R. D. *J. Colloid Interface Sci.* **2008**, *320*, 82-90.

(37) Daley, A. B.; Oleschuk, R. D. *J. Chromatogr., A* **2009**, *1216*, 772-780.

(38) Gibson, G. T. T.; Marecak, D. M.; Oleschuk, R. D. *J. Sep. Sci.* **2009**, *32*, 4025-4032.

(39) Brittain, S. M.; Ficarro, S. B.; Brock, A.; Peters, E. C. *Nat. Biotechnol.* **2005**, *23*, 463-468.

(40) Benskin, J. P.; Bataineh, M.; Martin, J. W. *Anal. Chem.* **2007**, *79*, 6455-6464.

(41) Sultan, M.; Stecher, G.; Stoeggl, W. M.; Bakry, R.; Zaborski, P.; Huck, C. W.; El Kousy, N. M.; Bonn, G. K. *Curr. Med. Chem.* **2005**, *12*, 573-588.

(42) Groleau, P. E.; Desharnais, P.; Cote, L.; Ayotte, C. *J. Mass Spectrom.* **2008**, *43*, 924-935.

(43) Gilar, M.; Neue, U. D. *J. Chromatogr., A* **2007**, *1169*, 139-150.

(44) Petersson, P.; Frank, A.; Heaton, J.; Euerby, M. R. *J. Sep. Sci.* **2008**, *31*, 2346-2357.

(45) de Nevers, N. *Fluid Mechanics for Chemical Engineers*, 3rd ed.; McGraw-Hill: New York, 2005.

(46) Guiochon, G. *J. Chromatogr., A* **2007**, *1168*, 101-168.

(47) Nishiyama, N.; Horie, K.; Asakura, T. *J. Appl. Polym. Sci.* **1987**, *34*, 1619-1630.

(48) Courtois, J.; Szumski, M.; Bystroem, E.; Iwasiewicz, A.; Shchukarev, A.; Irgum, K. *J. Sep. Sci.* **2006**, *29*, 14-24.

(49) Wirth, M. J.; Fatunmbi, H. O. *Anal. Chem.* **1992**, *64*, 2783-2786.

(50) Fairbank, R. W. P.; Xiang, Y.; Wirth, M. J. *Anal. Chem.* **1995**, *67*, 3879-3885.

(51) Wirth, M. J.; Fairbank, R. W. P.; Fatunmbi, H. O. *Science* **1997**, *275*, 44-47.

(52) Guo, Z.; Wang, C.; Liang, T.; Liang, X. *J. Chromatogr., A* **2010**, *1217*, 4555-4560.

Chapter 5: Summary and Project Outlook

The underlying theme throughout my project has been an attempt to expand the scope and applicability of fluorous separations away from the current domain that is largely limited to microsphere-based techniques. To this end, I have examined and discussed three main branches that are (or were) believed to offer advantages over conventional packed columns: entrapped microspheres, porous polymer monoliths and open-tubular liquid chromatography. Each of these options presented its own unique set of challenges (and presumed advantages) that were dealt with during development, with the ultimate benefits relative to original expectations being assessed upon the completion of each section.

In the realm of microsphere entrapment, the columns that were formed did not ultimately prove to have an advantage over unentrapped microspheres. Although affixing the spheres within a polymeric matrix is known to have benefits in terms of bed stability during repeated use (sphere movement and void formation is inhibited), the inclusion of a polymer coating proves to represent a greater concern with respect to the availability of the bead-based stationary phase. Thin layers of polymer forming over the entire surface of the column can be shown to limit the availability of the underlying microspheres to many target analytes, meaning that chromatographic efficiency will be decreased by the transformation (despite the efforts actually being to improve it). Conversely, one of the most useful conclusions drawn from these analyses was with respect to the effectiveness of fluorous acrylates as materials for fluorous selectivity. Their exhibition of preferential interactions with the fluorous microspheres as compared to any of the non-fluorous analogues was the driving force behind the examination of fluorous monolithic materials, as they seemed to represent the most viable option to explore in terms of a truly novel

stationary phase material. Additionally, directly forming monoliths rather than using them to entrap spheres was a significantly easier (and more practical) experimental technique, making it a logical avenue to pursue when the known benefits of monoliths for chromatography are considered.

The work with fluorous monoliths was perhaps the most conclusive of the results shown here, providing clear evidence of improved selectivity as compared to their direct competitors made without component fluorination. The topic of fluorous retention specificity was also effectively examined, with secondary effects (interactions of the analyte substrate outside of the fluorous region) probed and compared to those which had frequently been discussed for commercially-available microspheres. My results showed that the monoliths were very much in-line with what had already been seen and discussed for these sphere-based systems (fluorous affinity dominating the interactions), with residual substrate character also providing a slight contribution to the observed separation. Interestingly, the possibility of these secondary interactions serving as an additional dimension for chromatography (further separating fluorous subsets based on secondary structure) has never been explored, and after noting it here, it should be considered as one of the potential avenues for future research with these monolithic materials.

Subsequently, the optimized monoliths were also applied to preliminary fluorous proteomic examinations, separating a custom peptide with a fluorous tag from the non-fluorous species left in the reaction medium. Not only did this process help to confirm the viability of some of the tagging chemistries that are frequently cited in the literature as being amenable to fluorous methods, it also helped to demonstrate the online coupling of a fluorous separation method in a proteomic application. One of the limiting factors with

many fluorous separations (and a number of proteomic methods) is that they must first perform the separation as an offline step prior to using the collected fraction(s) for the actual analysis that is desired. Fluorous monoliths have been shown here to not need to be used in this fashion, being able to separate and interface with detection media simultaneously. This makes them desirable materials for further examination, as their versatility and specificity are generally unknown in online proteomic methods.

Development of open-tubular chromatographic columns based on microstructured optical fibers remains the most speculative of the projects discussed here. Fortunately, many of the current limitations are simply with respect to the availability of commercial materials with adequate hole tolerances; a factor that can be improved given the correct commercial impetus. The introduction of a fluorous stationary phase through silanization chemistry has been shown to be an effective method for imparting chromatographic selectivity into columns made with optical fibers, and controllable factors such as the treatment protocol and overall silane character have also been shown to affect the performance of the resulting columns. In particular, these open-tubular columns seem to present interesting options in the realm of trace analysis, as their limited internal volumes require only small amounts of both stationary phase and analyte to yield adequate separation results. With further optimization then, these materials (fluorous-functionalized or otherwise) could eventually be used in a variety of interesting realms outside of their original vision.

In terms of future research directions for this project, many of the possibilities lie in the realm of application. In particular, coupling fluorous tools like monoliths or open-tubular columns with online detection to facilitate proteomic applications remains the ultimate goal to be achieved. Fortunately, both of these substrates present reasonable

possibilities for achieving this goal, as they have been shown to possess the necessary specificity for sample analysis. Additionally, monoliths and optical fibers have also both been shown (by other work within our group) to be reasonable emitters for use in coupling liquid chromatography with mass spectrometry, suggesting that integrated fluorous systems using the materials presented here are indeed a possibility. To this end then, work on optimizing conditions that will permit both fluorous separation and electrospray mass spectrometry to be integrated into the same fluorous substrate remains a task to be undertaken.

Other future avenues for this project include some of the topics that were touched upon earlier. Using secondary interactions found in fluorous columns as a tool for improving separations is an interesting option, as it is conceivable that it could greatly impact an area such as proteomics. Here, it is common practice to introduce a fluorous tag into a peptide or protein to search for modifications to a particular amino acid residue. If this separation based on fluorous character could be further modified by analyte substrate (different amino acid polarities providing different secondary effects after initial grouping by fluorous tag), it seems possible to greatly improve the viability of the method. In general, finding ways to exploit these new fluorous substrates in unique realms like proteomics and microfluidics seems like the next logical step for the project to take, as with further integration they seem as though they have the potential to lead to a number of benefits in separation and overall sample analysis.

Looking back, one of the ideas discussed in Chapter 1 with respect to the general lack of fluorous separation tools appearing in more mainstream applications was that it might be the result of materials limitations and mechanistic uncertainty leading to hesitation. Difficulty applying packed beds of microspheres (the common fluorous

interface) to burgeoning media such as microchips, coupled with poorly-understood fluorous interaction specificity could easily lead people to shy away from fluorous tools in favour of more traditional options. Unfortunately, this line of thinking only serves to prevent fluorous techniques from finding their true role, which is something that my work hopefully helps to remedy. In particular, monolithic materials and open-tubular columns can serve as replacements for packed spheres in a number of applications where they wouldn't otherwise be applicable (particularly microfluidics), allowing the transition into newer fluorous applications as a result. Similarly, should these ideas and techniques continue to grow, they could one day be used to help elucidate the mechanism behind the fluorous affinity interaction by permitting new (and unique) analyses to be undertaken. At the very least then, the work presented here should hopefully encourage a wider examination of fluorous tools and their applicability in a number of unique areas; a key first step in the further growth and development of the field as a whole.

Appendices

Included on the following pages are the proton NMR spectra provided by Fluorous Technologies for the custom-synthesized carbamate mixtures used as some of the analytes in Chapter 3. Figure A1 is for the 4-nitro-benzyl substituted mixture ($C_{17+x}H_{17}F_{2x+1}N_2O_4$; x=3, 4, 6 and 8), while Figure A2 is for the 4-phenyl-benzyl substituted mixture ($C_{23+x}H_{22}F_{2x+1}NO_2$; x=3, 4, 6 and 8).

Figure A1

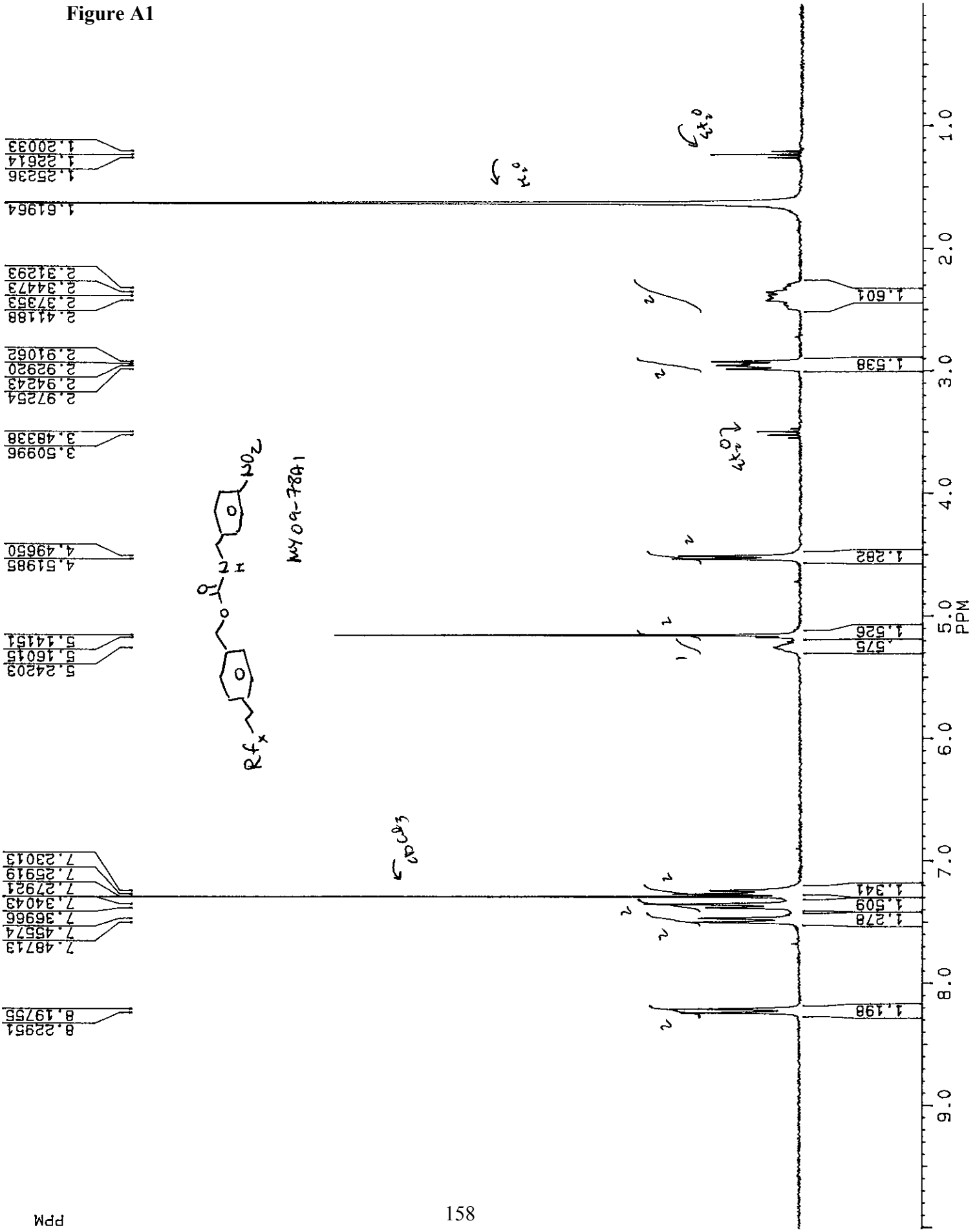

Figure A2

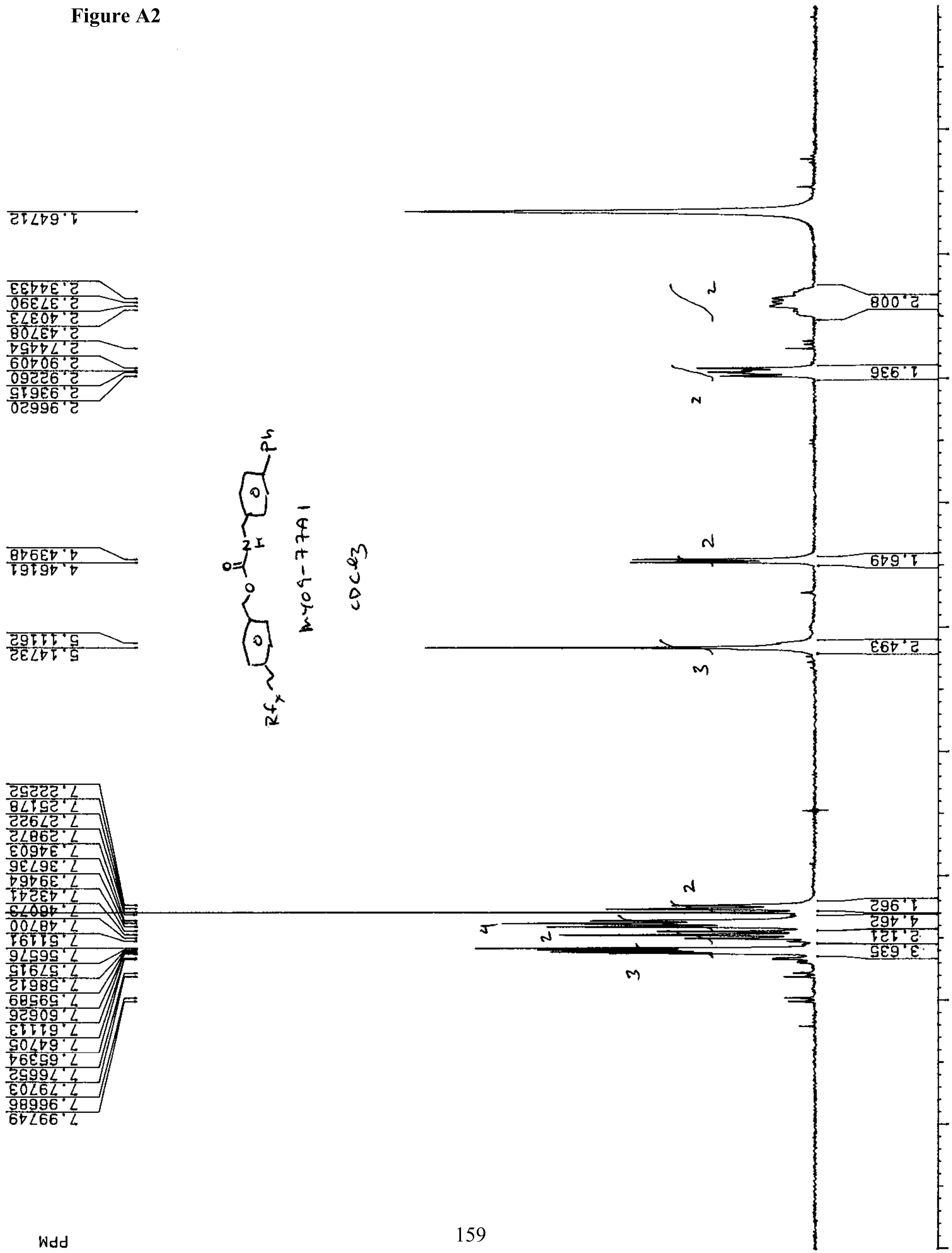
1.64712
2.34433
2.37390
2.40373
2.43708
2.74454
2.90409
2.92260
2.93615
2.96620
4.43948
4.46161
5.11162
5.14732
7.22252
7.25178
7.27922
7.29872
7.34603
7.36736
7.39464
7.43241
7.46073
7.48700
7.51191
7.56576
7.57915
7.58612
7.59589
7.60626
7.61113
7.64705
7.65394
7.76652
7.79703
7.96686
7.99749
2.008
1.936
1.649
2.493
1.962
4.462
2.121
3.635
my09-77A1
CDCl3
1.0
2.0
3.0
4.0
5.0
6.0
7.0
8.0
9.0
PPM
PPM